1997

Microstructures of poly(vinyl acetate) studied by nuclear magnetic resonance spectroscopy

Hongyang Yao
College of William & Mary - Arts & Sciences

MICROSTRUCTURES OF POLY(VINYL ACETATE) STUDIED BY NUCLEAR MAGNETIC RESONANCE SPECTROSCOPY

A Dissertation

Presented to

The Faculty of the Department of Applied Science

The College of William and Mary in Virginia

In Partial Fulfillment

Of the Requirements for the Degree of

Doctor of Philosophy

---

by

Hongyang Yao

1997

APPROVAL SHEET

This Dissertation is submitted in partial fulfillment of

the requirements for the degree of

Doctor of Philosophy

Author

Approved, April 1997

William H. Starnes, Jr.

Robert A. Orwoll

Robert L. Vold

Floyd L. Klavetter

Robert D. Pike
Department of Chemistry

TABLE OF CONTENTS

ACKNOWLEDGEMENTS

The author wishes to express his sincere appreciation to Professor William H. Starnes, Jr., for his patient guidance and constant encouragement throughout the performance of this work. He would like to thank the other committee members, Drs. Robert Orwoll, Robert Vold, Floyd Klavetter, and Robert Pike, for their valuable criticisms.

He thanks his colleagues, Drs. Haksoo Chung, Jong Paul Jeng, and Vadim Zaikov, for their help in the experiments. He also wishes to thank all of the other faculty and staff members of the Departments of Applied Science and Chemistry, and Dr. George M. Benedikt of the B. F. Goodrich Company, who provided several NMR spectra. Finally, he is deeply indebted to his wife, Rihong Xu, for her support.

LIST OF TABLES

LIST OF SCHEMES

LIST OF FIGURES

ABSTRACT

Carbon-13 NMR spectroscopy was used to investigate the microstructures of poly(vinyl acetate) prepared by solution polymerization in benzene. A series of aromatic compounds was synthesized in order to model the structures formed via chain transfer to solvent. The peaks near 126.5 and 128.5 ppm in the spectra of the polymer samples were assigned to a 1-phenyl-(2n + 1)-multi-acetoxyalkane (where n = 1, 2, 3, etc.) microstructure. The concentration of that structure obtained from NMR spectra was correlated with the concentration calculated from reported kinetic data.

Chain transfer to benzene was shown to occur by addition of the macroradical to benzene, followed by rearomatization involving loss of a hydrogen atom. No evidence was obtained for a transfer mechanism involving hydrogen abstraction from benzene, and the copolymerization of benzene with vinyl acetate also was shown to be absent. The transfer mechanism actually established accounts for the unexpectedly large transfer constant of benzene in vinyl acetate polymerization. General mechanisms are proposed for the solution polymerization of vinyl acetate in aromatic solvents.

MICROSTRUCTURES OF POLY(VINYL ACETATE) STUDIED BY NUCLEAR MAGNETIC RESONANCE SPECTROSCOPY

CHAPTER 1

INTRODUCTION

1.1 General

Materials have undergone a profound revolution in this century. Polymeric materials have changed our lives. Synthetic polymer materials (plastics, rubbers, fibers) not only have replaced the traditional materials (metal, glass, cotton) in many places, but also have created unique applications in areas such as electronics, automobiles, and health care.

The applications and processing of polymer materials are determined by their properties, such as glass transition temperature (Tg), melting temperature, solubility, melt and solution viscosities, strength, flexibility, and stability. These properties are determined, in turn, by structural factors, such as chemical compositions, molecular weights and their distributions, configurational and conformational microstructures, structural defects, and morphology. Furthermore, those characteristics are determined by the reaction mechanisms and kinetics of the polymerizations.

In order to design a polymeric material of controlled structure with the properties that are desired for specific applications, one needs to understand

the mechanism-structure-property-process-application relationships. This understanding requires the characterization of structures at the molecular level, the elucidation of the mechanisms of their formation, and their correlation with polymer properties. Knowledge of these features is very important for the manufacture and quality control of polymeric materials.

1.2 Poly(vinyl acetate) (PVAc)

Poly(vinyl acetate) (PVAc) is manufactured by the polymerization of vinyl acetate (VAc). In 1995, about 2.89 billion lb of VAc was produced in the United States, with 3% annual increases during 1985 – 1995. [1]

The free-radical polymerization of VAc may be an emulsion, bulk, solution, or suspension process. The initiators are usually peroxides, azo compounds, redox systems, light, or radiation. The polymerization kinetics are complicated by extensive chain transfer.

Poly(vinyl acetate) is amorphous and nontoxic. Its Tg is only 30 °C. [2] It is widely used in adhesives, emulsion paints, and coatings for paper and textiles. [2]

One of the most important applications of PVAc is as a precursor of poly(vinyl alcohol) (PVA) and poly(vinyl acetal)s, which cannot be prepared commercially by direct polymerization. Poly(vinyl alcohol) is made by alcoholysis or hydrolysis of PVAc (Eq. 1.1). It is used in fibers, coatings, water-based adhesives, thickening agents, and sizing agents. [3]

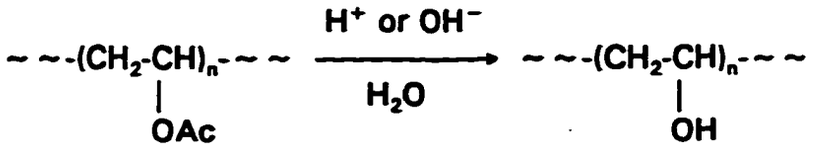

(1.1)

Poly(vinyl acetal)s are made by condensation of PVA with an aldehyde. Poly(vinyl butyral) is used as an interlayer in laminated safety glass, and poly(vinyl formal) as a wire enamel. [4]

1.3 Solution Polymerization

Solution polymerization minimizes many disadvantages of bulk polymerization. The lower solution viscosity allows easier stirring and better mixing. The greater ease of heat transfer (thermal control) avoids the bubbles or chars produced by the usually violent exothermic polymerization. However, solvents also may function as chain transfer agents for free-radical polymerization which lead to lower molecular weights. Polymer purification and subsequent solvent recycling may be problematical, both economically and environmentally. [5]

Free-radical solution polymerizations have a wide range of industrial applications for the production of various polymers with a broad range of properties. Organic solvent-borne polymers are widely used in coatings, adhesives, and inks; while water-borne polymers are used in detergents, water-treatment agents, and dispersants and as thickeners in paints and adhesives.

1.4 Chain Transfer

The mechanism of free radical polymerization can be represented by Scheme 1 – 1.[6]

Scheme 1 – 1

Initiation

$$I\text{-}I \longrightarrow 2\,I\cdot$$

$$I\cdot + M \xrightarrow{k_i} R_1\cdot$$

Propagation

$$R_n\cdot + M \xrightarrow{k_p} R_{(n+1)}\cdot$$

Transfer

$$R_n\cdot + SX \xrightarrow{k_{tr}} P_nX + S\cdot$$

$$S\cdot + M \xrightarrow{k_{p,tr}} R_1\cdot$$

Termination

$$R_n\cdot + R_m\cdot \xrightarrow{k_{tc}} P_{(n+m)}$$

$$R_n\cdot + R_m\cdot \xrightarrow{k_{td}} P_n + P_m$$

Here, I-I is the initiator, M is the monomer, SX is a chain transfer agent, the R·'s are propagating macroradicals, and P_n, P_m, and $P_{(n+m)}$ are polymer molecules.

The application of the steady-state approximation gives the following equations (Eqs. 1.2 and 1.3) for the rate of polymerization and the number-

average degree of polymerization without chain transfer.

$$r_p = k_p (2fk_i/2k_t)^{1/2} [I-I]^{1/2} [M] \qquad (1.2)$$

(where *f* is initiator efficiency)

$$(\overline{DP})_o^{-1} = \frac{(k_{tc} + 2k_{td})\, r_p}{k_p^2 [M]^2} + C_M \qquad (1.3)$$

The number-average degree of polymerization with chain transfer is given by the Mayo equation (Eq. 1.4).

$$(\overline{DP})^{-1} = (\overline{DP})_o^{-1} + \sum \{ C_{sx} \cdot [SX]/[M] \} \qquad (1.4)$$

The transfer agent SX may be monomer, initiator, solvent, or added substrate. The chain transfer reaction usually involves the abstraction of species X from the transfer agent by the propagating radical, $R_n\cdot$, in order to form a dead polymer, P_nX, and a radical, $S\cdot$, which reinitiates polymerization to form a new chain. The labile X may be an atom (usually hydrogen, chlorine, or bromine) or a group of atoms.

The chain transfer kinetic treatment may be very complex, depending upon the reactivity of the transfer radical, $S\cdot$. The conventional "transfer agent" is one that rapidly reinitiates polymerization; i.e., the reactivity of $S\cdot$ is comparable to that of $R_n\cdot$. Under such circumstances, the polymerization rate will not change, yet the average degree of polymerization will decrease.

The conventional "inhibitor" will not reinitiate the polymerization; i.e., the radical S• is stable and will not add to monomer. The polymerization essentially will not start until all of the inhibitor molecules are consumed, and only very low-molecular-weight oligomers may be produced during this inhibition period. The intermediate situation is that where the reactivity of S• is lower than that of R_n•, yet S• still can slowly reinitiate polymerization. Under these circumstances, both the rate of polymerization and the average degree of polymerization are expected to decrease.

1.5 Polymer Microstructures

The characterization of polymer microstructures is essential to an understanding of the physical and chemical properties of polymeric materials. Most microstructures are determined during polymerization by factors such as the direction of monomer addition, stereochemical selection, initiation, termination, and chain transfer. Postpolymerization chemical modification also can give new features such as branches, grafts, crosslinks, and new functional groups.

The low-concentration microstructures may have significant effects on certain properties of polymer materials, such as stability and crystallinity. With the use of powerful modern spectroscopic analytical methods, the characterization of polymer microstructures has been extended to lower concentrations and to more complex moieties. The structures,

concentrations, and formation mechanisms of the microstructures are very important for an understanding of the mechanism-structure-property relationship which is crucial to the design of new materials, the improvement of properties, and the control of manufacturing processes.

CHAPTER 2

BACKGROUND

2.1 Possible Microstructures Formed via Chain Transfer of PVAc Radicals to Aromatic Solvents

2.1.1 Experimental Phenomena

Aromatic compounds have unique chemical and physical properties, and aromaticity usually is exemplified by cyclic conjugated molecules containing $(4n+2)$ π-electrons. The aromaticity of benzene was probed recently by the synthesis of elusive cyclohexatrienyl compounds and by quantum mechanical computations which led to the hypothesis that the σ electrons may play a role in aromaticity.[1-5]

The high reactivity of the propagating radical and the relatively low addition reactivity of the monomer lead to extensive chain transfer during the vinyl acetate polymerization. This type of process results in various microstructural defects, lower molecular weight, and some degree of retardation of the rate of polymerization. Extensive research has been done on PVAc microstructures such as hydrolyzable and nonhydrolyzable

branches,[6,7] structures formed by head-to-head addition,[8-11] structures resulting from chain transfer to monomer,[12,13] and chain ends.[14,15]

The solvents also function as chain transfer agents in solution polymerization. During the polymerization of VAc in aromatics (usually benzene), several phenomena have been observed:

(1) Addition of a small amount of benzene drastically reduces the polymerization rate without a significant decrease of molecular weight, in contrast to the results obtained in many aliphatic solvents.[16-21]

(2) The chain transfer constant is higher than would be expected if a strong sp^2 C–H bond were broken.[22]

(3) Carbon-14 labeling experiments show some evidence for the incorporation of benzene.[23-26]

(4) Proton NMR supports benzene-ring incorporation into the polymer chain;[19] yet ^{13}C NMR has provided no evidence for the presence of aromatic structures.[27]

(5) The electron spin resonance (ESR) spectrum recorded during the polymerization in chlorobenzene shows some additional hyperfine splittings when compared with the spectrum obtained during bulk polymerization.[28]

(6) The resultant polymers have fewer branch points than those prepared in ethyl acetate.[19]

(7) There is no solvent effect on the PVAc tacticity, according to ^{13}C NMR.[29]

(8) There is no isotope effect on k_p or k_t in deuterated benzene.[18]

2.1.2 Proposed Mechanisms

Several mechanisms have been proposed to describe the role of benzene in the chain transfer reactions.

(1) The general degradative chain transfer proceeds through hydrogen abstraction from benzene by the propagating macroradical. The resultant phenyl radical is highly reactive, so its most probable reaction is to initiate a new chain, forming chain end structure **AR-I**, rather than to couple with P• in order to form **AR-II** (Scheme 2 – 1).[19, 30, 31]

This mechanism can explain the possible incorporation of benzene into the polymer chain, but it cannot explain most of the other experimental phenomena.

(2) The second approach is the copolymerization theory, in which the propagating macroradical adds to benzene rather than abstracting one of the strongly bonded hydrogen atoms.[21, 32] The resultant cyclohexadienyl radical has lower reactivity and may react with monomer to form structure **CHD-I** or **AR-II**, or terminate to form structure **CHD-II** or **AR-II**. Structures **CHD-I** and **CHD-II** may be oxidized to aromatic structures **AR-III** and **AR-IV** (Scheme 2 – 2).

An alternative route of radical addition to benzene is by means of a hydrogen atom instead of via P•, in order to form a 2,5-cyclohexadienyl

radical and a terminal double bond, **DB-V**, followed by reactions to form structure **CHD-III** or **CHD-IV**, which may be oxidized to **AR-I** or **AR-II** (Scheme 2−3).[32]

The copolymerization theory may explain most of the experimental results, yet it also is debated by several groups because of the absence of any conclusive evidence for copolymerization with benzene.[23, 26, 33, 34]

(3) The theory of complex formation of the propagating radical with the aromatic solvent was proposed to explain the decrease of propagation rate:[20, 35−38]

$$P_n\cdot + S \overset{K_c}{\rightleftharpoons} (P_n\cdot S)_\pi$$

$$P_n\cdot + M \xrightarrow{k_{po}} P_{n+1}\cdot$$

K_c: stability constant of the complex;

k_{po}: true propagation rate constant which is independent of the medium for polymerization.

Kamachi assumed that the complex radical $(P_n\cdot S)_\pi$ is the predominant species but inactive for the propagation, and he concluded that the observed propagation rate constant is given by: $k_p = k_{po}/(1 + K_c[S])$.

This theory may explain most of the kinetic data but not the possible aromatic microstructures in the polymer chain.

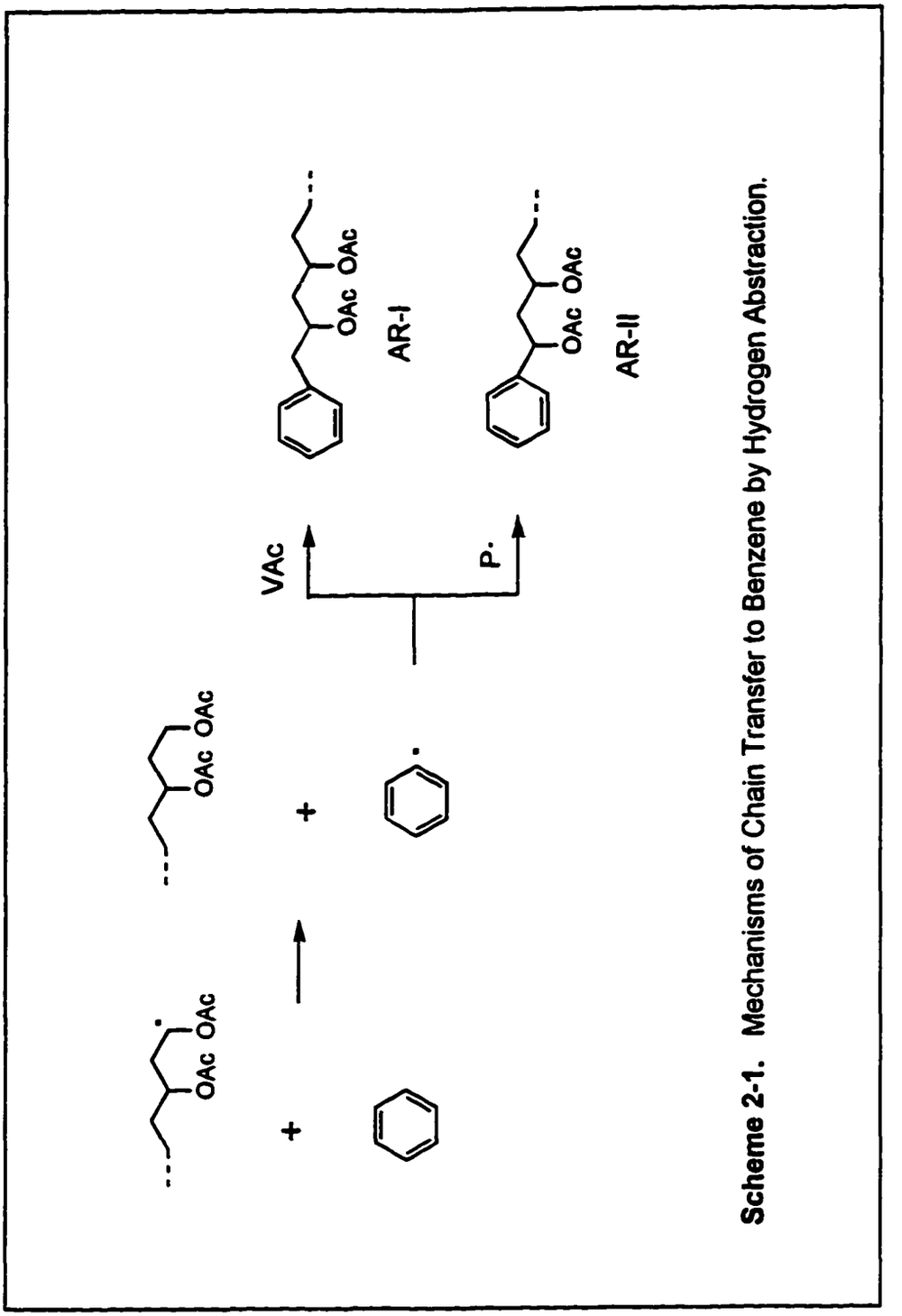

Scheme 2-1. Mechanisms of Chain Transfer to Benzene by Hydrogen Abstraction.

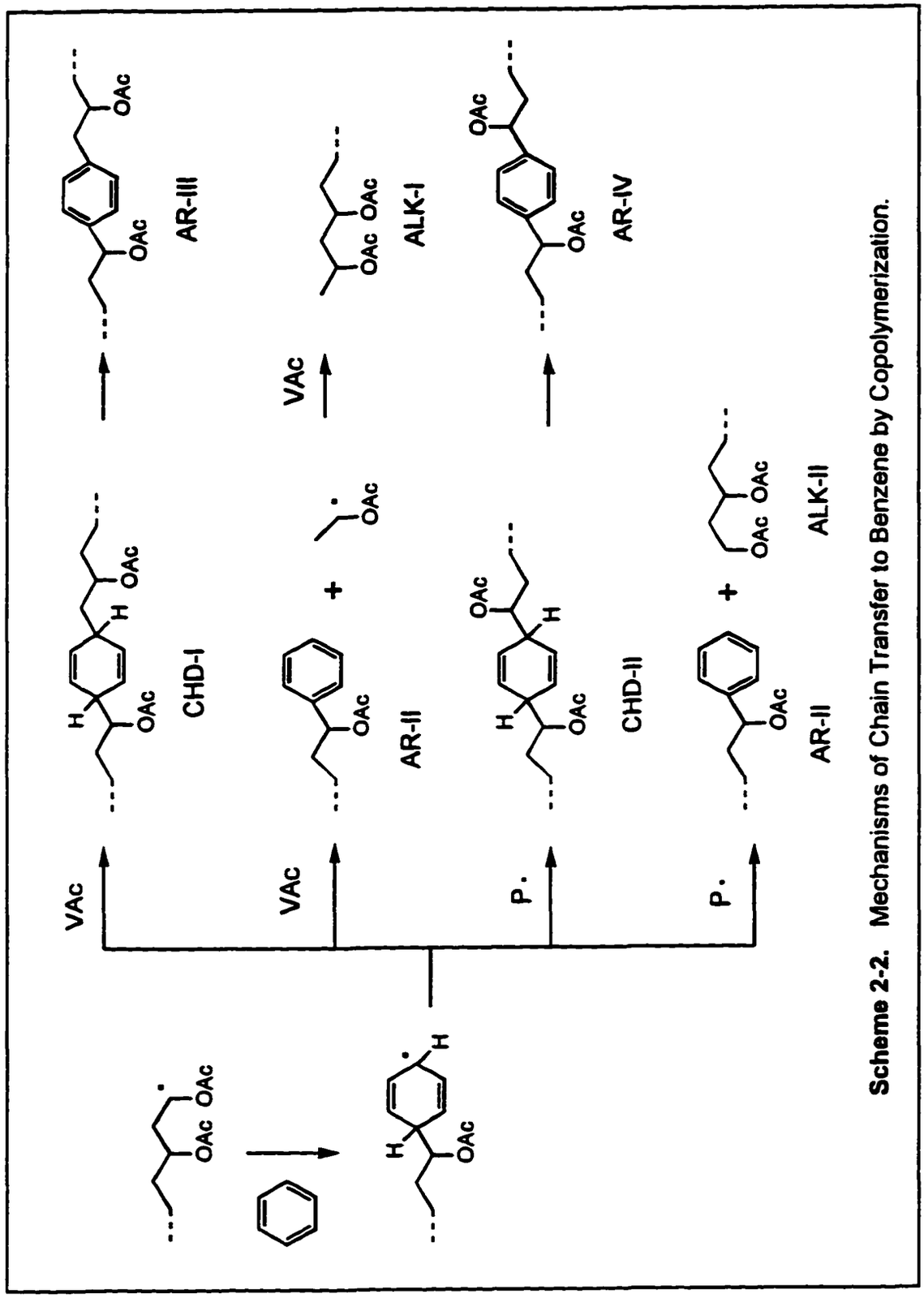

Scheme 2-2. Mechanisms of Chain Transfer to Benzene by Copolymerization.

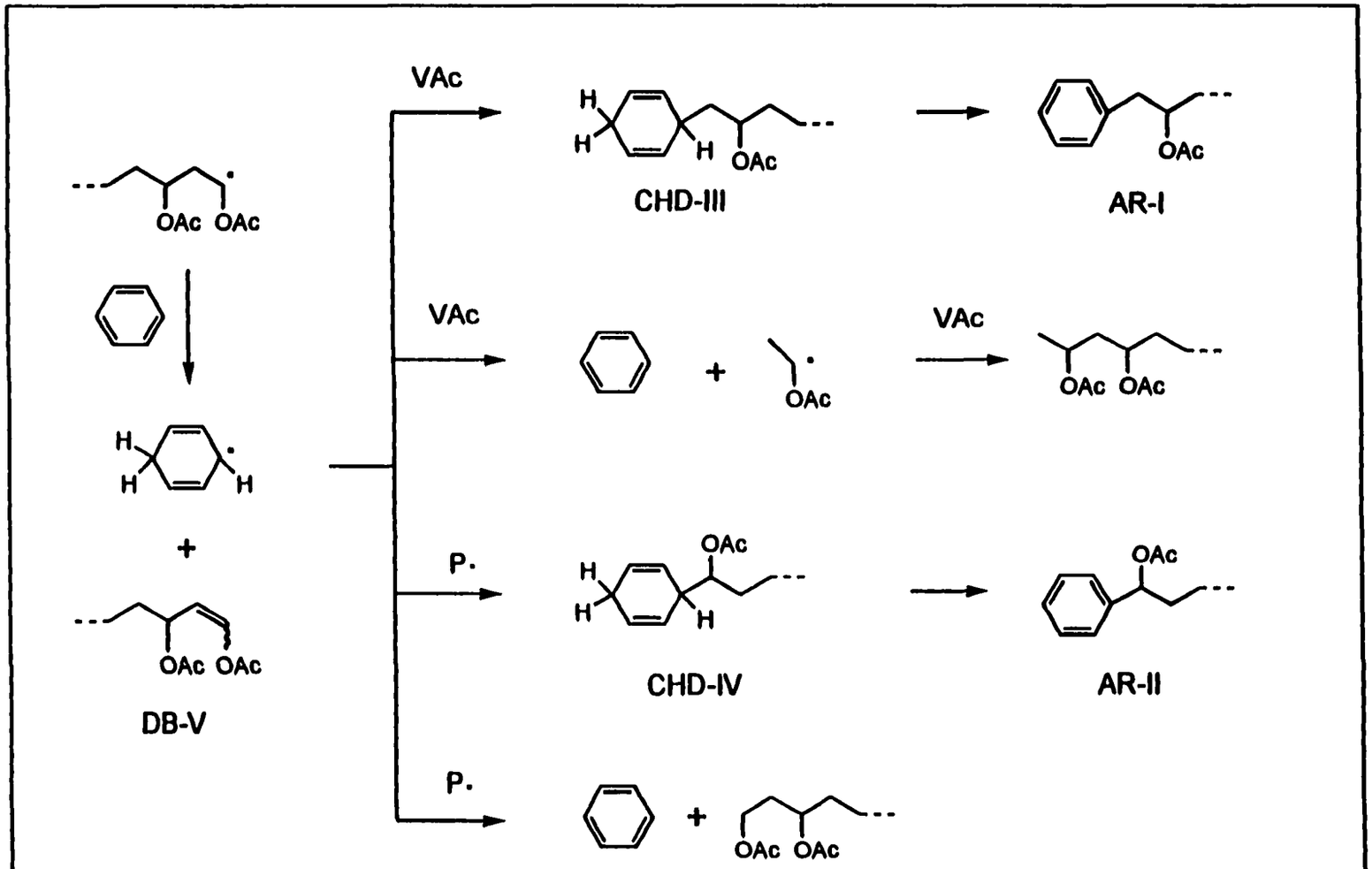

Scheme 2-3. Mechanisms of Chain Transfer to Benzene by Hydrogen Atom beta-Scission.

2.2 Microstructure of Alkene Groups

The ^{13}C NMR chemical shifts of alkene carbons are expected to be in the same region (100 – 150 ppm) as those of some of the carbons in the possible microstructures formed via chain transfer to benzene. Thus it is necessary to discuss the possible overlap of these peaks.

2.2.1 Degradation of PVAc

The internal double-bond moiety (DB-I) in PVAc may be formed through elimination of acetic acid along the polymer chain by thermal, photo–, or chemical degradation, or even during preparation and the purification process (Scheme 2 – 4). [39, 40]

Scheme 2 – 4

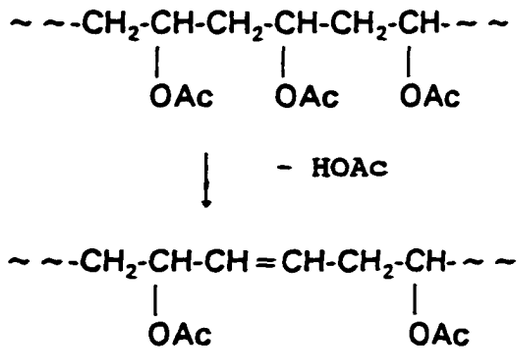

DB-I

2.2.2 Chain Transfer to Monomer

The chain transfer to monomer was shown to occur predominantly or exclusively by abstraction of a methyl hydrogen, followed by reinitiation by the transfer radical in order to form a structure (**DB-II**) containing a chain-end double bond (Scheme 2–5).[7, 27]

Scheme 2–5

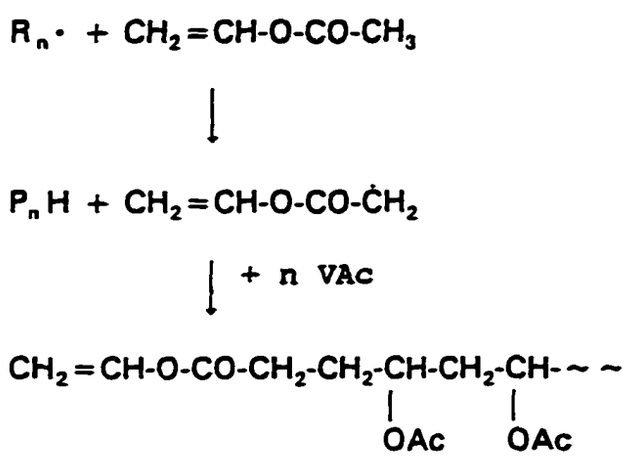

DB-II

The double-bond structures **DB-III** (conceivably formed via chain transfer to monomer by alkene-hydrogen abstraction) and **DB-IV** (conceivably formed via coupling of a transfer radical with a propagating macroradical) have not been detected.[27]

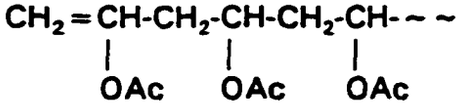

DB-III

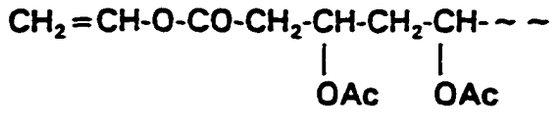

DB-IV

2.2.3 Termination

The propagating macroradicals may terminate through disproportionation to form one chain-end double-bond structure, **DB-V**, for every two polymer chains (Scheme 2-6).[41-43]

Scheme 2-6

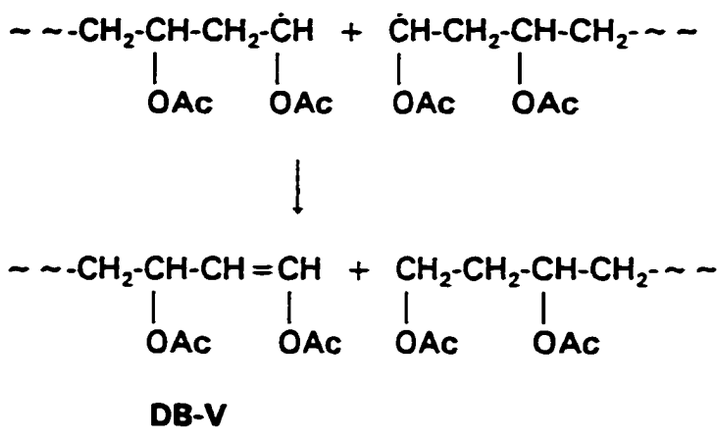

DB-V

2.2.4 Head-to-Head Addition

The double-bond structure **DB-VI** may be formed by head-to-head addition, followed by a 1,2 acyloxy shift and subsequent β-scission of an acetoxy radical (Scheme 2-7).[44, 45]

Scheme 2 – 7

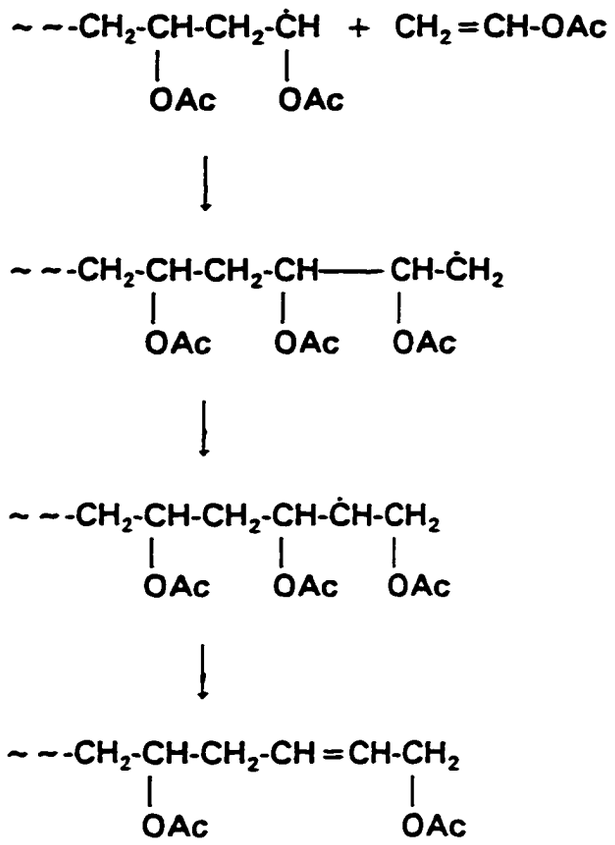

DB – VI

2.3 Model Compounds

A model compound, illustrated as follows, is a low-molecular-weight organic molecule that contains a structure that is similar to a part of polymer chain:

$$\sim\sim\text{-}(M)_x\text{-}(M)_a - Q - (M)_b\text{-}(M)_y\text{-}\sim\sim$$

Polymer Structure

$$R^{I}\text{-}(M)_a - Q - (M)_b\text{-}R^{II}$$

Model Compound

Q: Microstructure of interest, such as an n-ad, or a chain end;

M: Adjacent monomer unit, where a, b = 0−4;

M: Repeating monomer unit;

R^{I}, R^{II}: Usually linear alkyl groups.

By studying the structure and properties of the model compound, one may predict those of the modeled part of the polymer. This approach has been successfully applied in the investigation of stereoregularities, microstructural defects, chemical-shift assignments, and the chemical reactivities of functional groups (kinetics of polymerization and thermal degradation).

The accuracy of the prediction depends on the properties of interest and the degree of similarity of the model and the polymer structure. The ^{13}C NMR chemical shifts generally are sensitive to the presence of atoms in the α, β, γ, and δ positions, so one may expect the accuracy of the chemical shifts of microstructure Q to be within 0.2−0.3 ppm when the model compound $R^{I}\text{-}(M)_a - Q - (M)_b\text{-}R^{II}$ (a, b $\geq$ 2 for vinyl polymers) is used.

2.4 Chemical Modification of Polymers

Even though the reactivity of functional groups in polymers may be almost entirely independent of molecular size, the polymer reactions can have some complexities. A linear polymer chain generally is present in a random coil conformation in thermodynamically good solvents at very high dilutions. The concentration of functional groups is high within the polymer coils and near zero on the outside of them. The observed overall reaction rate is an average of the rates inside and outside the polymer coils. Kinetic effects also may come from additional steric effects, neighboring-group effects, and hydrophobic or hydrophilic interactions.

The side reactions of polymer modification have to be carefully considered, since the main products and byproducts may be present on the same macromolecule and thus cannot be separated by the usual separation processes. The complete transformation of a polymer into a derivative of equivalent molecular weight has been successful only in a few systems. One commercially successful example is the manufacture of PVA by hydrolysis of PVAc. A successful non-commercial example is the dechlorination of poly(vinyl chloride) (PVC) to polyethylene by tributyltin hydride, a process which has been particularly useful in elucidating the microstructures of PVC.[46-48]

Many other polymer reactions also are very useful for various reasons. Such reactions include graft copolymerization, block copolymerization, cross-linking, the formation of ion exchange resins, the use of polymers as

reagents and catalysts, Merrifield solid phase polypeptide synthesis, the esterification of cellulose, the synthesis of polyacetylene via a retro Diels-Alder reaction,[49, 50] and surface modifications.

2.5 Nuclear Magnetic Resonance (NMR) Spectroscopy

Nuclei with a 1/2 magnetic spin angular momentum (^{1}H, ^{13}C) in a homogeneous magnetic field, B_o, will partition between two states. For B_o = 7.0 T (1 T = 1 tesla = 10 kilogauss), the resonant frequencies of ^{1}H and ^{13}C are about 300 and 75 MHz, respectively.

The characteristic resonant frequency of a nucleus also depends upon the chemical and structural environment. The actual local field, B_{loc}, experienced by a nucleus is $B_{loc} = B_o(1 - \sigma)$, where σ is the screening constant. This constant is independent of B_o, yet sensitive to chemical environment, a property which makes NMR a powerful tool for chemists.

The resonance frequencies of nuclei are practically expressed in parts per million (ppm) relative to changes in B_o. The chemical shifts (δ's) are referred to an arbitrary reference substance (δ = 0), and tetramethylsilane (TMS) is used as such for ^{1}H and ^{13}C NMR spectroscopy.

The instrumental insensitivity of the ^{13}C nucleus is due to the low natural abundance of only 1.1% (vs. 99% for ^{1}H) and small magnetic moment (about 1/4 that of ^{1}H). Modern FT NMR makes it possible, however, to obtain ^{13}C spectra with suitable signal/noise ratios within

acceptable periods of time.

The principal advantage of ^{13}C NMR spectroscopy is the high sensitivity of the chemical shifts to local molecular structures, within a range of *ca.* 200 ppm (vs. *ca.* 10 ppm for ^{1}H). For this reason, ^{13}C NMR has become the method of choice for probing the microstructures of polymer chains.[51]

2.6 Objectives

The major objectives of the research described in this thesis were to identify various PVAc microstructures and to determine their mechanisms of formation.

Samples of PVAc were prepared by solution polymerization under conditions which would increase the concentrations of the possible microstructures formed via chain transfer to benzene. High resolution solution ^{13}C NMR was the primary tool for the detection of such structures, and a series of model compounds was obtained by multi-step syntheses in order to aid in the chemical-shift assignments. The expected concentrations of the structures were estimated from reported kinetic data and compared with those deduced from NMR spectra.

The characterization of the polymer microstructures contributed to an understanding of the mechanism of chain transfer to benzene during the free-radical polymerization of vinyl acetate.

CHAPTER 3

EXPERIMENTAL

3.1 Solution Polymerization of Vinyl Acetate in Benzene

3.1.1 Materials

(1) Vinyl acetate, $CH_3CO_2CH=CH_2$, V150-3, 99+%, bp 72−73 °C, Aldrich Chemical Company, Inc.

(2) Sodium bisulfite (sodium hydrogen sulfite), $NaHSO_3$, 24,397-3, Aldrich Chemical Company, Inc.

(3) Hydroxylamine hydrochloride, $H_2NOH \cdot HCl$, 15,941-7, 99%, Aldrich Chemical Company, Inc.

(4) Calcium chloride, $CaCl_2$, 22,231-3, 40 mesh, Aldrich Chemical Company, Inc.

(5) 2,2'-Azobis(isobutyronitrile) (AIBN) (2,2'-azobis-2-methylpropionitrile), $(CH_3)_2C(CN)N=NC(CH_3)_2CN$, A37,050, 98%, Pfaltz and Bauer, Inc., purified by recrystallization from methanol (mp 105−106 °C).

(6) Benzene, C_6H_6, 27,070-9, 99.9+%, HPLC grade, bp 80 °C, Aldrich Chemical Company, Inc.

(7) *n*-Hexane, $CH_3(CH_2)_4CH_3$, H303-4, Optima™, bp 68 – 72 °C, Fisher Scientific Co.

(8) Acetone, CH_3COCH_3, 27072-5, 99.9 + %, HPLC grade, bp 56 °C, Aldrich Chemical Company, Inc.

(9) Chloroform-*d*, $CDCl_3$, 15,185-8, 100 atom% *d*, bp 60.9 °C, Aldrich Chemical Company, Inc.

(10) Tetramethylsilane (TMS), $(CH_3)_4Si$, T2,400-7, 99.9%, NMR grade, bp 26 – 28 °C, Aldrich Chemical Company, Inc.

(11) Nitrogen, compressed gas, N_2, industrial grade, 99.998 vol. %, max. O_2 10.0 ppm (v/v), H_2O 3.5 ppm (v/v), Air Products and Chemicals, Inc.

3.1.2 Polymerization of Vinyl Acetate in Benzene

The commercially available vinyl acetate (VAc) was purified by the following procedure to remove impurities which might affect the polymerization process.[1, 2] The vinyl acetate was washed successively with 5% aqueous $NaHSO_3$, 5% aqueous $H_2NOH \cdot HCl$, and water, then dried with $CaCl_2$ overnight. The monomer was distilled through a 13-cm Vigreux column and prepolymerized by refluxing with AIBN (*ca.* 2 mg per 100 mL of VAc) for several minutes; then it was distilled again through the Vigreux column under a nitrogen atmosphere. The fraction boiling at 72 – 73 °C was collected.

Poly(vinyl acetate) samples were prepared by solution polymerization of vinyl acetate in benzene under a nitrogen atmosphere.[3,4] Benzene (96.4, 482, 964, or 1446 mL) was heated under reflux in a three-neck flask equipped with a magnetic stirrer, a reflux condenser, an addition funnel, and a pipet for bubbling nitrogen beneath the liquid surface. After nitrogen had been introduced for 10 min, a solution of AIBN (24.0, 87.2, 166.2, or 245.2 mg) in freshly distilled vinyl acetate (50.0 mL) was added during 2 min. The reflux was maintained for 2–4 h to reach the conversion of around 5%.

The solution was cooled to room temperature, concentrated under vacuum, and precipitated into 1 L of *n*-hexane. The resulting polymer was purified by successive precipitations from acetone solutions into *n*-hexane, water, and *n*-hexane. A polymer film deposited from an acetone solution was dried in a vacuum oven (*ca.* 2 torr) at 60 °C for 4 days.

3.1.3 Molecular Weight Measurements

Molecular weights of the poly(vinyl acetate) samples were determined by an intrinsic viscosity method.[5,6] Viscosities of the acetone solvent and polymer solutions (0.2–1.5 g/dL) were determined at 30 ± 0.1 °C with an Ubbelohde viscometer. The intrinsic viscosity was obtained by least–square linear extrapolation of η_{sp}/C versus C, where η_{sp} is specific viscosity and C is the polymer concentration in grams per deciliter.

3.1.4 Oxidation of Poly(vinyl acetate)

A procedure for oxidation of cyclohexadiene was modified for the polymer reaction.[7,8] A solution of poly(vinyl acetate) (1.0 g) and AIBN (10 mg) in benzene (30 mL) was placed in a three-neck flask equipped with a magnetic stirrer, a reflux condenser, a thermometer, and a pipet for bubbling oxygen beneath the liquid surface. The solution was heated under reflux for 20 h in purging oxygen, then cooled to room temperature and concentrated under vacuum. The polymer was purified by successive precipitations from acetone solutions into *n*-hexane, water, and *n*-hexane. A polymer film deposited from an acetone solution was dried in a vacuum oven (*ca.* 2 torr) at 60 °C for 4 days.

3.1.5 Carbon-13 NMR Spectroscopy

The proton-decoupled 75.57 MHz ^{13}C NMR spectra of the poly(vinyl acetate) samples were obtained on a General Electric QE 300 FT-NMR spectrometer, at ambient temperature and with a sweep width of 10,000 Hz. At least 20K transients were accumulated. The pulse angle was 30 – 60 °, and the delay time was 5 – 10 s. The solution concentrations were 10 – 20 wt % in $CDCl_3$, and TMS (Me_4Si) was used as internal reference.[9,10]

Similar conditions were used to obtain 125.76 MHz ^{13}C NMR spectra on a Bruker WH 500 FT-NMR spectrometer. These spectra were recorded by Dr. G. M. Benedikt of the B. F. Goodrich Company.

3.2 Model Compounds for Possible Microstructures Formed via Chain Transfer to Benzene

3.2.1 Materials

(1) Hexylmagnesium bromide, $CH_3(CH_2)_4CH_2MgBr$, 25,502-5, 2.0 M solution in diethyl ether, Aldrich Chemical Company, Inc.

(2) Hydrocinnamaldehyde, $C_6H_5CH_2CH_2CHO$, 39,319-3, tech., 90%, bp 97 – 98 °C/12mm, Aldrich Chemical Company, Inc.

(3) Magnesium sulfate, $MgSO_4$, M65-500, anhydrous, Fisher Scientific Co.

(4) Acetic anhydride, $(CH_3CO)_2O$, 32,010-2, 99 + %, bp 138 – 140 °C, Aldrich Chemical Company, Inc.

(5) Pyridine, C_5H_5N, 27,097-0, anhydrous, 99.8%, bp 115 °C, Aldrich Chemical Company, Inc.

(6) (Methoxymethyl)triphenylphosphonium chloride, $[CH_3OCH_2P(C_6H_5)_3]^+Cl^-$, 30,956-7, 97%, mp 178 – 185 °C, Aldrich Chemical Company, Inc.

(7) Phenyllithium, C_6H_5Li, 22,102-3, 1.8 M solution in cyclohexane/ether (70/30), Aldrich Chemical Company, Inc.

(8) Mercury(II) acetate (mercuric acetate), $(CH_3CO_2)_2Hg$, 17,610-9, 98 + %, mp 179 – 182 °C, Aldrich Chemical Company, Inc.

(9) Tetrahydrofuran (THF), C_4H_8O, 18,656-2, anhydrous, 99.9 + %, bp 65 – 67 °C, Aldrich Chemical Company, Inc.

(10) Potassium iodide, KI, 22,194-5, 99+%, Aldrich Chemical Company, Inc.

(11) Dichloromethane, CH_2Cl_2, D6,510-0, 99.6%, bp 40 °C, Aldrich Chemical Company, Inc.

(12) 1-Benzoylacetone (1-phenyl-1,3-butanedione), $C_6H_5COCH_2COCH_3$, B1,190-7, 99%, mp 58–60 °C, Aldrich Chemical Company, Inc.

(13) Sodium borohydride (sodium tetrahydriborate), $NaBH_4$, 34,772-8, granules, 10–40 mesh, 98%, Aldrich Chemical Company, Inc.

(14) Sodium hydride, NaH, 19,923-0, 60% dispersion in mineral oil, Aldrich Chemical Company, Inc.

(15) Ethylene glycol dimethyl ether (1,2-dimethoxyethane, monoglyme), $CH_3OCH_2CH_2OCH_3$, 27,952-7, anhydrous, 99.5%, bp 85 °C, Aldrich Chemical Company, Inc.

(16) Methyl benzoate, $C_6H_5CO_2CH_3$, M2,990-8, 99%, bp 198–199 °C, Aldrich Chemical Company, Inc.

(17) 2,4-Pentanedione (acetylacetone), $CH_3COCH_2COCH_3$, P775-4, 99+%, bp 140 °C, Aldrich Chemical Company, Inc.

(18) 1-Phenyl-2,4-pentanedione, $C_6H_5CH_2COCH_2COCH_3$, P14,130, 95%, bp 142–145 °C/15 mm, Pfaltz and Bauer, Inc.

(19) Terephthalaldehyde (terephthaldicarboxaldehyde), C_6H_4-1,4-$(CHO)_2$, T220-7, 99%, mp 115–116 °C, Aldrich Chemical Company, Inc.

(20) Terephthalaldehyde *mono*(diethyl acetal) [4-(diethoxymethyl)-

benzaldehyde], *p*-CHO-C_6H_4-$CH(OC_2H_5)_2$, 27,486-0, 97%, Aldrich Chemical Company, Inc.

(21) 1,1,1,3,3,3-Hexamethyldisilazane, $(CH_3)_3SiNHSi(CH_3)_3$, 37,921-2, 99.9%, bp 125 °C, Aldrich Chemical Company, Inc.

(22) Trimethylchlorosilane (chlorotrimethylsilane), $(CH_3)_3SiCl$, C7,285-4, 98%, bp 57 °C, Aldrich Chemical Company, Inc.

(23) Nitrogen, compressed gas, N_2, industrial grade, 99.998 vol. %, max. O_2 10.0 ppm (v/v), H_2O 3.5 ppm (v/v), Air Products and Chemicals, Inc.

(24) Silica gel, S744-1, 100-200 mesh, 150 Å pore size, Fisher Scientific Co.

3.2.2 NMR and GC/MS Measurements

The 75 MHz ^{13}C and 300 MHz ^{1}H NMR spectra were obtained on a GE QE 300 FT-NMR spectrometer with *ca.* 10 wt % solutions in $CDCl_3$ and TMS as internal reference.

The (gas chromatography)–(mass spectroscopy) (GC/MS) measurements were performed on a Hewlett-Packard HP 5890A/5988A or HP 5890/5971A apparatus equipped with a fused-silica capillary GC column. The mass spectrometer operated in total ion concentration (TIC) mode. Helium was used as the carrier gas, and the heating rate was 5 – 20 °C/min.

3.2.3 Synthesis of γ-Acetoxynonylbenzene

General scheme 3 – 1

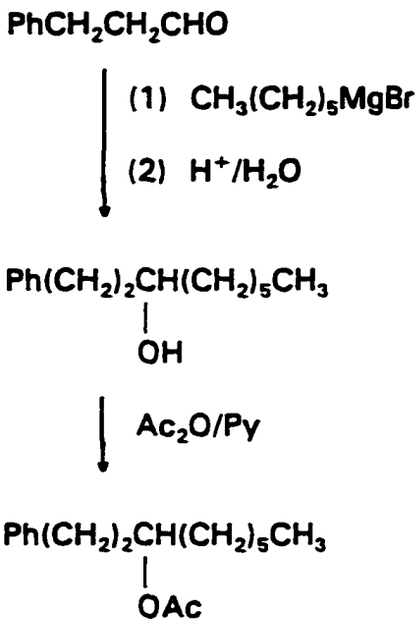

(i) Grignard Reaction

A Grignard reaction was used to make the desired alcohol from the aldehyde.[11] Under a nitrogen atmosphere, a solution of hydrocinnamaldehyde (6.7 g, 50 mmol) in 50 mL of anhydrous ether was added dropwise at about 5 °C to a stirred solution of 60 mmol of hexylmagnesium bromide in 100 mL of ether contained in a three-neck flask that was equipped with a reflux condenser, a dropping funnel, and a nitrogen inlet tube. The mixture was heated under reflux for 1 h, cooled to room temperature, diluted with 100 mL of ether, and decomposed with 200

mL of cold 2% aqueous sulfuric acid.

The ether layer was separated, combined with 2 x 50 mL of ether extracts of the aqueous layer, washed with 4 x 150 mL of water, dried with anhydrous magnesium sulfate, and concentrated under vacuum. Short path distillation of the residue under reduced pressure gave 8.8 g (80% yield) of *γ*-hydroxynonylbenzene (95% purity by GC/MS), bp 158–161 °C (10 torr); mass spectrum (Fig. 3–1), m/e(%): 220 (0.6, $M^{\cdot+}$), 202 (11), 117 (28), 104 (57), 91 (100), 65 (17), 43 (26), 41 (30), and 29 (21); ^{13}C NMR (75.57 MHz, $CDCl_3$) (Fig. 3–2) δ 142.30, 128.40, 128.34, 125.72, 71.25, 39.11, 37.60, 32.10, 31.88, 29.42, 25.65, 22.65, and 14.10 ppm.

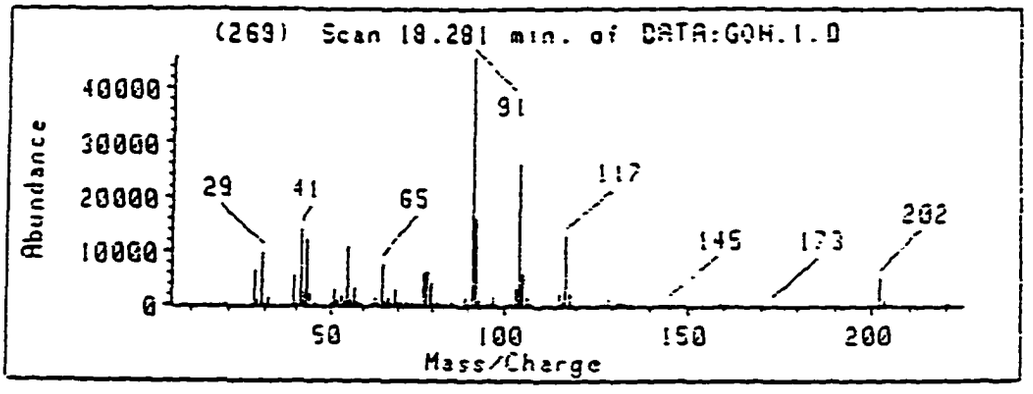

Figure 3–1. Mass spectrum of *γ*-hydroxynonylbenzene.

(ii) Acetylation

The acetylation reagents used were acetic anhydride and pyridine.[12]

A solution of γ-hydroxynonylbenzene (6.6 g, 30 mmol) in 50 mL of ether was added to 60 mL of acetic anhydride/pyridine (1/2, v/v). The solution was stirred at about 35 °C for 8 h in flowing nitrogen, then cooled to room temperature and diluted with 200 mL of ether. The ether layer was separated, washed with 4 x 100 mL of water, dried over anhydrous magnesium sulfate, and concentrated under vacuum. Short path distillation of the residue under reduced pressure gave 7.0 g (90% yield) of γ-acetoxynonylbenzene (90% purity by GC/MS), bp 165 – 168 °C (10 torr); mass spectrum (Fig. 3 – 3), m/e (%): 202 (22), 117 (43), 104 (100), 91 (60), 43 (74), and 29 (8); ^{13}C NMR (75.57 MHz, $CDCl_3$) (Fig. 3 – 4) δ 170.81, 141.75, 128.39, 128.31, 125.88, 74.01, 35.84, 34.21, 31.83, 31.74, 29.19, 25.22, 22.58, 21.18, and 14.04 ppm.

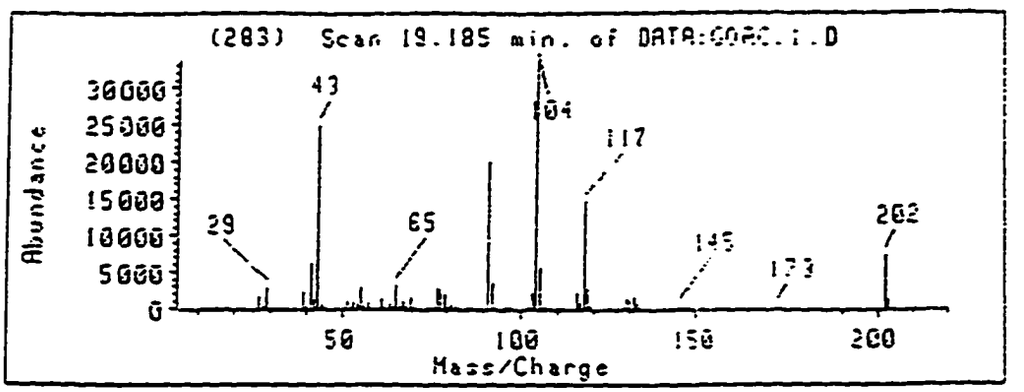

Figure 3 – 3. Mass spectrum of γ-acetoxynonylbenzene.

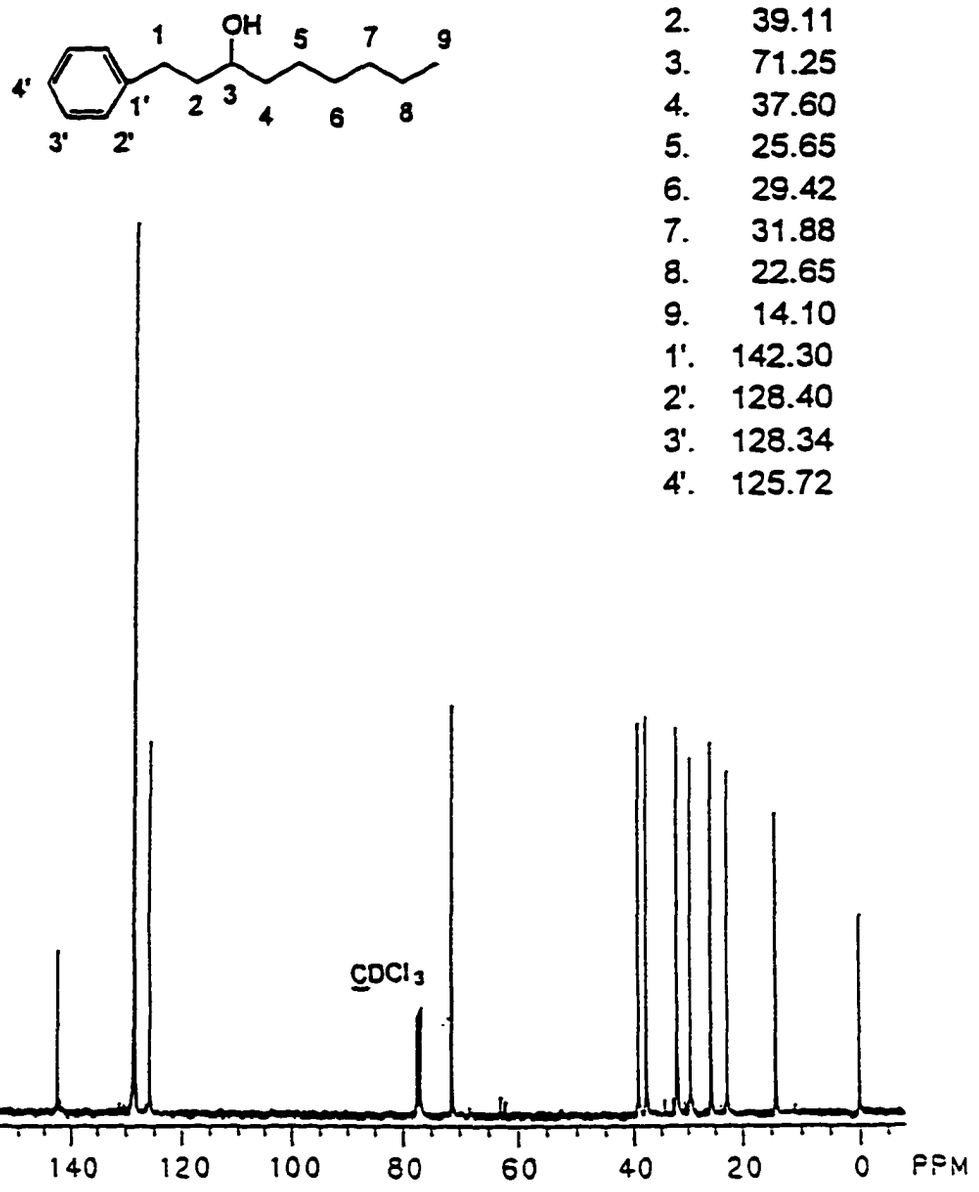

Figure 3-2. Carbon-13 NMR spectrum (75.57 MHz) and peak assignments of gamma-hydroxynonylbenzene.

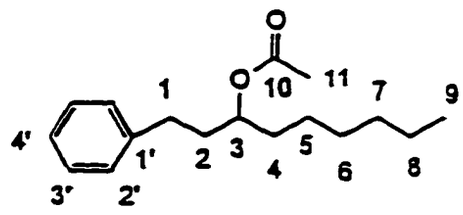

1.	31.83
2.	35.84
3.	74.01
4.	34.21
5.	25.22
6.	29.19
7.	31.74
8.	22.58
9.	14.04
10.	170.81
11.	21.18
1'.	141.75
2'.	128.39
3'.	128.31
4'.	125.88

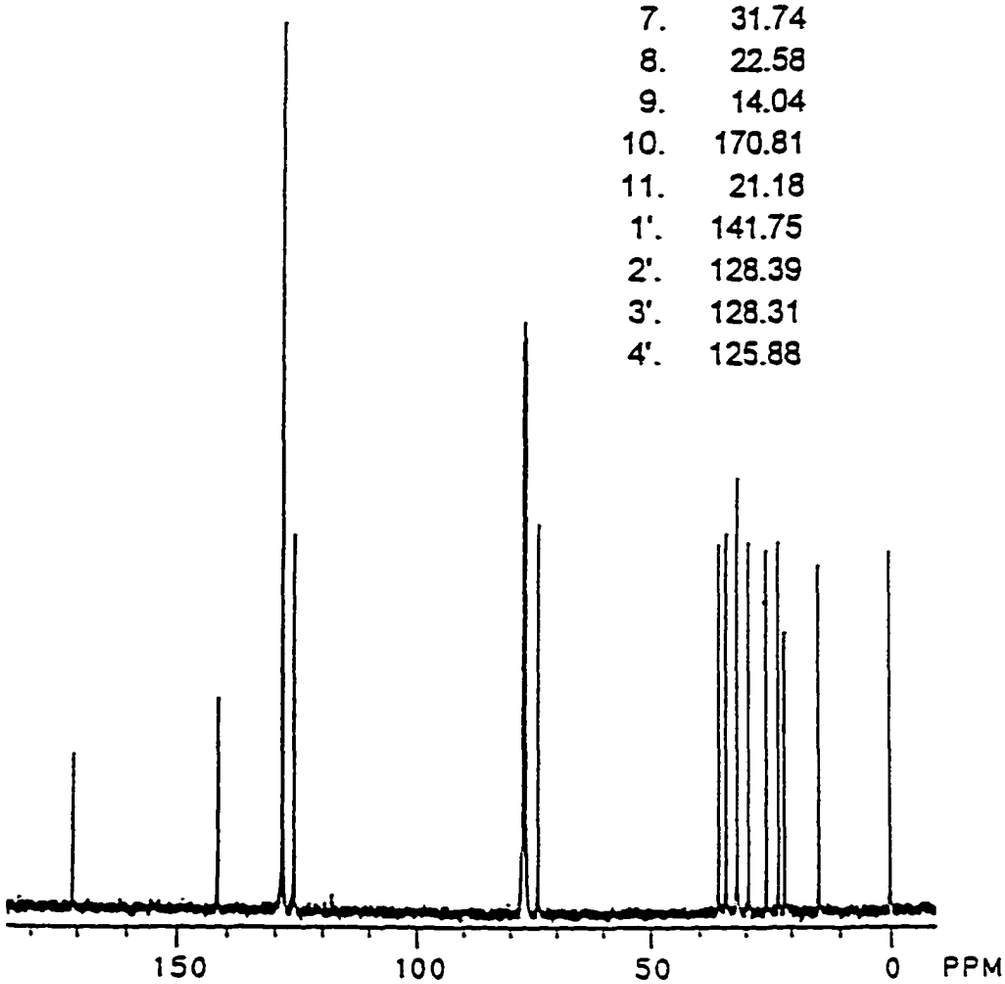

Figure 3-4. Carbon-13 NMR spectrum (75.57 MHz) and peak assignments of gamma-acetoxynonylbenzene.

3.2.4 Synthesis of δ-Acetoxydecylbenzene

General scheme 3 – 2

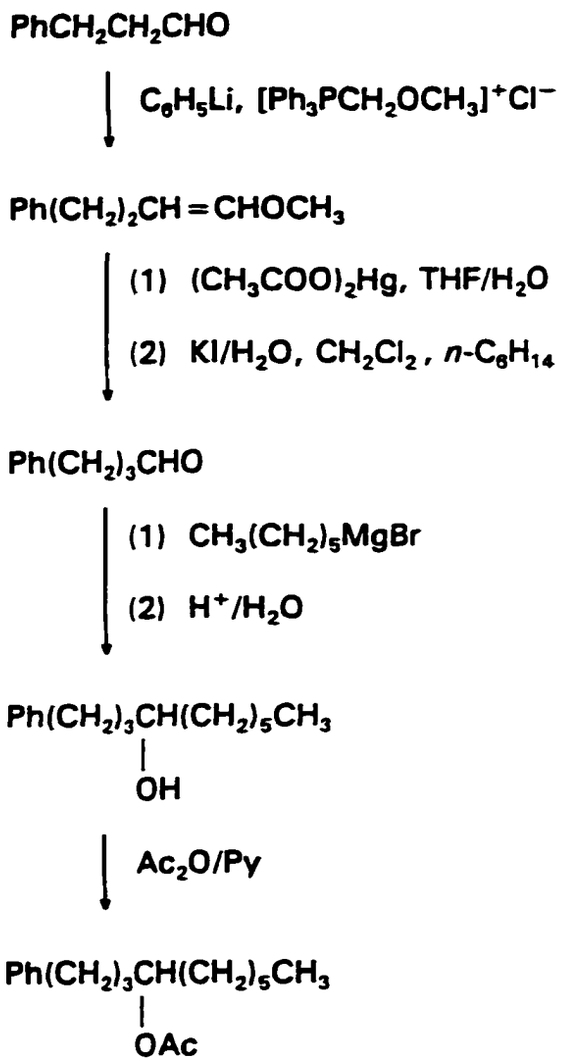

(i) Wittig Reaction

A Wittig reaction was used to extend the carbon skeleton.[13, 14] Under a nitrogen atmosphere, a solution of phenyllithium (50 mmol) in cyclohexane/ether (70/30) was added dropwise at about 0 °C to a stirred suspension of finely powdered (methoxymethyl)triphenylphosphonium chloride (17.7 g, 50 mmol) in 250 mL of anhydrous ether contained in a three-neck flask. The mixture was kept at 0 °C for 1 h and at room temperature for 1/2 h. After dropwise addition of a solution of hydrocinnamaldehyde (4.70 g, 35 mmol) in 50 mL of anhydrous ether, the mixture was stirred at room temperature for 1/2 h to complete the reaction. The ether solution was separated by suction filtration, washed with 4 x 100 mL of water, dried over anhydrous magnesium sulfate, and concentrated under vacuum. Short path distillation of the residue under reduced pressure gave 4.2 g (74% yield) of 1-methoxy-4-phenyl-1-butene (70% purity by GC/MS), bp 125 – 128 °C (10 torr); mass spectrum (Fig. 3 – 5), m/e (%): 162 (20, $M\cdot^{+}$), 115 (8), 91 (24), 71 (100), 65 (10), and 41 (37).

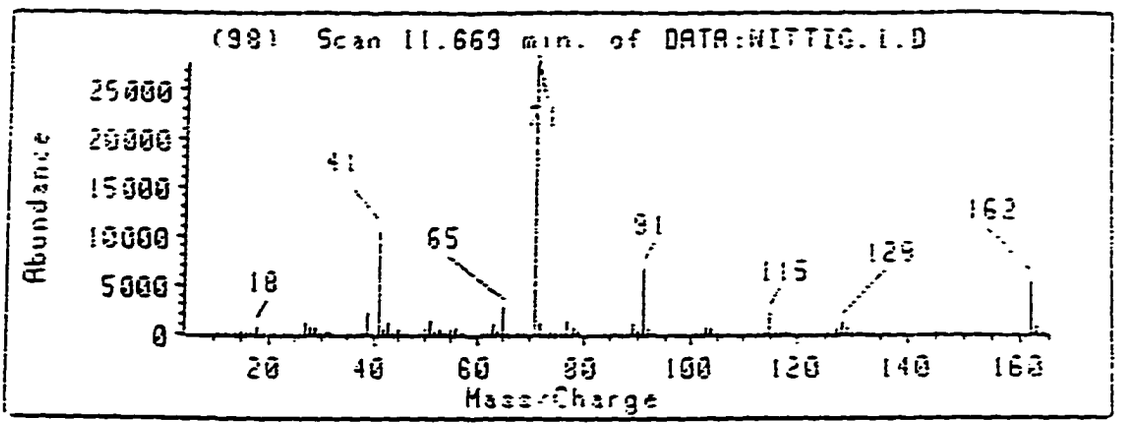

Figure 3 – 5. Mass spectrum of 1-methoxy-4-phenyl-1-butene.

(ii) Hydrolysis of the Enol Ether

The neutral hydrolysis was performed with mercuric acetate.[15] A solution of the above enol ether (2.42 g, 15 mmol) and mercuric acetate (14.2 g, 45 mmol) in 275 mL of THF/H_2O (10/1, v/v) was heated under reflux for 1/2 h. A saturated aqueous solution of potassium iodide (50 mL) was added, and reflux was maintained for 2 h. The reaction mixture was cooled to room temperature and extracted with 3 x 200 mL of CH_2Cl_2; then the combined extracts were concentrated under vacuum. The partially solid residue was extracted with 3 x 150 mL of *n*-hexane, and the combined extracts were concentrated under vacuum. Short path distillation of the residue under reduced pressure gave 1.95 g (88% yield) of 4-phenylbutanal (70% purity by GC/MS), bp 105 – 107 °C (10 torr) [lit.[16] bp 129 – 130 (17

torr)]; mass spectrum (Fig. 3–6), m/e (%): 148 (9, $M^{\cdot+}$), 115 (8), 104 (100), 91 (75), 65 (30), 51 (14), and 39 (18).

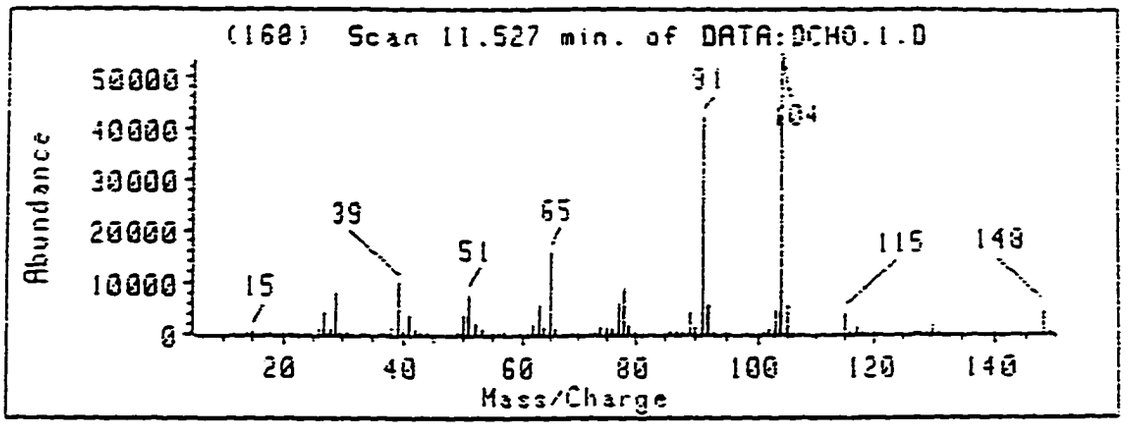

Figure 3–6. Mass spectrum of 4-phenylbutanal.

(iii) Grignard Reaction

Under a nitrogen atmosphere, a solution of 4-phenylbutanal (1.3 mL, 10 mmol) in 50 mL of anhydrous ether was added dropwise at about 5 °C to a stirred solution of hexylmagnesium bromide (20 mmol) in 100 mL of ether contained in a three-neck flask. The mixture was heated under reflux for 1 h, cooled to room temperature, diluted with 250 mL of ether, and decomposed with 300 mL of cold 2% aqueous sulfuric acid. The ether layer was separated, combined with 2 x 50 mL of ether extracts of the aqueous layer, washed with 4 x 150 mL of water, dried with anhydrous magnesium sulfate, and concentrated under vacuum. Short path distillation of the

residue under reduced pressure gave 1.3 g (55% yield) of δ-hydroxydecylbenzene (85% purity by GC/MS), bp 168 – 171 °C (10 torr); mass spectrum (Fig. 3 – 7), m/e(%): 216 (1.5), 131 (13), 104 (100), 91 (43), 65 (10), 55 (20), 43 (21), 41 (23), and 29 (15).

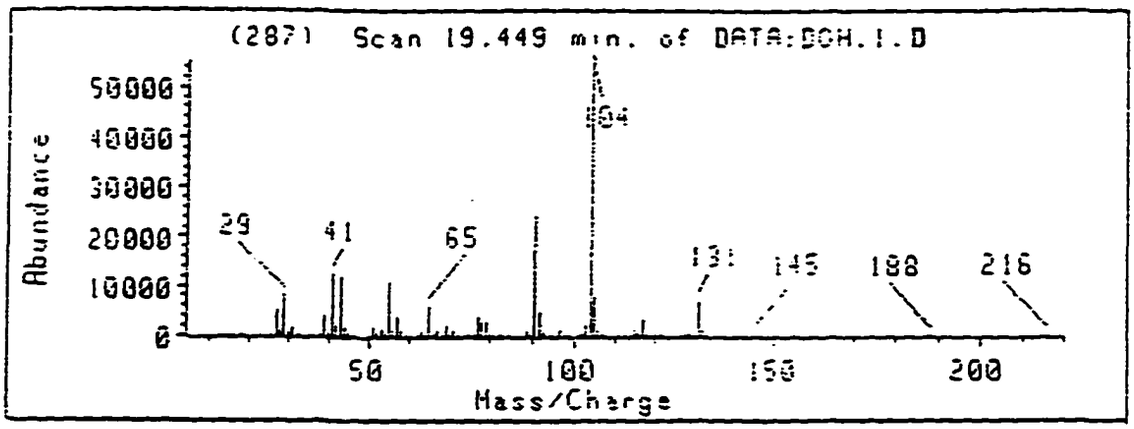

Figure 3 – 7. Mass spectrum of δ-hydroxydecylbenzene.

(iv) Acetylation

A solution of δ-hydroxydecylbenzene (1.5 g, 6.4 mmol) in 50 mL of ether was added to 60 mL of acetic anhydride/pyridine (1/2, v/v). The solution was stirred at about 35 °C for 8 h in flowing nitrogen, cooled to room temperature, and diluted with 200 mL of ether. The ether layer was separated, washed with 4 x 100 mL of water, dried over anhydrous magnesium sulfate, and concentrated under vacuum. Short path distillation of the residue under reduced pressure gave 1.3 g (74% yield) of δ-

acetoxydecylbenzene (90% purity by GC/MS), bp 176–179 °C (10 torr); mass spectrum (Fig. 3–8), m/e(%): 276 (0.1, $M\cdot^+$), 216 (7), 131 (6), 117 (8), 104 (100), 91 (40), 43 (42), and 41 (8); ^{13}C NMR (75.57 MHz, $CDCl_3$) (Fig. 3–9) δ 170.84, 142.17, 128.37, 128.31, 125.77, 74.10, 35.72, 34.16, 33.73, 31.74, 29.18, 27.14, 25.27, 22.58, 21.23, and 14.05 ppm.

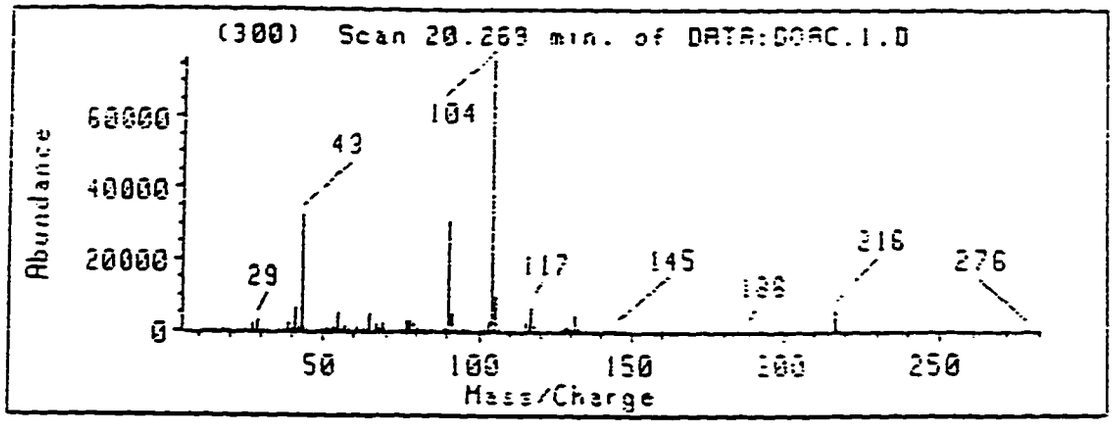

Figure 3–8. Mass spectrum of δ-acetoxydecylbenzene.

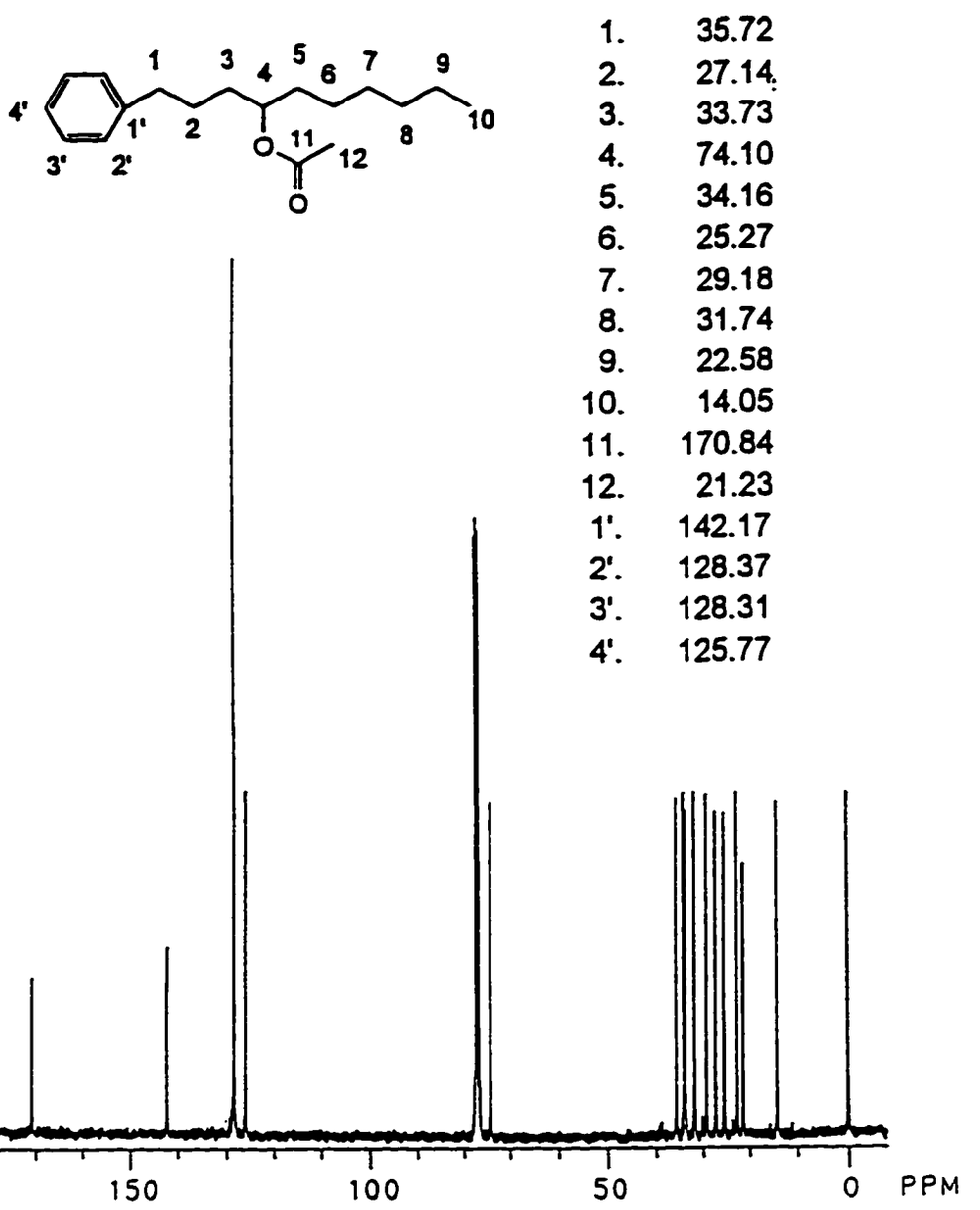

Figure 3-9. Carbon-13 NMR spectrum (75.57 MHz) and peak assignments of delta-acetoxydecylbenzene.

3.2.5 Synthesis of 1-Phenyl-1,3-diacetoxybutane

General scheme 3 – 3

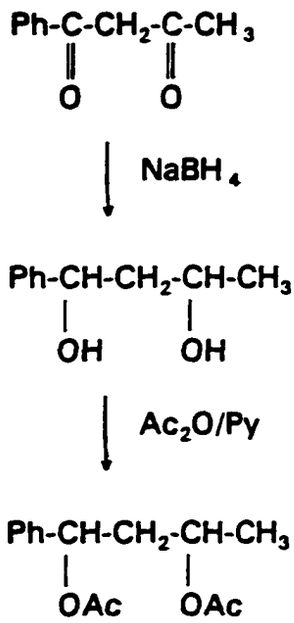

(i) Reduction

The reduction was done with borohydride under mild conditions.[16] A solution of sodium borohydride (4.0 g, 125 mmol) and sodium hydroxide (1.0 g) in 200 mL of water was added dropwise at about 10 °C to a stirred solution of 1-phenyl-1,3-butanedione (4.86 g, 30 mmol) in 200 mL of ethanol. The mixture was stirred for 12 h at room temperature, neutralized with dilute aqueous hydrochloric acid, and extracted with 3 x 300 mL of ether. The combined extracts were washed with 3 x 400 mL of brine, dried over anhydrous magnesium sulfate, and concentrated under vacuum. Short

path distillation of the residue under reduced pressure gave 4.28 g (86% yield) of 1-phenyl-1,3-butanediol (98% purity by GC/MS), bp 209 – 214 °C (10 torr); mass spectrum (Fig. 3 – 10), m/e (%): 166 (5, $M^{\bullet+}$), 148 (19), 133 (11), 107 (47), 105 (50), 91 (14), 79 (100), 77 (85), 51 (21), 43 (18), and 29 (12); ^{13}C NMR (75.57 MHz, $CDCl_3$) (Fig. 3 – 11) δ 144.51, 144.44, 128.34, 128.27, 127.40, 127.09, 125.65, 125.58, 74.74, 71.22, 68.43, 64.94, 46.81, 46.25, 23.78, and 23.28 ppm.

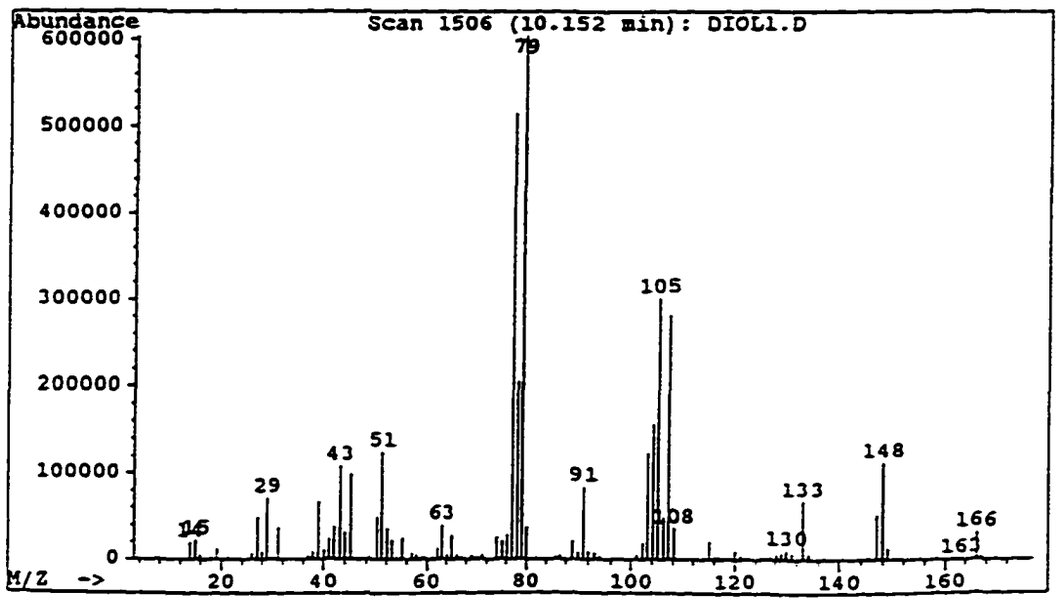

Figure 3 – 10. Mass spectrum of 1-phenyl-1,3-butanediol.

(ii) Acetylation

A solution of 1-phenyl-1,3-butanediol (1.15 g, 6.9 mmol) in 20 mL of

anhydrous ether was added to 30 mL of acetic anhydride/pyridine (1/2, v/v). The solution was stirred at about 35 °C for 16 h in flowing nitrogen, cooled to room temperature, and diluted with 100 mL of ether. The ether layer was separated, washed with 4 x 100 mL of water, dried over anhydrous magnesium sulfate, and concentrated under vacuum. Short path distillation of the residue under reduced pressure gave 1.35 g (78% yield) of 1-phenyl-1,3-diacetoxybutane (98% purity by GC/MS), bp 210 – 212 °C (10 torr); mass spectrum (Fig. 3 – 12), *m/e* (%): 250 (0.8, $M\cdot^{+}$), 190 (58), 148 (90), 147 (72), 133 (52), 107 (38), 105 (100), 91 (27), 77 (52), and 43 (95); ^{13}C NMR (75.57 MHz, $CDCl_3$) (Fig. 3 – 13) δ 170.56, 170.32, 170.11, 170.03, 140.38, 139.93, 128.55, 128.16, 128.03, 126.49, 126.34, 73.14, 72.16, 67.92, 67.09, 42.66, 42.21, 21.19, 21.15, 21.07, 20.44, and 20.08 ppm.

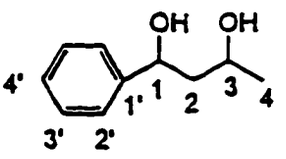

1.	74.74,	71.22
2.	46.81,	46.25
3.	68.43,	64.94
4.	23.78,	23.28
1'.	144.51,	144.44
2'.	125.65,	125.58
3'.	128.34,	128.27
4'.	127.40,	127.09

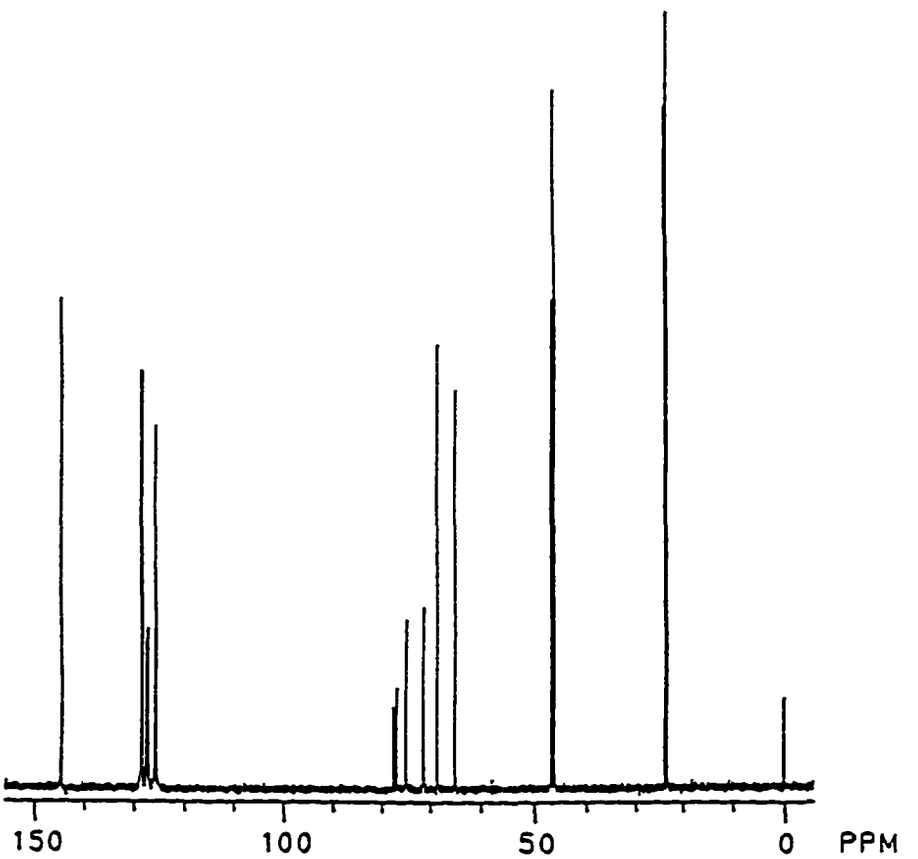

Figure 3-11. Carbon-13 NMR spectrum (75.57 MHz) and peak assignments of 1-phenyl-1,3-butanediol.

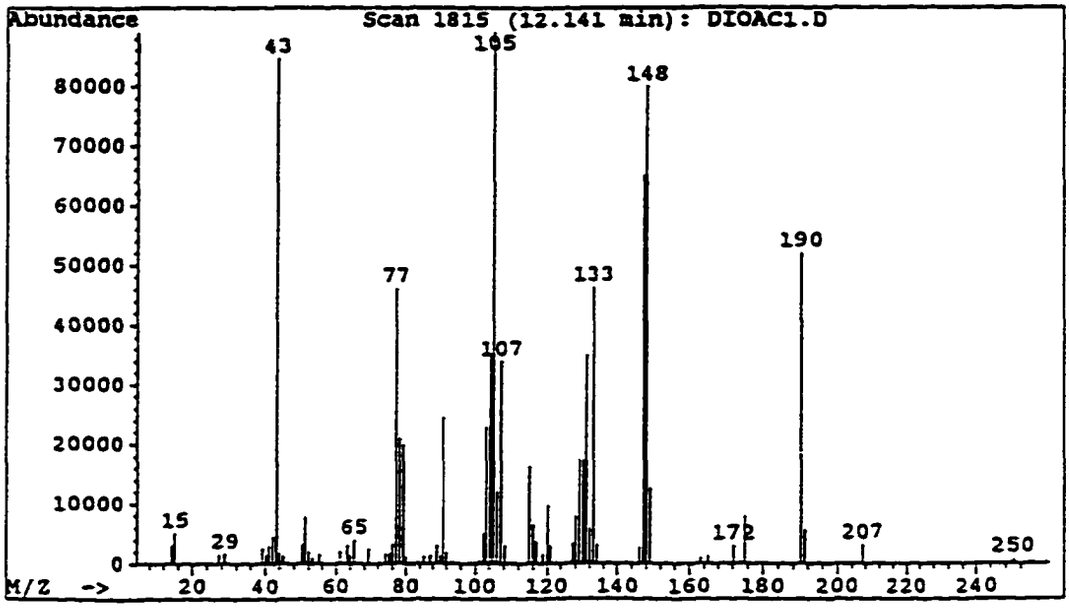

Figure 3 – 12. Mass spectrum of 1-phenyl-1,3-diacetoxybutane.

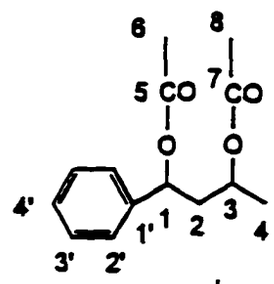

1.	73.14,	72.16
2.	42.66,	42.21
3.	67.92,	67.09
4.	20.44,	20.08
5, 7.	170.56,	170.32,
	170.11,	170.03
6, 8.	21.99,	21.15,
	21.07	
1'.	140.38,	139.93
2'.	126.49,	126.34
3'.	128.55	
4'.	128.16,	128.03

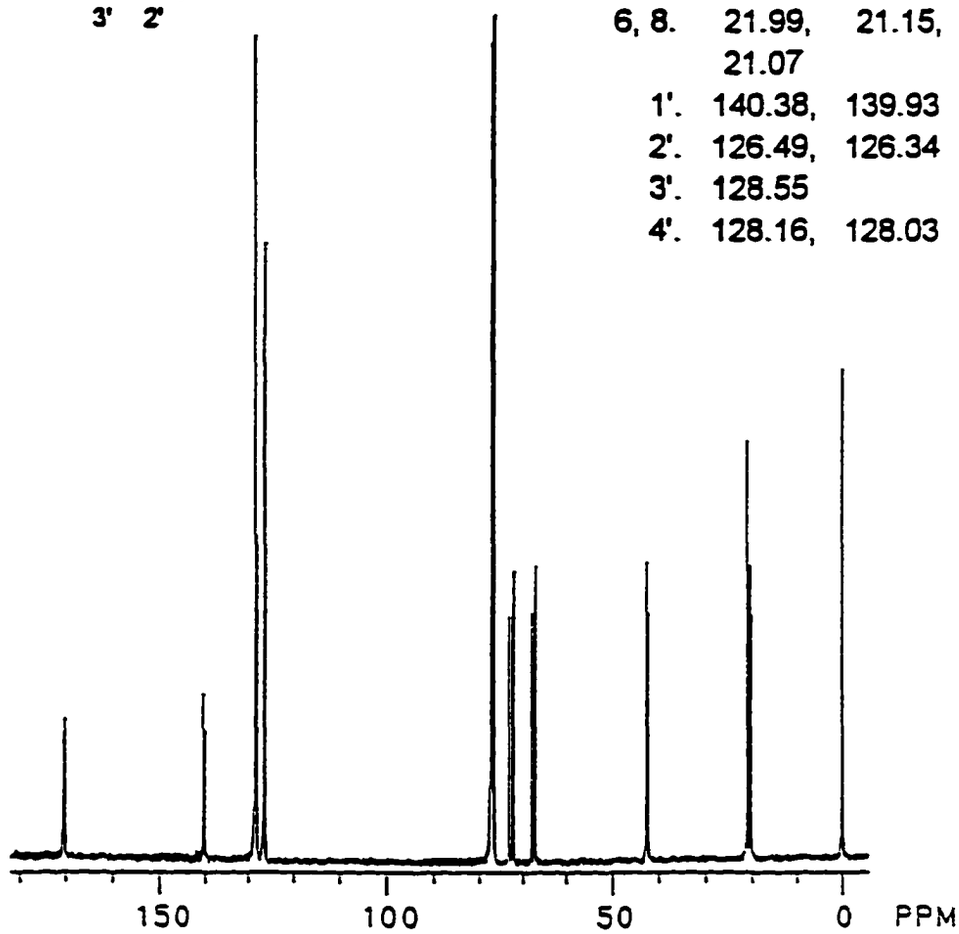

Figure 3-13. Carbon-13 NMR spectrum (75.57 MHz) and peak assignments of 1-phenyl-1,3-diacetoxybutane.

3.2.6 Synthesis of 1-Phenyl-1,3,5-triacetoxyhexane

General scheme 3 – 4

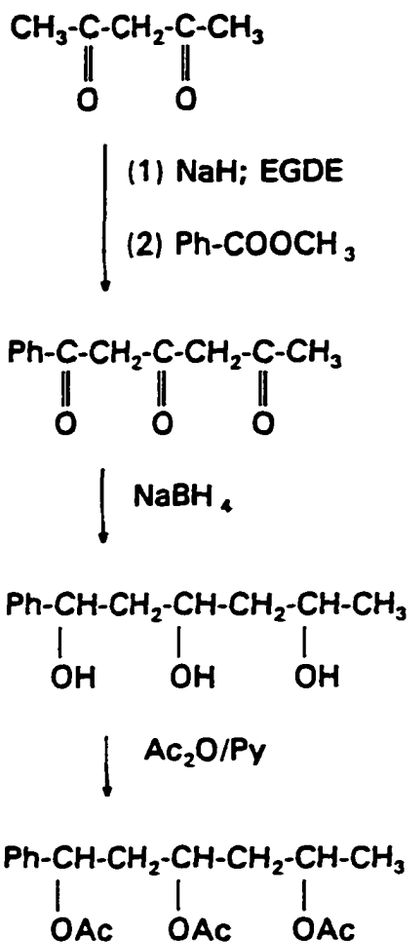

(i) Extension of Carbon Skeleton

Benzoylation of the *β*-diketone was accomplished with sodium hydride as the basic reagent.[17] Under a nitrogen atmosphere, a solution of 2,4-pentanedione (5.0 g, 50 mmol) in 50 mL of ethylene glycol dimethyl ether

(EGDE) was added to a stirred slurry of sodium hydride (3.6 g, 150 mmol) in 100 mL of EGDE under reflux. After 45 min of reflux, a solution of methyl benzoate (6.8 g, 50 mmol) in 50 mL of EGDE was added. The mixture was heated under reflux for 2 h. Most of the solvent was removed under reduced pressure, and the pasty residue was cooled to 0 °C; then ether (100 mL) and water (100 mL) were added successively. The ether layer was extracted with 2 x 100 mL of cold water and 100 mL of cold 1% aqueous sodium hydroxide solution, and the combined aqueous layers were poured onto a mixture of 50 mL of 12 N hydrochloric acid and 200 g of crushed ice. The resulting viscous organic layer was separated by gravity filtration, washed with water, and crystallized from 95% ethanol to give 1.0 g (10% yield) of 1-phenyl-1,3,5-hexanetrione (80% purity by GC/MS), mp 101 – 103 °C; mass spectrum (Fig. 3 – 14), m/e (%): 204 (5, $M\cdot^{+}$), 203 (6), 202 (33), 201 (33), 186 (36), 161 (32), 147 (20), 125 (18), 105 (100), 77 (77), 69 (33), 51 (24), and 43 (20).

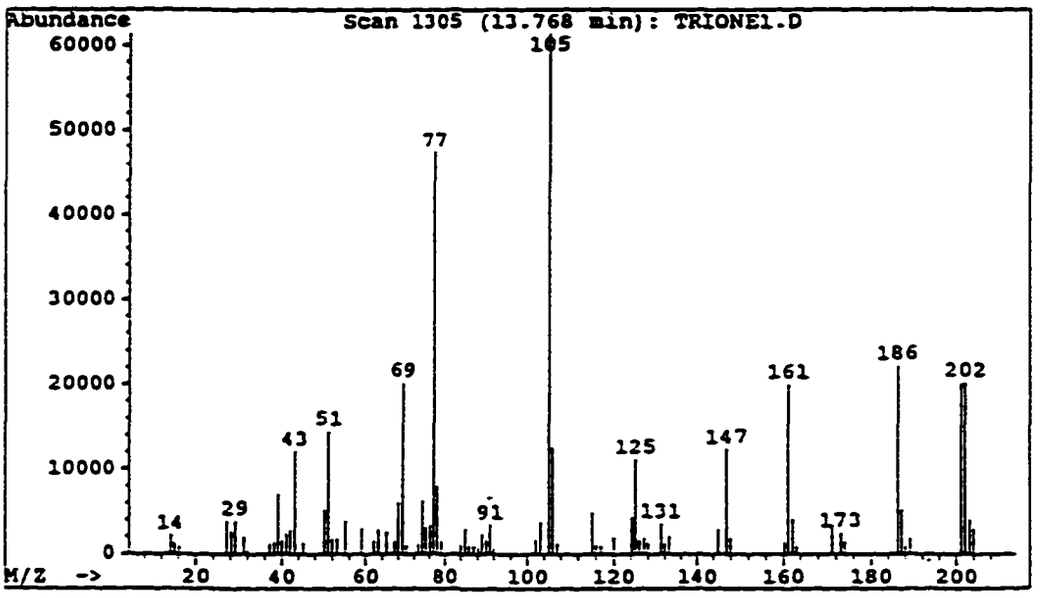

Figure 3 – 14. Mass spectrum of 1-phenyl-1,3,5-hexanetrione.

(ii) Reduction

A solution of sodium borohydride (2.0 g, 63 mmol) and sodium hydroxide (0.50 g) in 100 mL of water was added dropwise at about 10 °C to a stirred solution of 1-phenyl-1,3,5-hexanetrione (1.82 g, 9.0 mmol) in 200 mL of ethanol, cooled with an ice bath. The mixture was stirred for 18 h at room temperature, neutralized with dilute aqueous hydrochloric acid, and extracted with 3 x 300 mL of ether. The combined extracts were washed with 3 x 400 mL of brine, dried over anhydrous magnesium sulfate, and concentrated under vacuum to give 1.47 g (78% yield) of residual 1-

phenyl-1,3-5-hexanetriol (80% purity by GC/MS); mass spectrum (Fig. 3 – 15), m/e (%): 192 (3), 186 (45), 158 (100), 129 (13), 115 (14), 102 (38), 77 (34), 51 (9), and 43 (9).

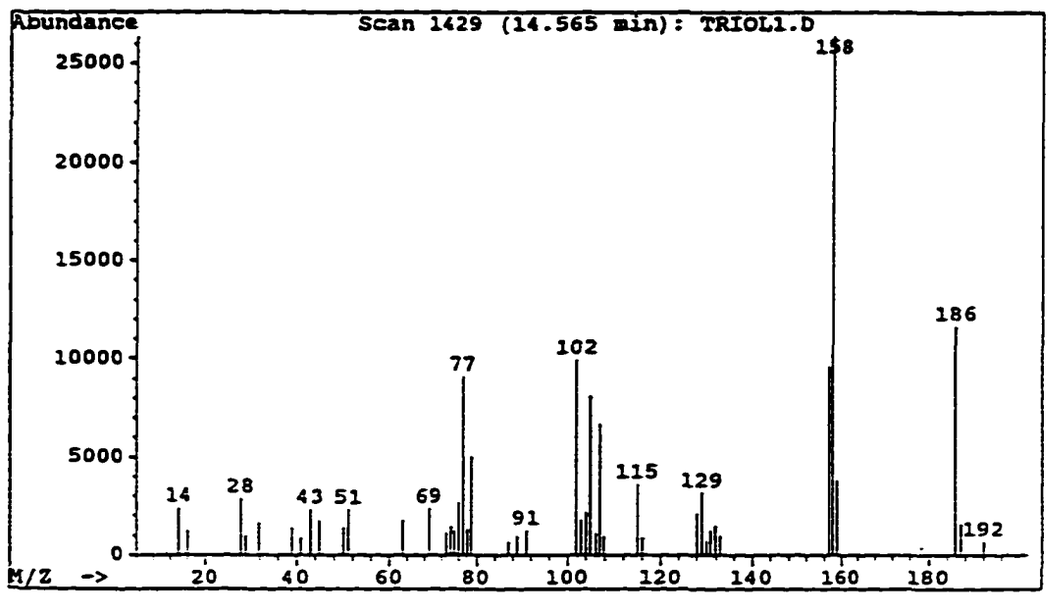

Figure 3 – 15. Mass spectrum of 1-phenyl-1,3-5-hexanetriol.

(iii) Acetylation

A solution of 1-phenyl-1,3,5-hexanetriol (0.63 g, 3.0 mmol) in 50 mL of anhydrous ether was added to 60 mL of acetic anhydride/pyridine (1/2, v/v). The solution was stirred at about 35 °C for 8 h in flowing nitrogen, cooled to room temperature, and diluted with 200 mL of ether. The ether layer was separated, washed with 4 x 100 mL of water, dried over

anhydrous magnesium sulfate, and concentrated under vacuum. The crude product was purified by column chromatography on a 35 cm x 2.2 cm (*i. d.*) column, packed with 100 – 200 mesh silica gel, using ethyl acetate/hexanes (1/10, v/v) as elution solvent, to give 0.34 g (33% yield) of 1-phenyl-1,3,5-triacetoxyhexane (96% purity by GC/MS); mass spectrum (Fig. 3 – 16), m/e (%): 276 (7), 216 (4), 174 (31), 157 (16), 105 (70), 91 (12), 77 (17), and 43 (100); ^{1}H NMR (300 MHz, $CDCl_3$) (Fig. 3 – 17) δ 7.32 (m, 5H), 5.78 (m, 1H), 4.92 (m, 2H), 2.01 (m, 13H), and 1.21 (m, 3H) ppm; ^{13}C NMR (75.57 MHz, $CDCl_3$) (Fig. 3 – 18) δ 170.37, 170.31, 170.16, 170.04, 169.95, 140.20, 140.01, 139.71, 128.57, 128.20, 128.09, 126.62, 126.53, 126.36, 73.03, 72.04, 71.85, 68.33, 67.81, 67.62, 67.56, 67.41, 66.89, 66.81, 41.31, 41.06, 40.99, 40.90, 40.74, 40.42, 40.20, 39.93, 21.21, 21.15, 21.03, 20.85, 20.36, and 20.14 ppm.

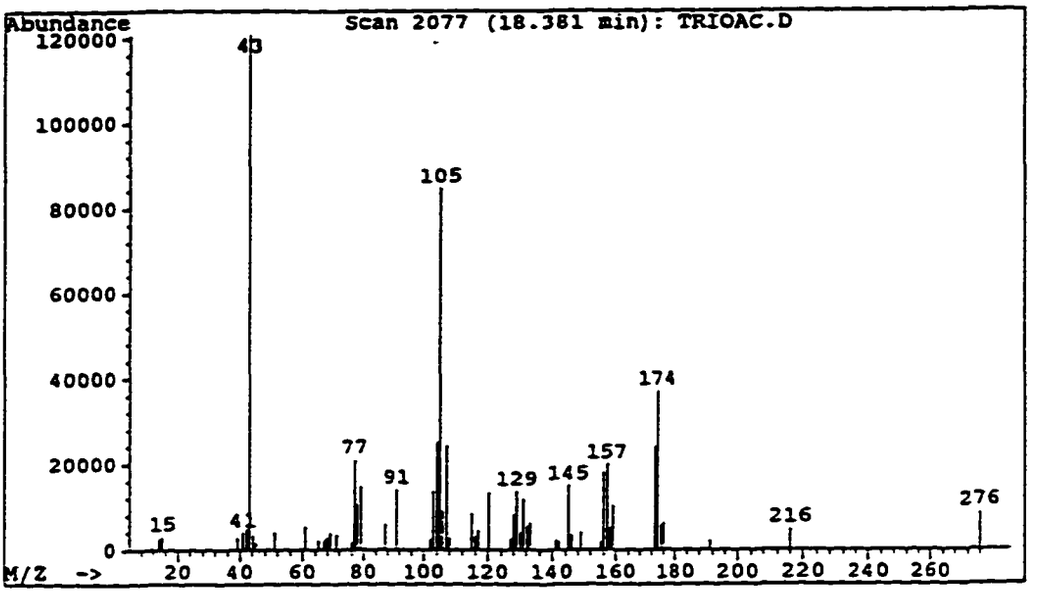

Figure 3 – 16. Mass spectrum of 1-phenyl-1,3,5-triacetoxyhexane.

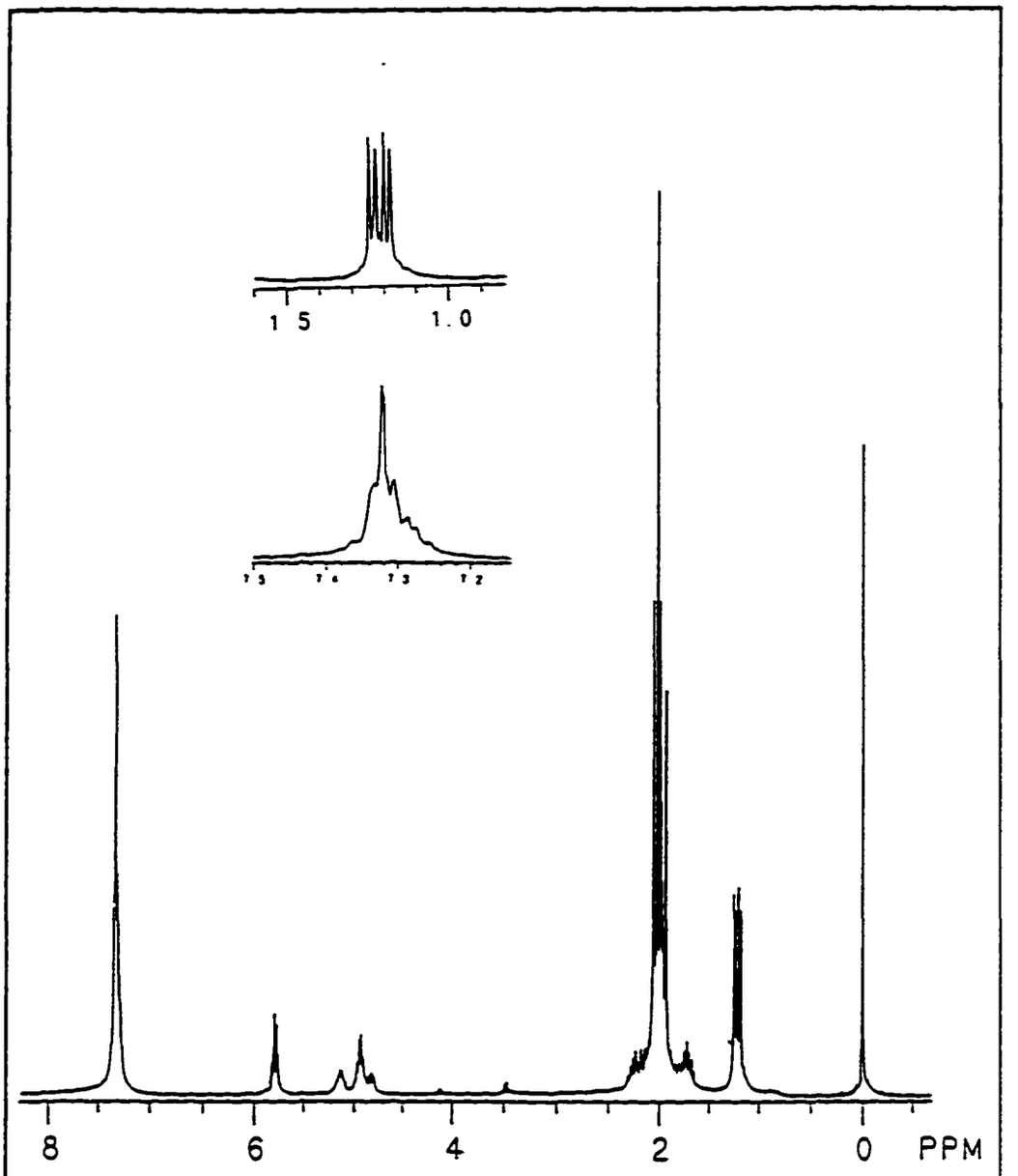

Figure 3-17. Proton NMR spectrum (300 MHz) of 1-phenyl-1,3,5-triacetoxyhexane.

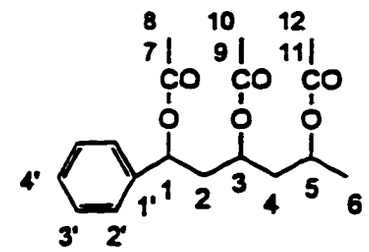

1.	73.03,	72.04,	71.85
2,4.	41.31,	41.06,	40.99,
	40.90,	40.74,	40.42,
	40.20,	39.93	
3,5.	68.33,	67.81,	67.62,
	67.56,	67.41,	66.89,
	66.81		
6.	20.36,	20.14	
7,9,11.	170.37,	170.31,	170.16
	170.04,	169.95	
8,10,12.	21.21,	21.15,	21.03,
	20.85		
1'.	140.20,	140.01,	139.71
2'.	126.62,	126.53,	126.36
3'.	128.57,		
4'.	128.20,	128.09	

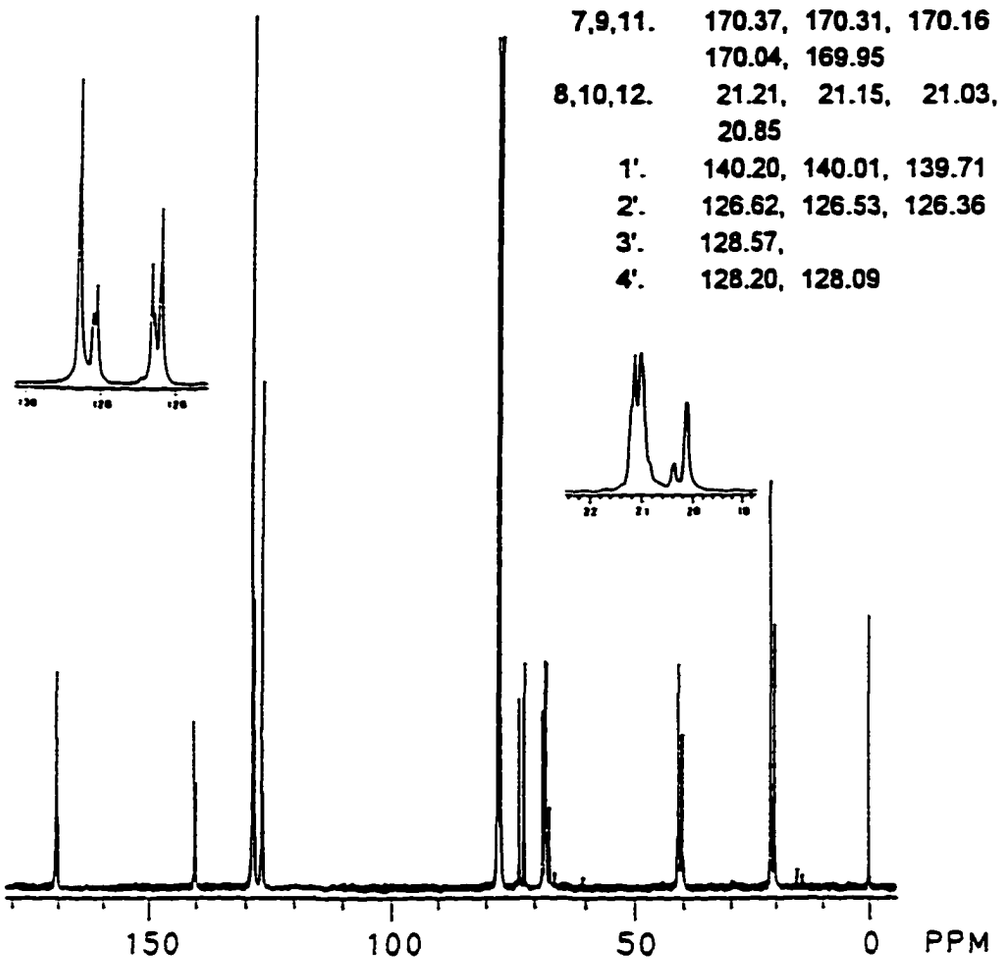

Figure 3-18. Carbon-13 NMR spectrum (75.57 MHz) and peak assignments of 1-phenyl-1,3,5-triacetoxyhexane.

3.2.7 Synthesis of 1-Phenyl-2,4-diacetoxypentane

General scheme 3 – 5

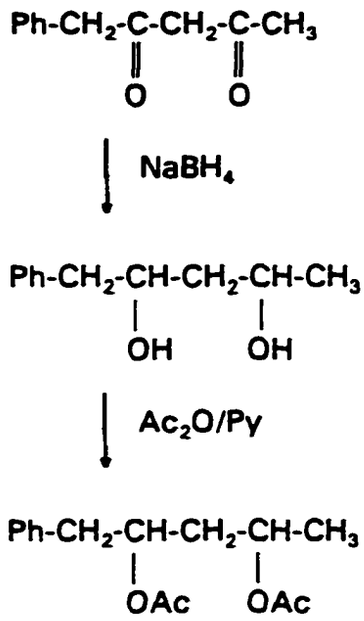

(i) Reduction

A solution of sodium borohydride (2.80 g, 88 mmol) and sodium hydroxide (0.60 g) in 100 mL of water was added dropwise at about 10 °C to a stirred solution of 3.52 g (20 mmol) of 1-phenyl-2,4-pentanedione in 100 mL of ethanol. The mixture was stirred for 16 h at room temperature, neutralized with dilute aqueous hydrochloric acid, and extracted with 3 x 300 mL of ether. The combined extracts were washed with 3 x 400 mL of brine, dried over anhydrous magnesium sulfate, and concentrated under vacuum. Short path distillation of the residue under reduced pressure gave

2.7 g (75% yield) of 1-phenyl-2,4-pentanediol (95% purity by GC/MS), bp 215 – 225 °C (10 torr); mass spectrum (Fig. 3 – 19), m/e (%): 180 (1, $M^{\cdot +}$), 162 (5), 117 (5), 103 (4), 92 (100), 91 (54), 77 (4), 71 (17), 45 (33), and 43 (16); ^{13}C NMR (75.57 MHz, $CDCl_3$) (Fig. 3 – 20) δ 138.52, 138.06, 129.40, 129.37, 128.41, 126.36, 126.30, 73.63, 69.78, 68.64, 64.92, 44.53, 43.90, 43.57, 23.79, and 23.33 ppm.

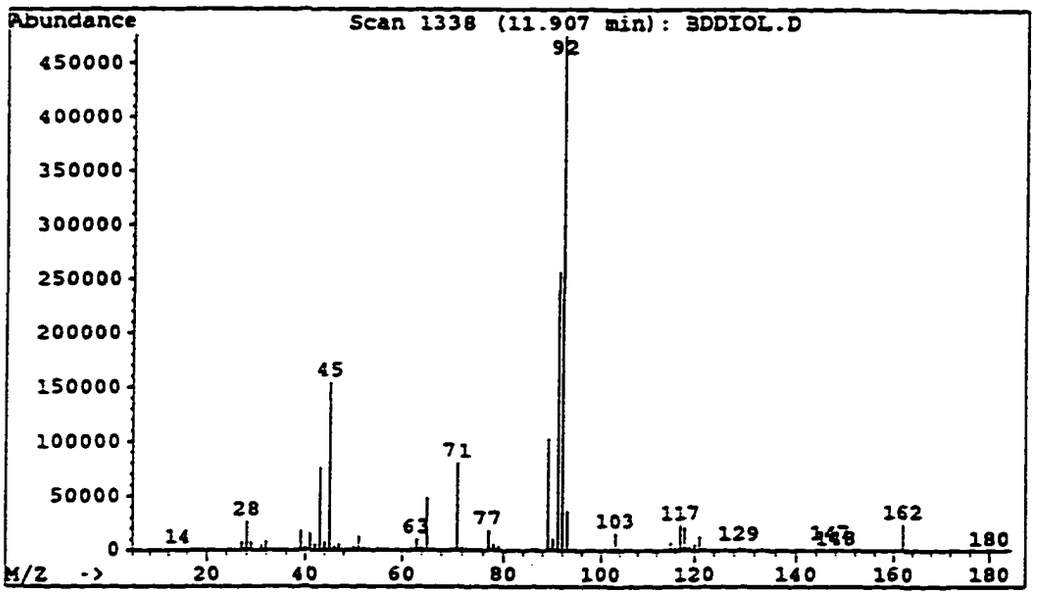

Figure 3 – 19. Mass spectrum of 1-phenyl-2,4-pentanediol.

(ii) Acetylation

A solution of 1-phenyl-2,4-pentanediol (0.90 g, 5 mmol) in 20 mL of anhydrous ether was added to 30 mL of acetic anhydride/pyridine (1/2, v/v). The solution was stirred at about 35 °C for 16 h in flowing nitrogen, cooled

to room temperature, and diluted with 200 mL of ether. The ether layer was separated, washed with 4 x 100 mL of water, dried over anhydrous magnesium sulfate, and concentrated under vacuum to give 1.04 g (79% yield) of residual 1-phenyl-2,4-diacetoxypentane (90% purity by GC/MS); mass spectrum (Fig. 3-21), m/e (%): 173 (1), 144 (100), 129 (50), 117 (18), 91 (44), 77 (4), 71 (13), and 43 (80); ^{1}H NMR (300 MHz, $CDCl_3$) (Fig. 3-22) δ 7.25 (m, 5H), 5.16 (m, 1H), 4.96 (m, 1H), 2.83 (m, 2H), 1.97 (m, 6H), 1.73 (m, 2H), and 1.18 (m, 3H); ^{13}C NMR (75.57 MHz, $CDCl_3$) (Fig. 3-23) δ 170.46, 170.22, 137.05, 136.97, 129.46, 129.43, 128.37, 126.58, 71.74, 70.58, 68.03, 66.83, 40.94, 40.65, 39.71, 39.49, 21.23, 21.12, 21.06, 20.95, 20.42, and 19.88 ppm.

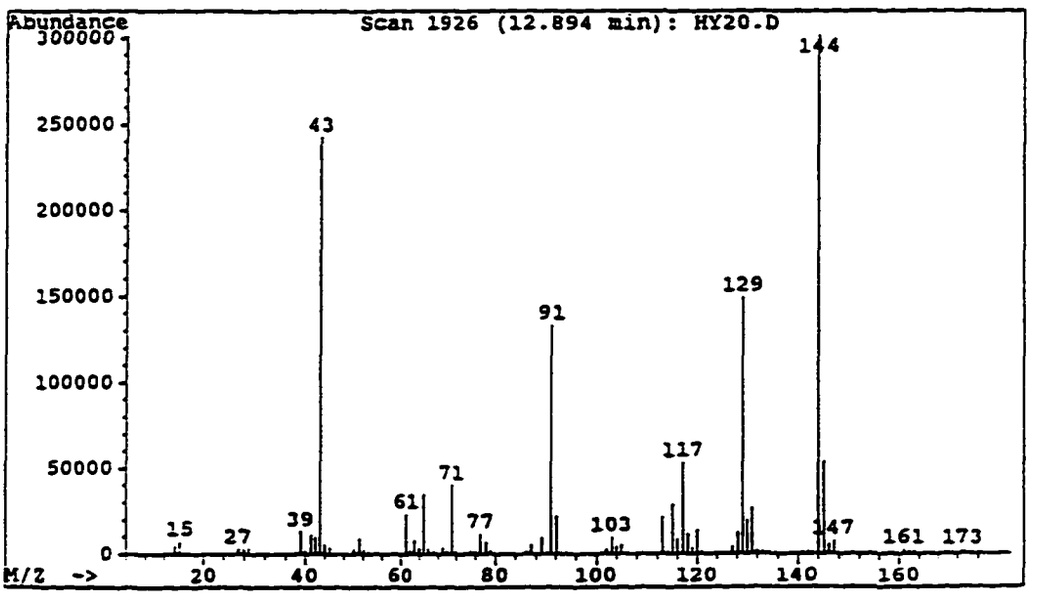

Figure 3-21. Mass spectrum of 1-phenyl-2,4-diacetoxypentane.

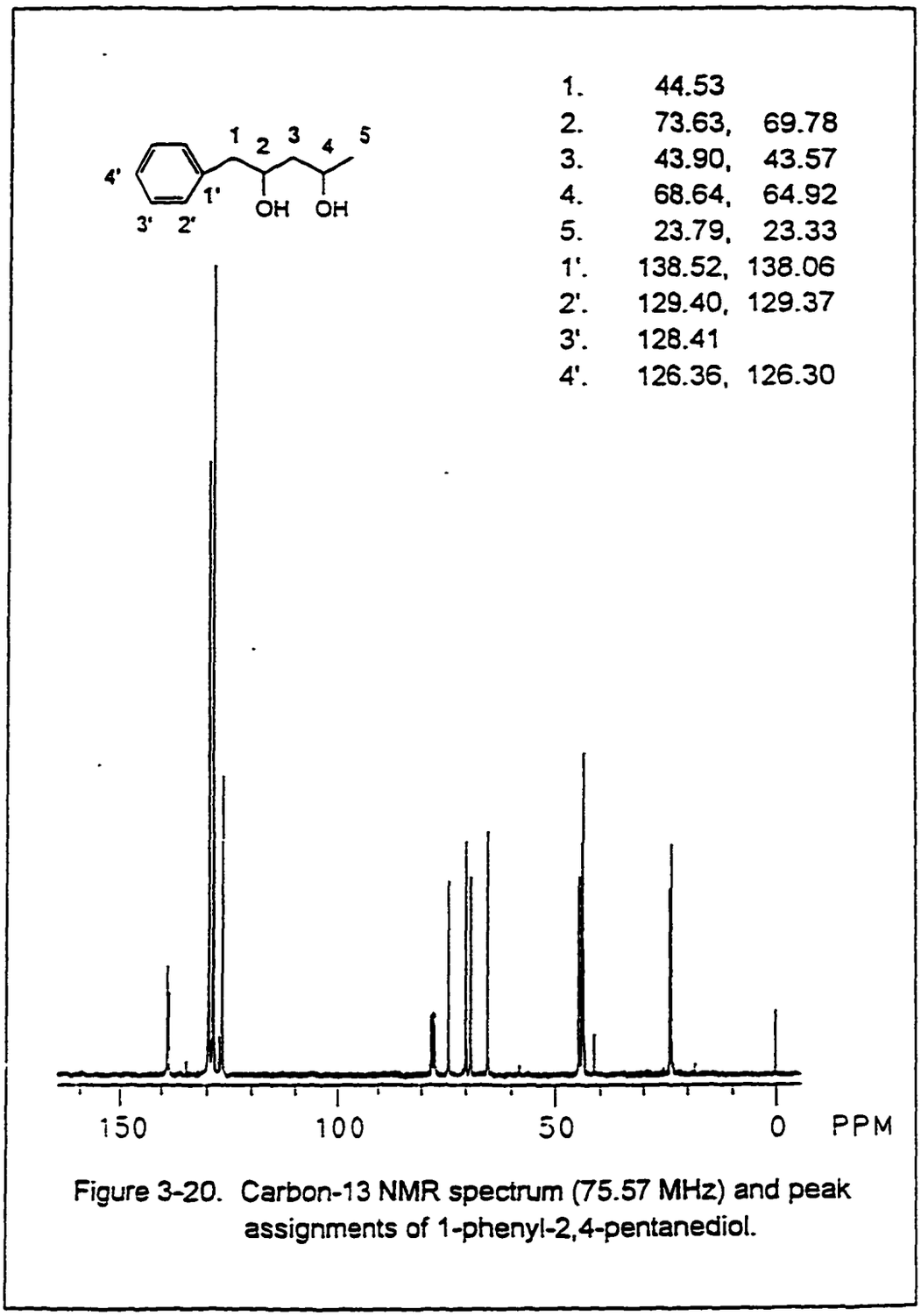

Figure 3-20. Carbon-13 NMR spectrum (75.57 MHz) and peak assignments of 1-phenyl-2,4-pentanediol.

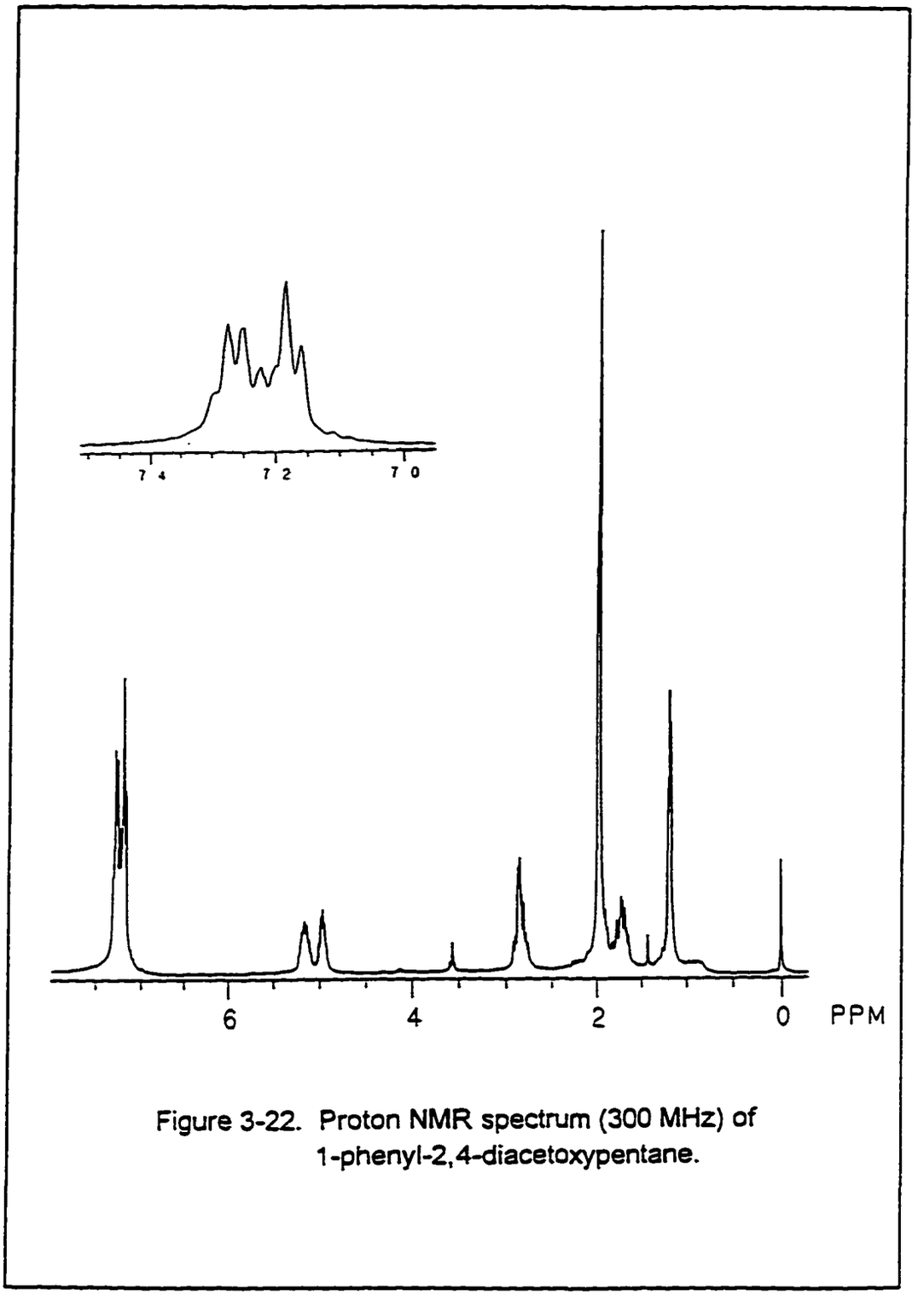

Figure 3-22. Proton NMR spectrum (300 MHz) of 1-phenyl-2,4-diacetoxypentane.

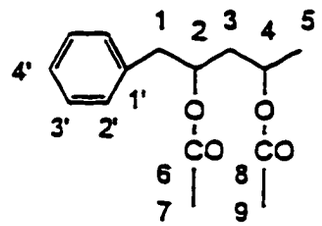

1,3.	40.94,	40.65
	39.71,	39.49
2.	71.74,	70.58
4.	68.03,	66.83
5,7,9.	21.23,	21.12
	21.06,	20.95
	20.42,	19.88
6,8.	170.46	170.22
1'.	137.05,	136.97
2'.	129.46,	129.43
3'.	128.37	
4'.	126.58	

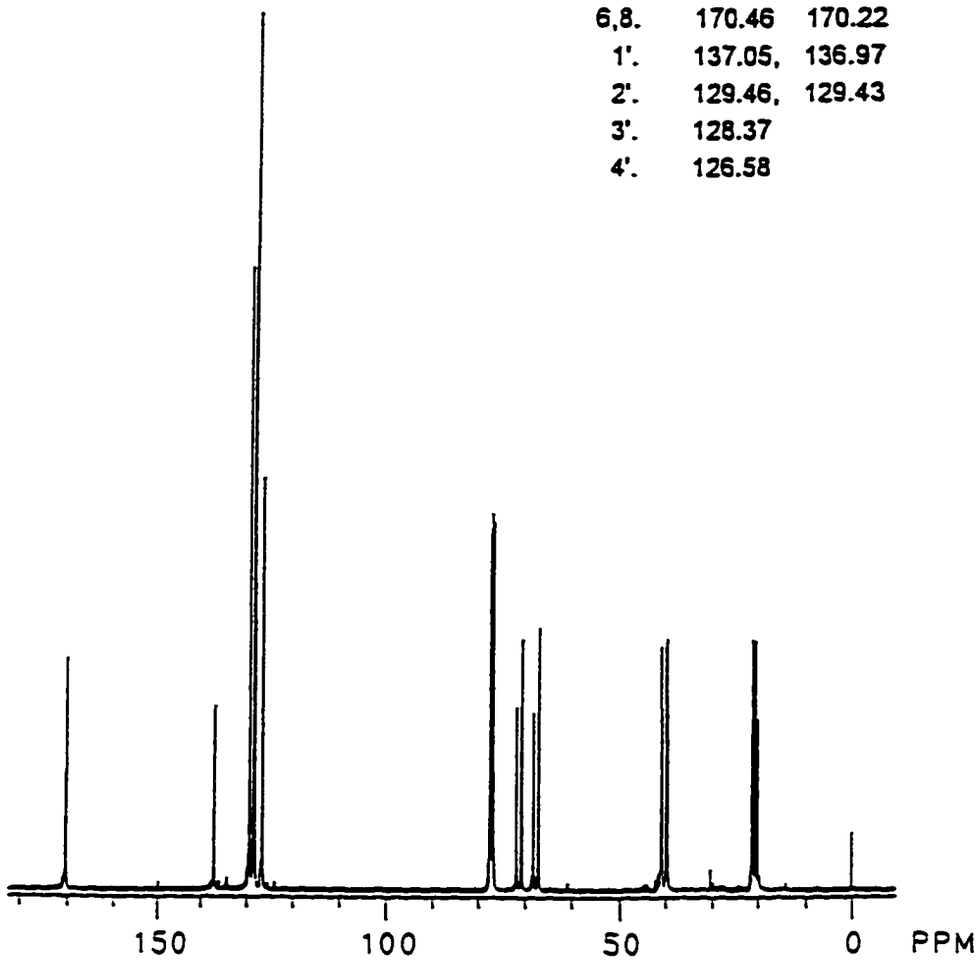

Figure 3-23. Carbon-13 NMR spectrum (75.57 MHz) and peak assignments of 1-phenyl-2,4-diacetoxypentane.

3.2.8 Synthesis of 1,4-Bis(α-acetoxyheptyl)benzene

General scheme 3 – 6

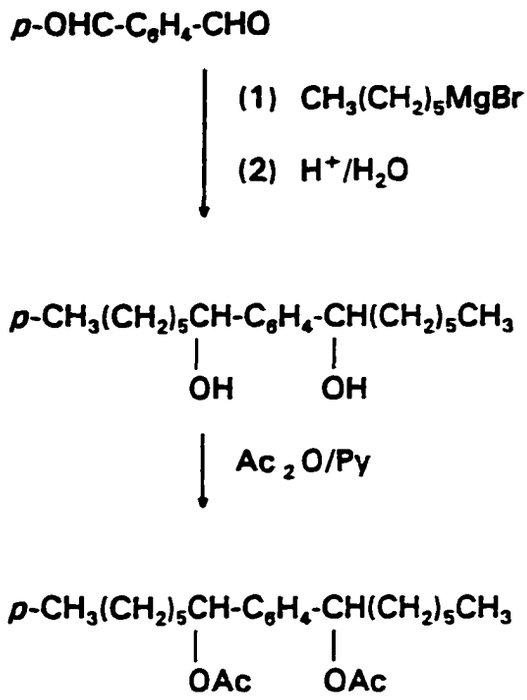

(i) Grignard Reaction

Under a nitrogen atmosphere, a solution of terephthaldicarboxaldehyde (6.7 g, 50 mmol) in 100 mL of anhydrous ether was added dropwise at about 5 °C to a stirred solution of hexylmagnesium bromide (120 mmol) in 100 mL of ether contained in a three-neck flask. The mixture was heated under reflux for 1 h, cooled to room temperature, diluted with 100 mL of ether, and decomposed with 200 mL of cold 2% aqueous sulfuric acid. The ether layer was separated, combined with

2 x 100 mL of ether extracts of the aqueous layer, washed with 4 x 150 mL of water, dried with anhydrous magnesium sulfate, and concentrated under vacuum. Short path distillation of the residue under reduced pressure gave 12.7 g (82% yield) of 1,4-bis(α-hydroxyheptyl)benzene (80% purity by GC/MS), bp 207–210 °C (10 torr); mass spectrum (Fig. 3–24), m/e (%): 306 (0.3, $M^{\cdot+}$), 288 (0.5), 270 (0.5), 221 (100), 203 (13), 136 (25), 107 (33), 91 (32), 79 (41), 55 (30), 43 (82), 41 (41), and 29 (30); ^{13}C NMR (75.57 MHz, $CDCl_3$) (Fig. 3–25) δ 144.08, 125.93, 74.33, 39.10, 31.81, 29.25, 25.83, 22.64, and 14.08 ppm.

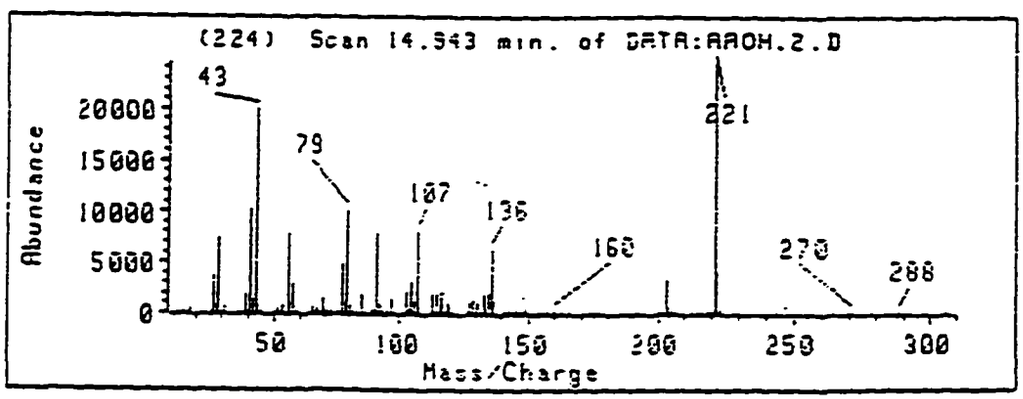

Figure 3–24. Mass spectrum of 1,4-bis(α-hydroxyheptyl)benzene.

(ii) Acetylation

A solution of 1,4-bis(α-hydroxyheptyl)benzene (6.12 g, 20 mmol) in

50 mL of anhydrous ether was added to 60 mL of acetic anhydride/pyridine (1/2, v/v). The solution was stirred at about 35 °C for 8 h in flowing nitrogen, cooled to room temperature, and diluted with 200 mL of ether. The ether layer was separated, washed with 4 x 100 mL of water, dried over anhydrous magnesium sulfate, and concentrated under vacuum. Short path distillation of the residue under reduced pressure gave 5.85 g (75% yield) of 1,4-bis(*α*-acetoxyheptyl)benzene (90% purity by GC/MS), bp 214 – 218 °C (10 torr); mass spectrum (Fig. 3 – 26), m/e (%): 330 (2), 288 (42), 217 (6), 203 (21), 175 (9), 133 (11), 117 (13), 105 (14), 91 (34), 55 (8), 43 (100), 41 (16), and 29 (10); ^{13}C NMR (Fig. 3 – 27), (75.57 MHz, $CDCl_3$) δ 170.33, 140.42, 126.58, 75.86, 36.30, 31.66, 28.99, 25.48, 22.56, 21.26, and 14.03 ppm.

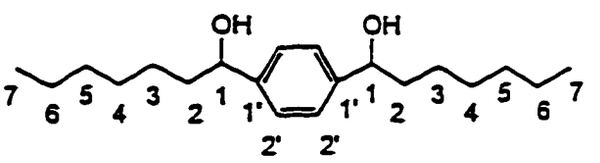

1. 74.33
2. 39.10
3. 25.83
4. 29.25
5. 31.81
6. 22.64
7. 14.08
1'. 144.08
2'. 125.93

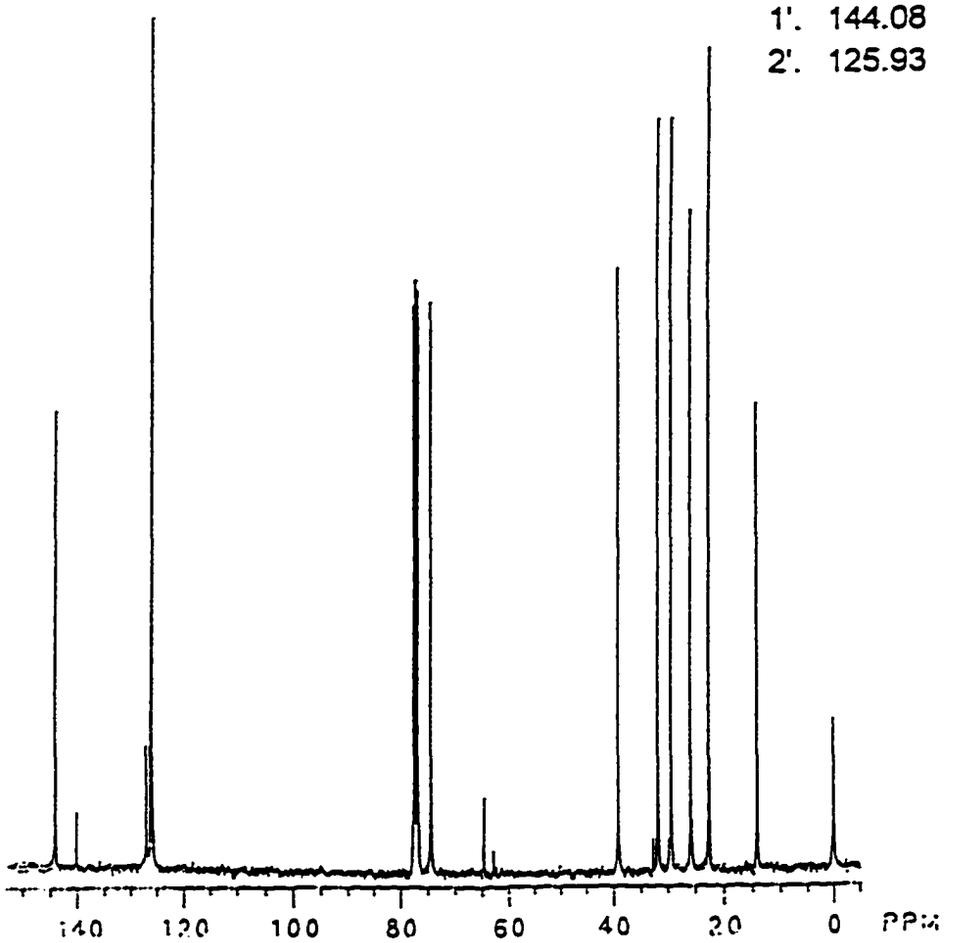

Figure 3-25. Carbon-13 NMR spectrum (75.57 MHz) and peak assignments of 1,4-bis(alpha-hydroxyheptyl)benzene.

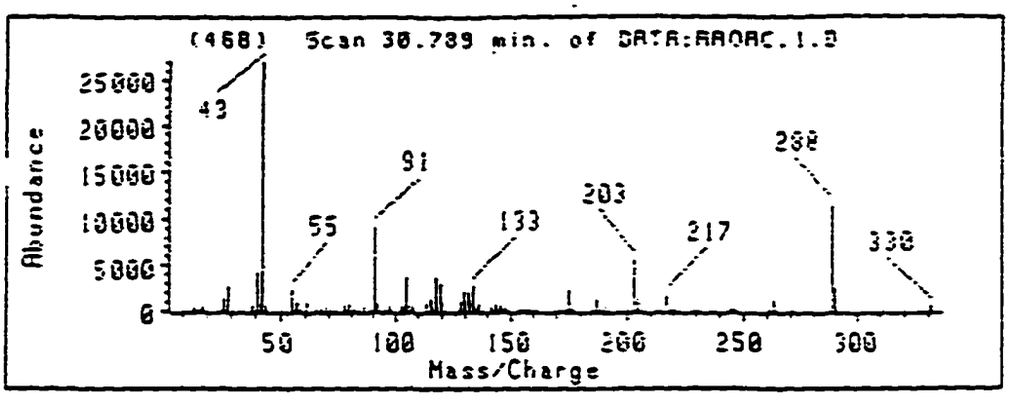

Figure 3 – 26. Mass spectrum of 1,4-bis(α-acetoxyheptyl)benzene.

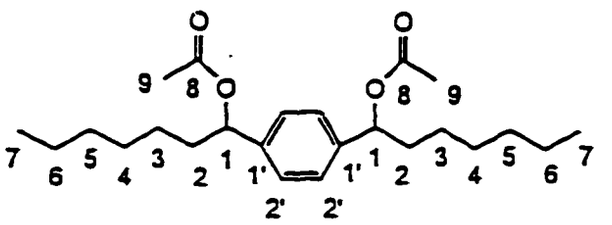

1. 75.86
2. 36.30
3. 25.48
4. 28.99
5. 31.66
6. 22.56
7. 14.03
8. 170.33
9. 21.26
1'. 140.42
2'. 126.58

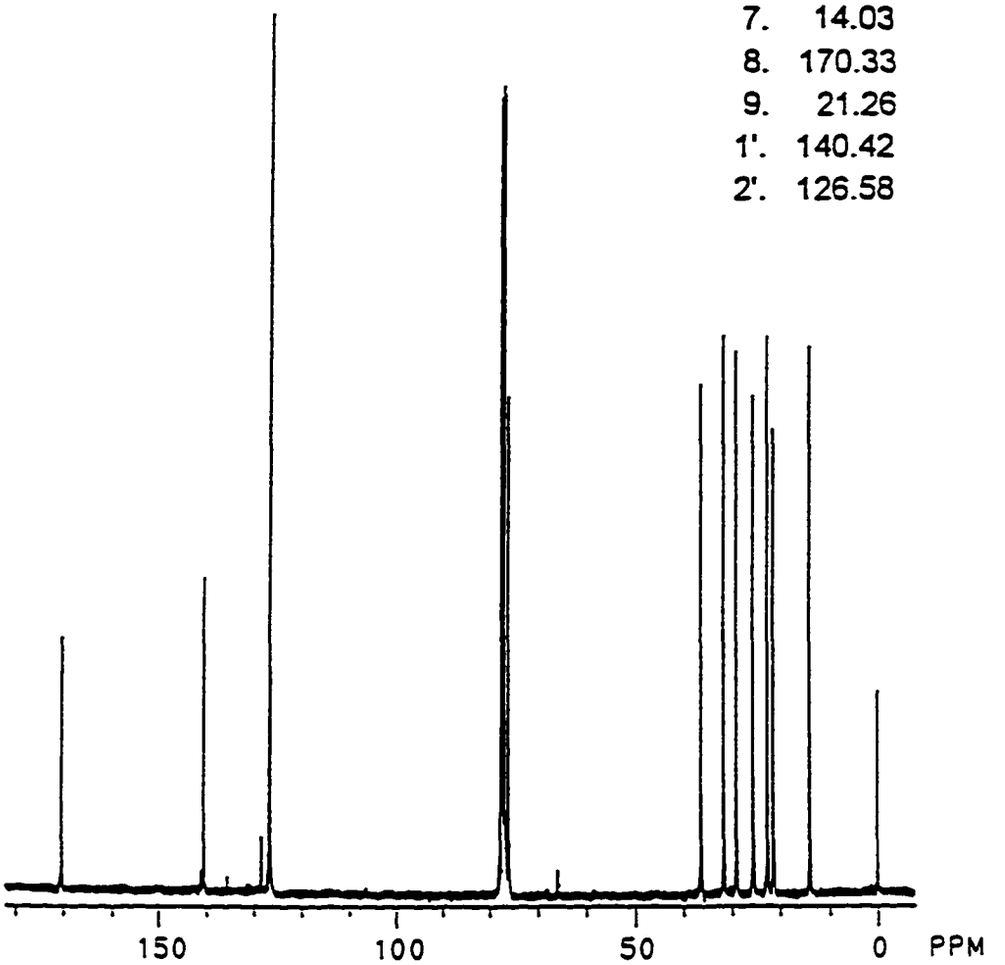

Figure 3-27. Carbon-13 NMR spectrum (75.57 MHz) and peak assignments of 1,4-bis(alpha-acetoxyheptyl)benzene.

3.2.9 Synthesis of 1-(α-Acetoxyheptyl)-4-(β-acetoxyoctyl)benzene

General scheme 3 – 7

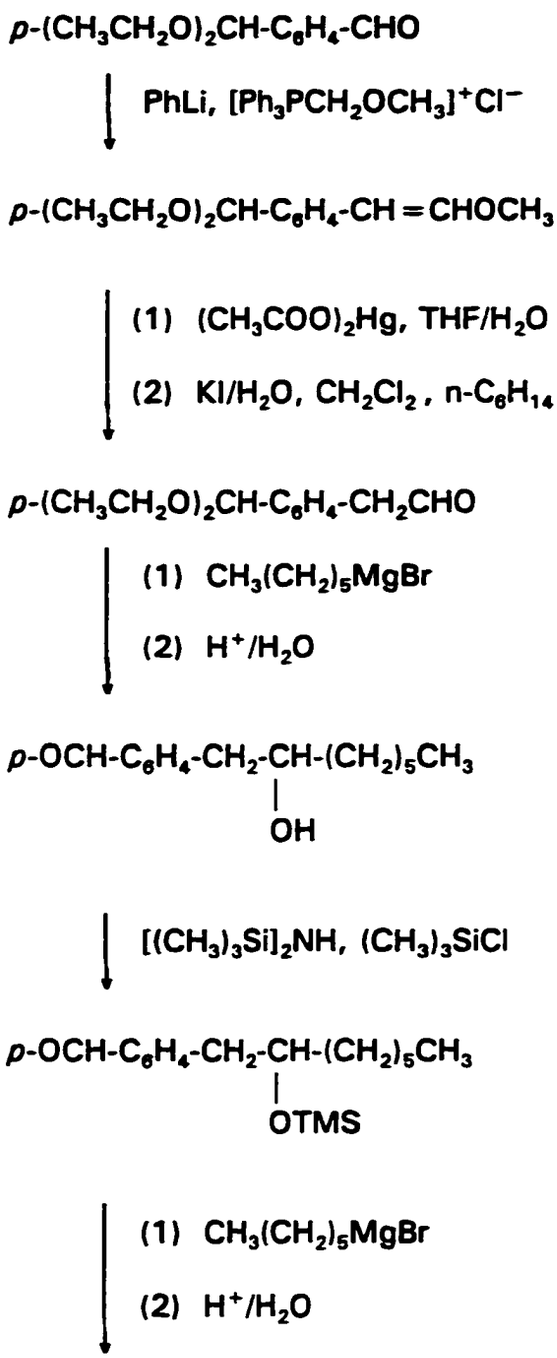

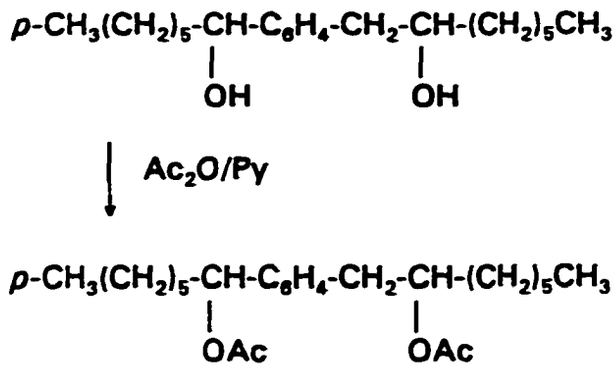

(i) Wittig Reaction

Under a nitrogen atmosphere, a solution of phenyllithium (50 mmol) in cyclohexane/ether (70/30) was added dropwise at about 0 °C to a stirred suspension of finely powdered (methoxymethyl)triphenylphosphonium chloride (17.7 g, 50 mmol) in 250 mL of anhydrous ether contained in a three-neck flask. The mixture was kept at 0 °C for 1 h and at room temperature for 1/2 h. After dropwise addition of a solution of terephthalaldehyde *mono*(diethyl acetal) (6.4 g, 30 mmol) in 50 mL of anhydrous ether, the mixture was stirred at room temperature for 1/2 h to complete the reaction. The ether layer was separated by suction filtration, washed with 4 x 100 mL of water, dried over anhydrous magnesium sulfate, and concentrated under vacuum. Short path distillation of the residue under reduced pressure gave 2.8 g (60% yield) of 1-(diethoxymethyl)-4-(β-methoxyvinyl)benzene (90% purity by GC/MS), bp 110–115°C (10 torr); mass spectrum (Fig. 3–28), m/e (%): 236 (4, $M\cdot^{+}$), 191 (40), 161 (47), 135 (12), 103 (50), 91 (100), 65 (16), and 29 (51).

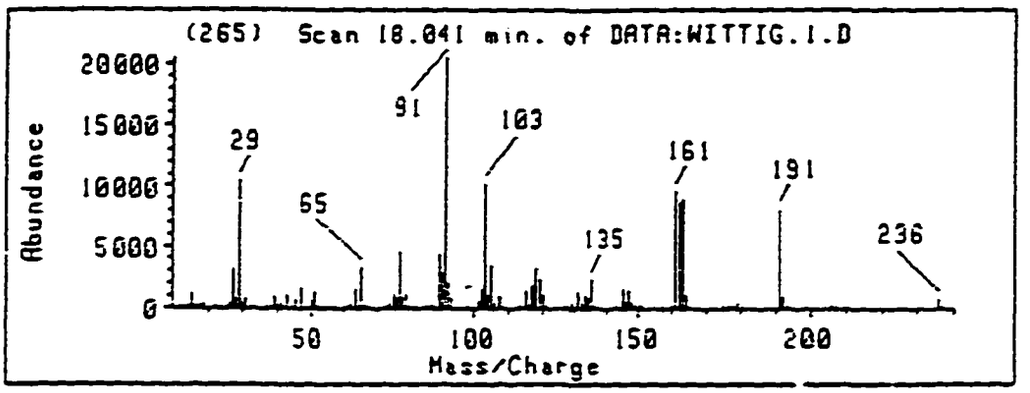

Figure 3 – 28. Mass spectrum of 1-(diethoxymethyl)-4-(β-methoxyvinyl)benzene.

(ii) Hydrolysis of Enol Ether

A solution of the above enol ether (6.7 g, 28 mmol) and mercuric acetate (28.6 g, 90 mmol) in 330 mL of THF/H_2O (10/1, v/v) was heated under reflux for 1/2 h. A saturated aqueous solution of potassium iodide (210 mL) was added, and reflux was maintained for 2 h. The reaction mixture was cooled to room temperature and extracted with 3 x 300 mL of CH_2Cl_2. Then the combined extracts were concentrated under vacuum, and the resultant brown oil was extracted with 3 x 250 mL of *n*-hexane. The combined extracts were concentrated under vacuum to give 2.56 g (42% yield) of residual 4-(diethoxymethyl)phenylacetaldehyde (80% purity by GC/MS); mass spectrum (Fig. 3 – 29), m/e (%): 177 (37), 149 (40), 103 (44), 91 (91), 65 (25), and 29 (100).

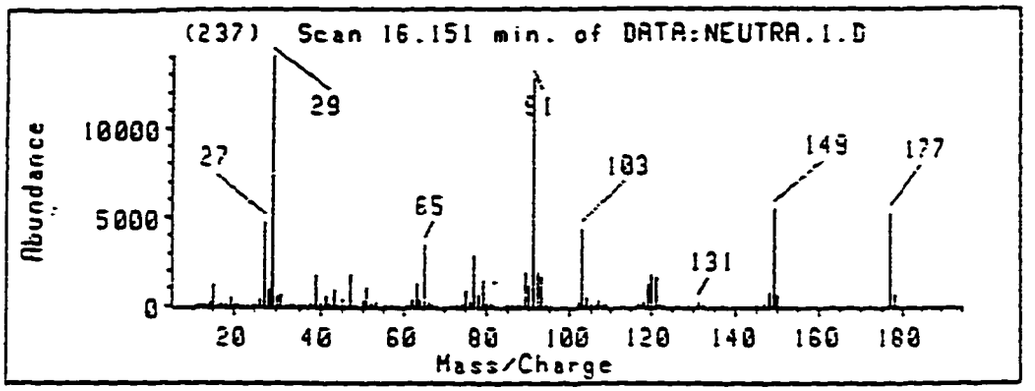

Figure 3–29. Mass spectrum of 4-(diethoxymethyl)-phenylacetaldehyde.

(iii) Grignard Reaction

Under a nitrogen atmosphere, a solution of the above acetal aldehyde (2.0 g, 9.1 mmol) in 100 mL of anhydrous ether was added dropwise at about 5 °C to a stirred solution of 20 mmol of hexylmagnesium bromide in 100 mL of ether contained in a three-neck flask. The mixture was heated under reflux for 1 h, cooled to room temperature, diluted with 100 mL of ether, and decomposed with 200 mL of cold 2% aqueous sulfuric acid. The ether layer was separated, combined with 2 x 150 mL of ether extracts of the aqueous layer, washed with 4 x 250 mL of water, dried with anhydrous magnesium sulfate, and concentrated under vacuum to give 1.9 g (88% yield) of residual 4-(β-hydroxyoctyl)benzaldehyde (70% purity by GC/MS); mass spectrum (Fig. 3–30), m/e (%): 147 (2), 120 (100), 91 (59), 65 (9),

55 (17), and 29 (25).

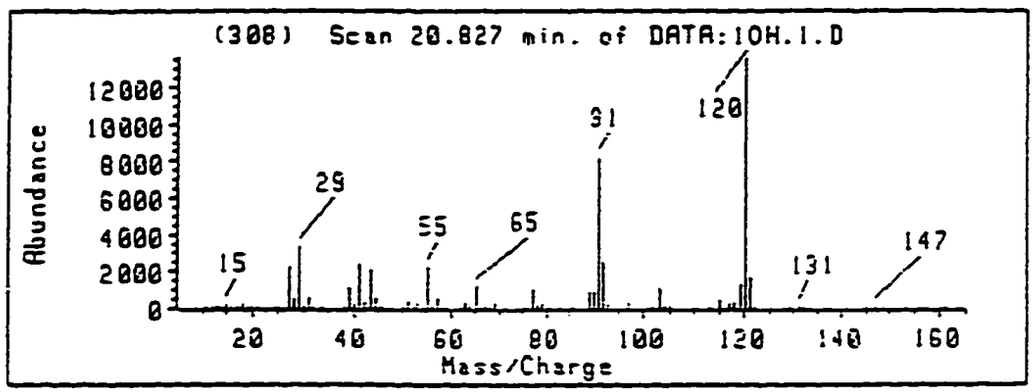

Figure 3 – 30. Mass spectrum of 4-(β-hydroxyoctyl)benzaldehyde.

(iv) Protection of Hydroxy Group

The 4-(β-hydroxyoctyl)benzaldehyde (0.79 g, 3.4 mmol) was treated with 1,1,1,3,3,3-hexamethyldisilazane (4 mL) and trimethylchlorosilane (2 mL) in 20 mL of anhydrous pyridine for 10 min.[19] The solution was diluted with 100 mL of ether, washed with 3 x 100 mL of water, and dried over 4 Å molecular sieves. The ether solution was concentrated under vacuum to give 0.98 g (94% yield) of residual 4-(β-trimethylsiloxyoctyl)benzaldehyde (85% purity by GC/MS); mass spectrum (Fig. 3 – 31), m/e (%): 306 (0.1, $M\cdot^+$), 291 (13), 221 (11), 192 (100), 187 (92), 103 (26), 73 (78), and 55 (11).

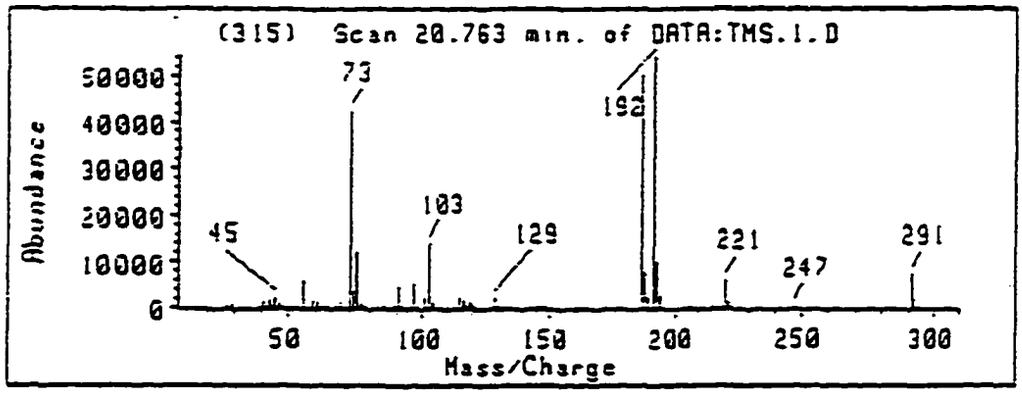

Figure 3 – 31. Mass spectrum of 4-(β-trimethylsiloxyoctyl)-benzaldehyde.

(v) Grignard Reaction

Under a nitrogen atmosphere, a solution of 4-(β-trimethylsiloxyoctyl)benzaldehyde (0.92 g, 3.0 mmol) in 20 mL of anhydrous ether was added dropwise at about 5 °C to a stirred solution of 18 mmol of hexylmagnesium bromide in 100 mL of ether contained in a three-neck flask. The mixture was heated under reflux for 2 h, cooled to room temperature, diluted with 100 mL of ether, and treated with 100 mL of cold 2% aqueous sulfuric acid. The ether layer was separated, combined with 2 x 100 mL of ether extracts of the aqueous layer, washed with 4 x 150 mL of water, dried with anhydrous magnesium sulfate, and concentrated under vacuum. The crude product, 1-(α-hydroxyheptyl)-4-(β-hydroxyoctyl)benzene, was used directly in the next step.

(vi) Acetylation

A solution of 1-(*α*-hydroxyheptyl)-4-(*β*-hydroxyoctyl)benzene (1.3 g, 4.0 mmol) in 50 mL of anhydrous ether was added to 30 mL of acetic anhydride/pyridine (1/2, v/v). The solution was stirred at about 35 °C for 8 h in flowing nitrogen, cooled to room temperature, and diluted with 200 mL of ether. The ether layer was separated, washed with 4 x 100 mL of water, dried over anhydrous magnesium sulfate, and concentrated under vacuum. The crude product was purified by column chromatography on a 35 cm x 2.2 cm (*i.d.*) column, packed with 100–200 mesh silica gel, using ethyl acetate/hexanes (1/10, v/v) as elution solvent, to give 0.4 g (*ca.* 25% yield) of 1-(*α*-acetoxyheptyl)-4-(*β*-acetoxyoctyl)benzene (94% purity by GC/MS); mass spectrum (Fig. 3–32), m/e (%): 345 (16), 344 (61), 302 (13), 284 (4), 259 (6), 217 (100), 129 (9), 117 (16), 104 (27), 91 (13), 55 (4), and 43 (46); ^{13}C NMR (75.57 MHz, $CDCl_3$) (Fig. 3–33) δ 170.57, 170.32, 138.98, 137.31, 129.44, 126.55, 75.94, 74.73, 40.28, 36.27, 33.58, 33.52, 31.71, 31.69, 29.11, 29.00, 25.49, 25.34, 22.56, 21.28, 21.16, and 14.02 ppm.

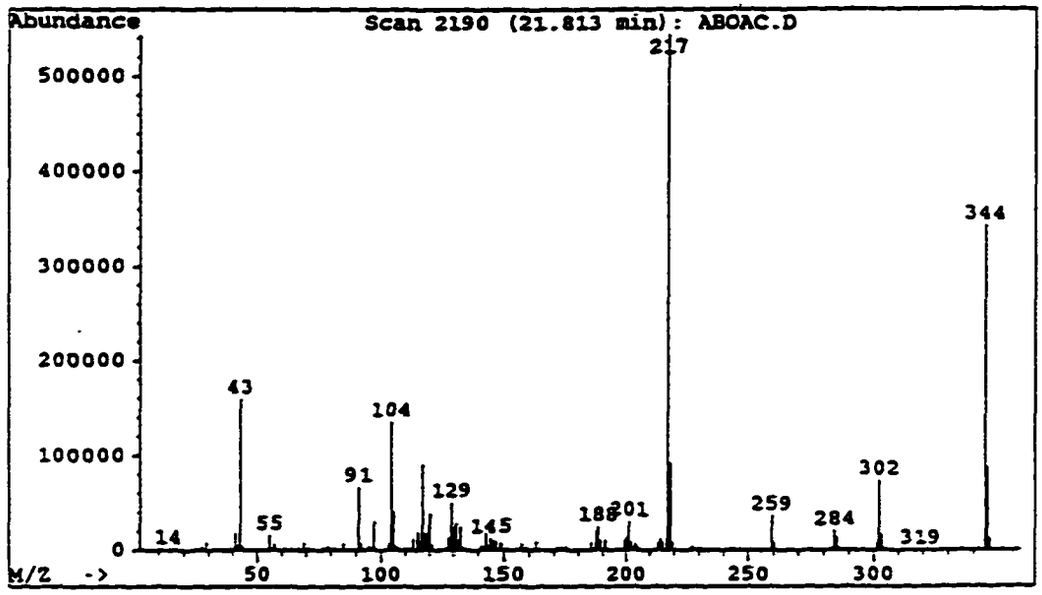

Figure 3 – 32. Mass spectrum of 1-(*α*-acetoxyheptyl)-4-(*β*-acetoxyoctyl)benzene.

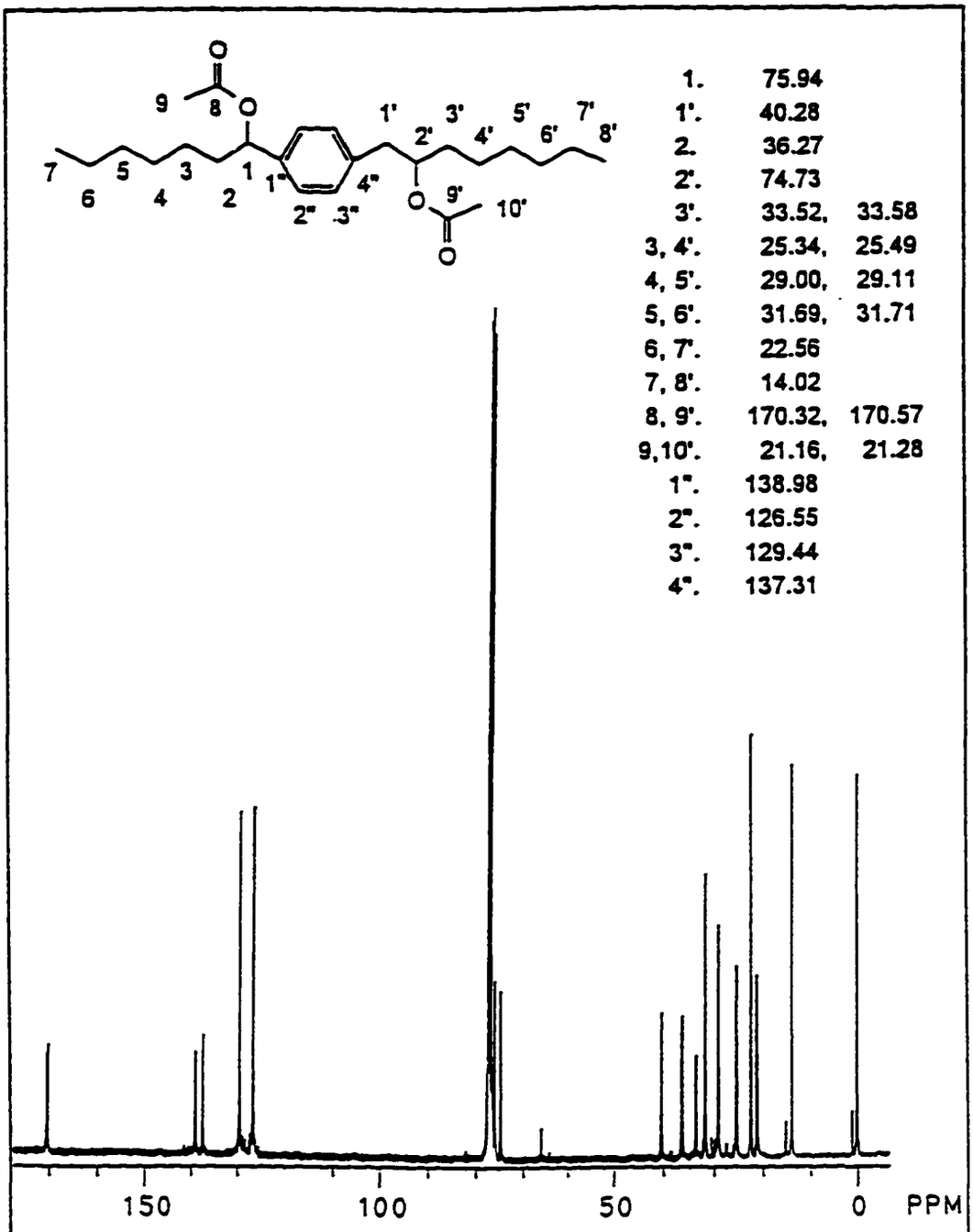

Figure 3-33. Carbon-13 NMR spectrum (75.57 MHz) and peak assignments of 1-(alpha-acetoxyheptyl)-4-(beta-acetoxyoctyl)benzene.

3.3 Preparation and Characterization of Poly(vinyl acetate - *co* - acetylene)

3.3.1 Materials

(1) *trans*-2-Nonenal, $CH_3(CH_2)_5CH=CHCHO$, 25,565-3, 97%, bp 88 – 90 °C/12 mm, Aldrich Chemical Company, Inc.

(2) Hexylmagnesium bromide, $CH_3(CH_2)_4CH_2MgBr$, 25,502-5, 2.0 M solution in ether, Aldrich Chemical Company, Inc.

(3) Magnesium sulfate, $MgSO_4$, M65-500, anhydrous, Fisher Scientific Co.

(4) Sodium bicarbonate (sodium hydrogen carbonate), $NaHCO_3$, S233-500, Fisher Scientific Co.

(5) Pyridine, C_5H_5N, 27,097-0, anhydrous, 99.8%, bp 115 °C, Aldrich Chemical Company, Inc.

(6) Acetic anhydride, $(CH_3CO)_2O$, 32,010-2, 99+%, bp 138 – 140 °C, Aldrich Chemical Company, Inc.

(7) 1-Heptyne, $CH_3(CH_2)_4C\equiv CH$, 24,441-4, 98%, bp 99 – 100 °C, Aldrich Chemical Company, Inc.

(8) Diisobutylaluminum hydride, $[(CH_3)_2CHCH_2]_2AlH$, 25685-4, 1.0 M in heptane, Aldrich Chemical Company, Inc.

(9) *n*-Butyllithium, $CH_3(CH_2)_3Li$, 30,212-0, 2.0 M solution in cyclohexane, Aldrich Chemical Company, Inc.

(10) 1,2-Epoxyhexane, $C_6H_{12}O$, 37,717-1, bp 118 – 120 °C, Aldrich

Chemical Company, Inc.

(11) *trans*-4-Decenal, $CH_3(CH_2)_4CH=CH(CH_2)_2CHO$, 36,733-8, 95%, bp 90–100 °C/15 mm, Aldrich Chemical Company, Inc.

(12) 6-Undecanol, $CH_3(CH_2)_4CH(OH)(CH_2)_4CH_3$, 94,080, 98+%, mp 23–26 °C, Fluka Chemical Corp.

(13) Bromine, Br_2, B385-250, bp 59.5 °C, Fisher Scientific Co.

(14) Triphenylphosphine, $(C_6H_5)_3P$, T8,440-9, 99%, mp 79–81 °C, Aldrich Chemical Company, Inc.

(15) *N,N*-Dimethylformamide (DMF), $HCON(CH_3)_2$, 22,705-6, anhydrous, 99.8%, bp 153 °C, Aldrich Chemical Company, Inc.

(16) 1,8-Diazabicyclo[5.4.0]undec-7-ene (DBU), 13,900-9, 98%, bp 80–83 °C/0.6 mm, Aldrich Chemical Company, Inc.

(17) Dimethyl sulfoxide (DMSO), $(CH_3)_2SO$, 27,685-5, anhydrous, 99.8%, mp 18.4 °C, bp 189 °C, Aldrich Chemical Company, Inc.

(18) 2-Hepten-4-ol, $CH_3CH=CHCH(OH)(CH_2)_2CH_3$, 3206.00, 98%, Wiley Organics, Inc.

(19) Poly(vinyl acetate) (40% hydrolyzed), 17,561, nominal MW (presumably M_n) *ca.* 72,000, Polysciences, Inc.

(20) *n*-Hexane, $CH_3(CH_2)_4CH_3$, H303-4, Optima™, bp 68–72 °C, Fisher Scientific Co.

(21) Chloroform-*d*, $CDCl_3$, 15,185-8, 100 atom% *d*, bp 60.9 °C, Aldrich Chemical Company, Inc.

(22) Tetramethylsilane (TMS), $(CH_3)_4Si$, T2,400-7, 99.9%, NMR grade, bp 26–28 °C, Aldrich Chemical Company, Inc.

(23) Nitrogen, compressed gas, N_2, industrial grade, 99.998 vol. %, max. O_2 10.0 ppm (v/v), H_2O 3.5 ppm (v/v), Air Products and Chemicals, Inc.

(24) Silica gel, S744-1, 100-200 mesh, 150 Å pore size, Fisher Scientific Co.

3.3.2 Synthesis of *trans*-9-Acetoxy-7-pentadecene

General scheme 3 – 8

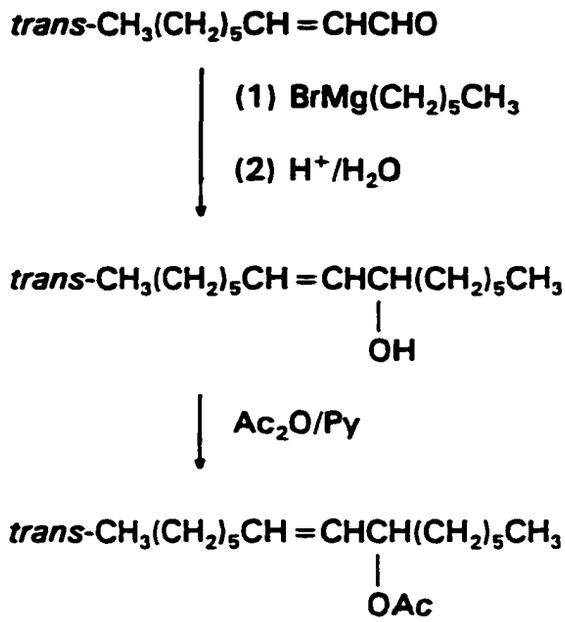

(i) Grignard Reaction

Under a nitrogen atmosphere, a solution of hexylmagnesium bromide (36 mmol) in ether was added dropwise at about 0 °C to a stirred solution of *trans*-2-nonenal (3.6 g, 27 mmol) in 50 mL of ether contained in a three-neck flask. The mixture was heated under reflux for 1 h, cooled to room temperature, diluted with 200 mL of ether, and decomposed with 200 mL of cold 2% aqueous sulfuric acid. The ether layer was separated, combined with 2 x 100 mL of ether extracts of the aqueous layer, and washed successively with water, 10% aqueous $NaHCO_3$, and water. The ether

solution was dried over anhydrous magnesium sulfate and concentrated under vacuum; then the mixture was purified by column chromatography on a 35 cm x 2.2 cm (*i. d.*) column, packed with 100 – 200 mesh silica gel, using ethyl actate/hexanes (1/10, v/v) as elution solvent, to give 1.5 g (25% yield) of *trans*-9-hydroxy-7-pentadecene (95% purity by GC/MS); mass spectrum (Fig. 3 – 34), m/e (%): 226 (7, $M^{\cdot+}$), 208 (5), 141 (100), 113 (39), 96 (41), 95 (30), 81 (60), 67 (63), and 43 (74).

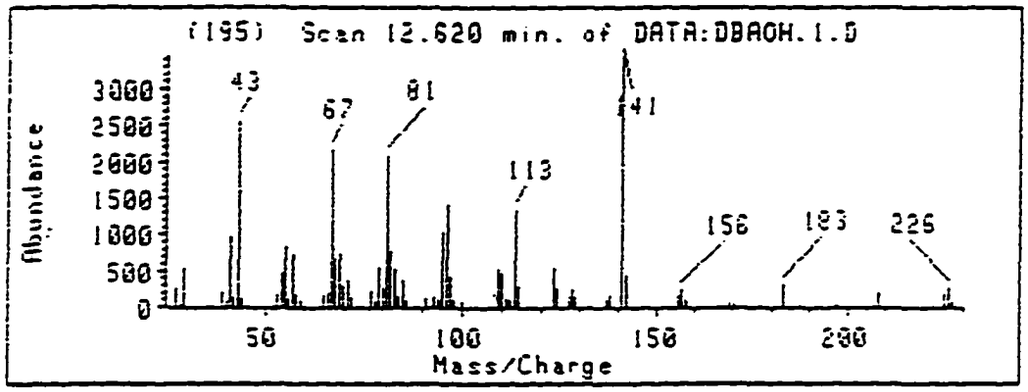

Figure 3 – 34. Mass spectrum of *trans*-9-hydroxy-7-pentadecene.

(ii) Acetylation

A solution of *trans*-9-hydroxy-7-pentadecene (0.56 g, 2.5 mmol) in 50 mL of ether was added to 15 mL of acetic anhydride/pyridine (1/2, v/v). The solution was stirred at about 35 °C overnight in flowing nitrogen, then cooled to room temperature and diluted with 100 mL of ether. The ether

layer was separated, washed with 3 x 100 mL of water, and dried over anhydrous magnesium sulfate. The solution was concentrated to give 0.64 g (95% yield) of residual *trans*-9-acetoxy-7-pentadecene (95% purity by GC/MS); mass spectrum (Fig. 3-35), m/e (%): 268 (0.4, $M^{\cdot+}$), 226 (15), 225 (12), 208 (13), 183 (11), 141 (82), 113 (21), 95 (33), 81 (55), 67 (61), and 43 (100); ^{13}C NMR (75.57 MHz, $CDCl_3$) (Fig. 3-36) δ 170.01, 134.21, 128.99, 75.07, 34.86, 32.33, 32.08, 31.89, 31.84, 31.61, 29.84, 29.47, 29.21, 28.88, 25.31, 22.66, 21.18, and 13.94 ppm.

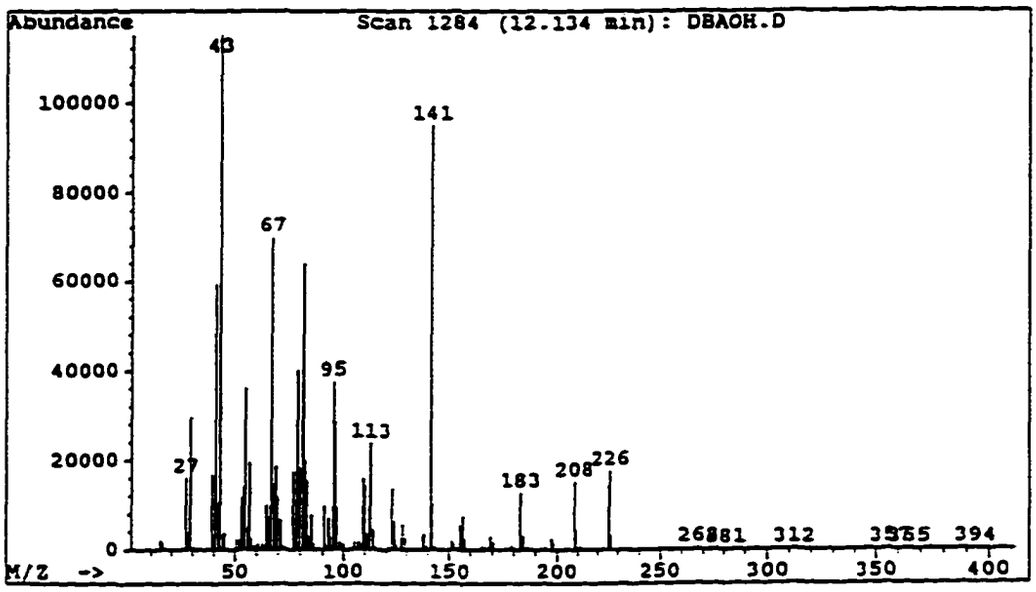

Figure 3-35. Mass spectrum of *trans*-9-acetoxy-7-pentadecene.

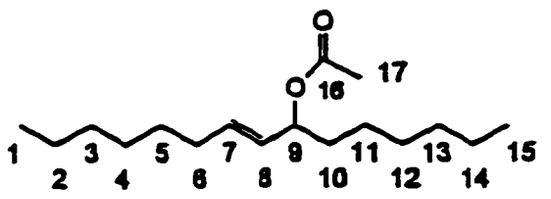

1, 15.	13.94	
2, 14.	22.66	
3, 6, 13.	32.33,	32.08
	31.89,	31.84
	31.61	
4, 5, 12.	29.84,	29.47
	29.21,	28.88
7.	134.21	
8.	128.99	
9.	75.07	
10.	34.86	
11.	25.31	
16.	170.01	
17.	21.18	

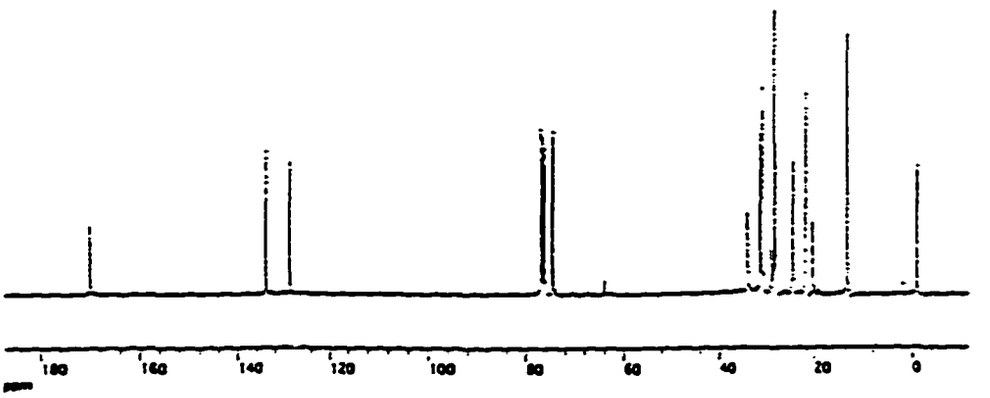

Figure 3-36. Carbon-13 NMR spectrum (75.57 MHz) and peak assignments of *trans*-9-acetoxy-7-pentadecene.

3.3.3 Synthesis of *trans*-9-Acetoxy-6-tridecene

General scheme 3 – 9

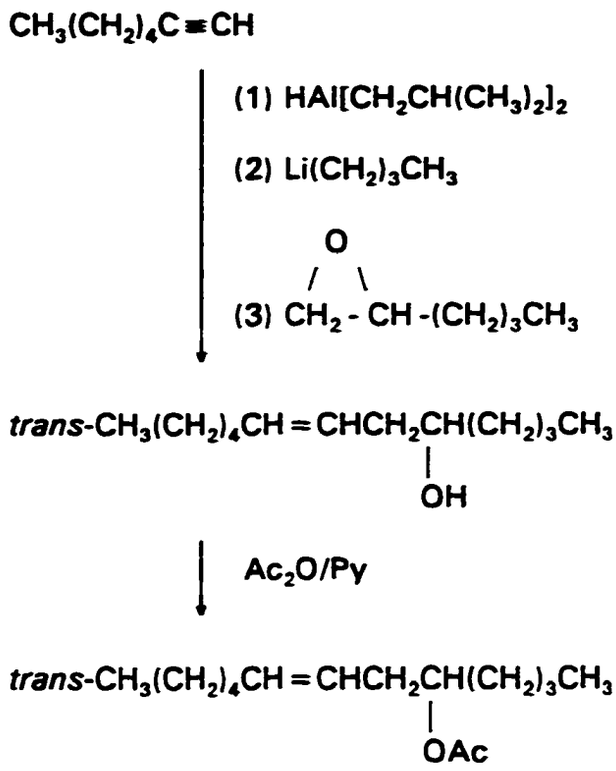

(i) Synthesis of *trans*-9-Hydroxy-6-tridecene

An organoaluminate intermediate was utilized to make the *β*-hydroxyalkene.[20-22] Under a nitrogen atmosphere in a three-neck flask, a solution of diisobutylaluminum hydride (50 mmol) in heptane was added dropwise with stirring at about 0 °C to 1-heptyne (9.6 g, 100 mmol). After the mixture had been stirred for 2 h at 50 °C, the excess 1-heptyne was removed under vacuum, and 200 mL of ether was added at room

temperature; then a solution of *n*-butyllithium (50 mmol) in cyclohexane was added dropwise at 0 °C. After the mixture had been stirred at 40 °C for 1/2 h, 1,2-epoxyhexane (5.0 g, 50 mmol) was added dropwise at room temperature. The mixture was heated under reflux for 1 h, then cooled to 0 °C and hydrolyzed with 10% aqueous hydrochloric acid. The organic layer was separated, combined with 2 x 200 mL of ether extracts of the aqueous layer, dried with anhydrous magnesium sulfate, and concentrated under vacuum. Short path distillation of the residue under reduced pressure gave 1.5 g (15% yield) of *trans*-9-hydroxy-6-tridecene (92% purity by GC/MS), bp 170–180 °C (10 torr); mass spectrum (Fig. 3–37), m/e (%): 198 (0.5, $M\cdot^+$), 180 (1), 112 (61), 83 (39), 69 (100), 56 (34), 41 (47), and 29 (17).

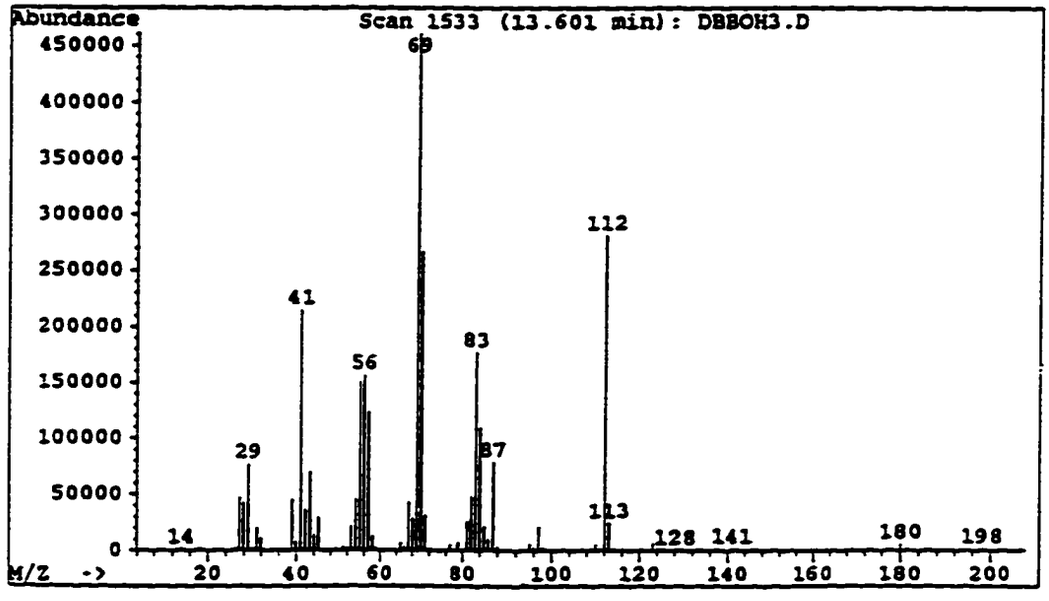

Figure 3–37. Mass spectrum of *trans*-9-hydroxy-6-tridecene.

(ii) Acetylation

A solution of *trans*-9-hydroxy-6-tridecene (1.0 g, 5 mmol) in 50 mL of ether was added to 30 mL of acetic anhydride/pyridine (1/2, v/v). The solution was stirred at about 35 °C overnight under a nitrogen atmosphere, then cooled to room temperature and diluted with 200 mL of ether. The ether layer was separated, washed with 4 x 150 mL of water, and dried over anhydrous magnesium sulfate. The solution was concentrated under vacuum to give 1.1 g (92% yield) of residual *trans*-9-acetoxy-6-hexadecene (*ca.* 99% purity by NMR); mass spectrum (Fig. 3 – 38), m/e (%): 197 (0.3), 180 (35), 129 (8), 110 (13), 96 (25), 81 (20), 67 (22), 55 (11), and 43 (100); ^{13}C NMR (75.57 MHz, $CDCl_3$) (Fig. 3 – 39) δ 170.54, 133.89, 125.13, 73.98, 37.59, 33.38, 32.62, 31.44, 29.24, 27.61, 22.64, 21.14, 14.00, and 13.96 ppm.

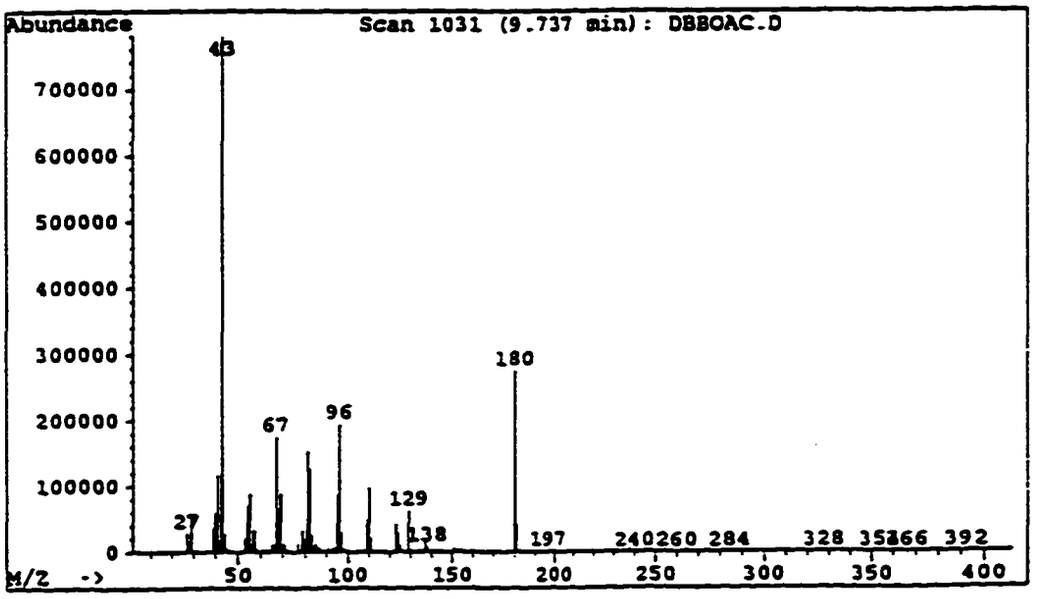

Figure 3 – 38. Mass spectrum of *trans*-9-acetoxy-6-tridecene.

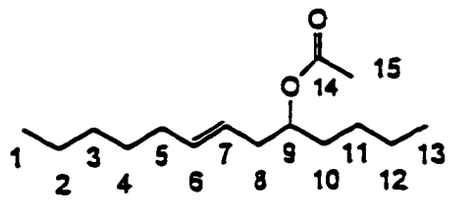

1, 13.	13.96, 14.00
2, 12.	22.64
3.	32.62
4.	29.24
5.	31.44
6.	133.89
7.	125.13
8.	33.38
9.	73.98
10.	37.59
11.	27.61
14.	170.54
15.	21.14

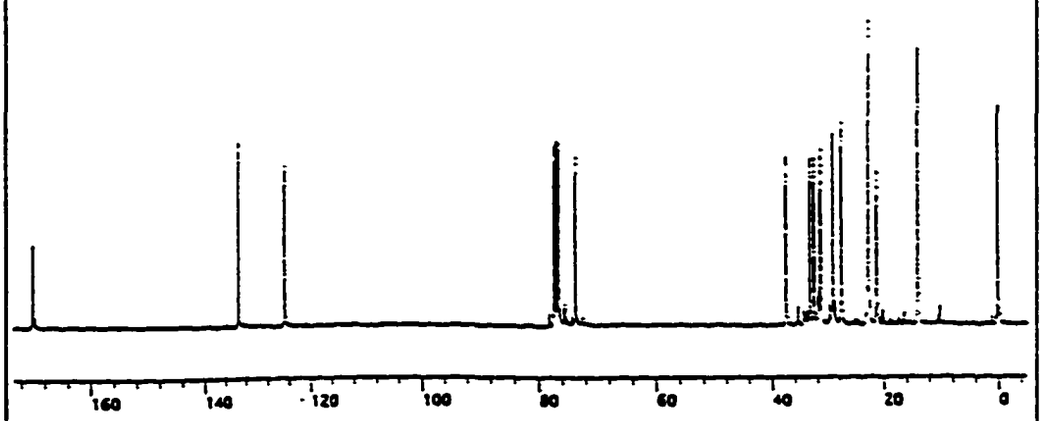

Figure 3-39. Carbon-13 NMR spectrum (75.57 MHz) and peak assignments of *trans*-9-acetoxy-6-tridecene.

3.3.4 Synthesis of *trans*-10-Acetoxy-6-hexadecene

General scheme 3 – 10

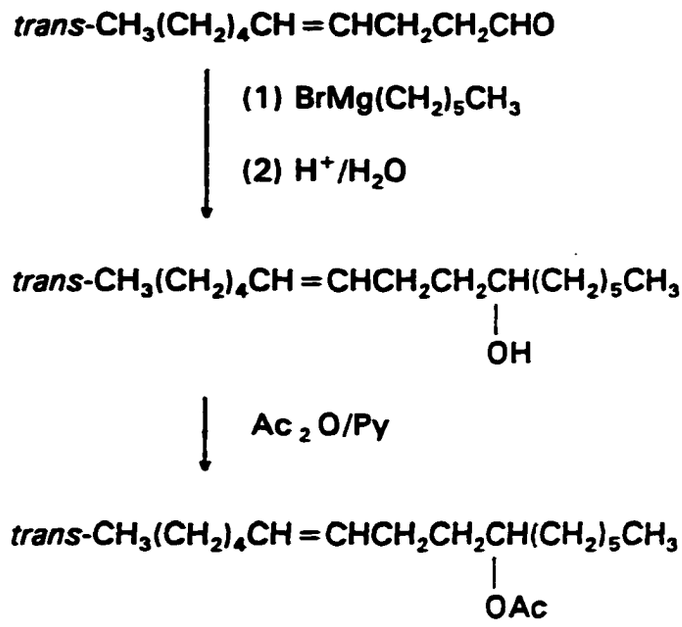

(i) Grignard Reaction

Under a nitrogen atmosphere, a solution of hexylmagnesium bromide (40 mmol) in ether was added dropwise at about 5 °C to a stirred solution of *trans*-4-decenal (3.12 g, 20 mmol) in 50 mL of ether contained in a three-neck flask. The mixture was heated under reflux for 1 h, cooled to room temperature, diluted with 200 mL of ether, and then decomposed with 200 mL of cold 2% aqueous sulfuric acid. The ether layer was separated, combined with 2 x 100 mL of ether extracts of the aqueous layer, and washed successively with water, 10% aqueous $NaHCO_3$, and water. The

ether solution was dried over anhydrous magnesium sulfate and concentrated under vacuum. The mixture was separated by column chromatography on a 35 cm x 2.2 cm (*i. d.*) column packed with 100 – 200 mesh silica gel, using ethyl acetate/hexanes (1/10, v/v) as elution solvent, to give 0.5 g (10% yield) of *trans*-10-hydroxy-6-hexadecene (95% purity by GC/MS); mass spectrum (Fig. 3 – 40), m/e (%): 240 (6, $M^{+}\cdot$), 222 (96), 197 (10), 183 (33), 155 (100), 137 (22), 124 (42), 113 (34), 95 (42), 81 (40), 69 (28), 55 (33), 43 (17), and 41 (22).

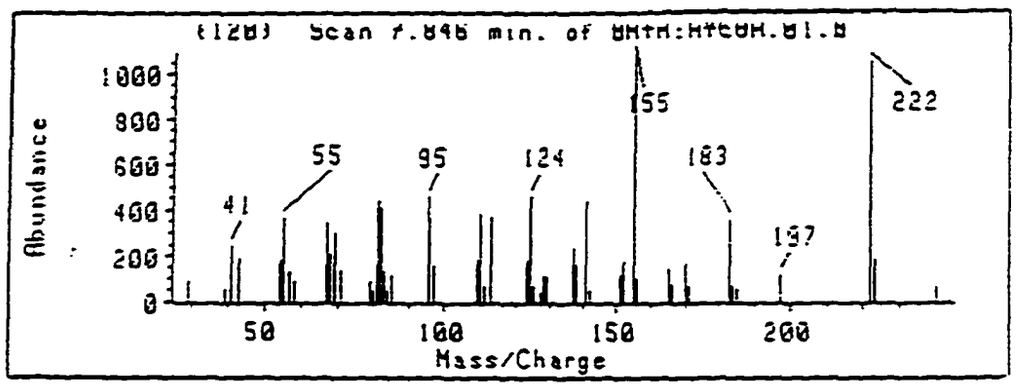

Figure 3 – 40. Mass spectrum of *trans*-10-hydroxy-6-hexadecene.

(ii) Acetylation

A solution of *trans*-10-hydroxy-6-hexadecene (0.3 g, 1.25 mmol) in 50 mL of ether was added to 15 mL of acetic anhydride/pyridine (1/2, v/v). The solution was stirred at about 35 °C overnight in flowing nitrogen, then

cooled to room temperature and diluted with 100 mL of ether. The ether layer was separated, washed with 4 x 100 mL of water, and dried over anhydrous magnesium sulfate. Then the solution was concentrated under vacuum to give 0.34 g (96% yield) of residual *trans*-10-acetoxy-6-hexadecene (95% purity by GC/MS); mass spectrum (Fig. 3-41), m/e (%): 222 (11), 152 (6), 124 (54), 96 (86), 95 (73), 82 (92), 81 (91), 67 (91), 55 (49), 43 (100), and 41 (44); ^{13}C NMR (75.57 MHz, $CDCl_3$) (Fig. 3-42) δ 170.51, 131.29, 129.36, 129.25, 74.16, 34.36, 32.60, 31.86, 31.53, 29.37, 29.30, 28.58, 25.36, 22.60, 21.10, and 13.94 ppm.

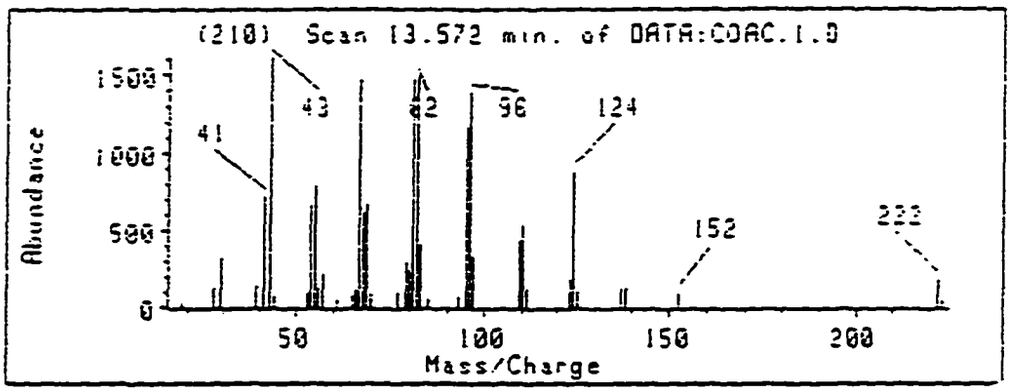

Figure 3-41. Mass spectrum of *trans*-10-acetoxy-6-hexadecene.

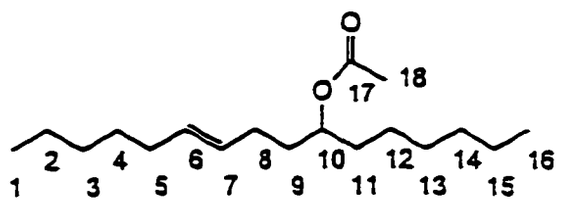

1, 16.	13.94	
2, 8, 15.	22.60	
3, 14.	31.53,	31.86
4, 13.	29.30,	29.37
5.	28.58	
6.	131.29	
7.	129.25,	129.36
8.	32.60	
10.	74.16	
11.	34.36	
12.	25.36	
17.	170.51	
18.	21.10	

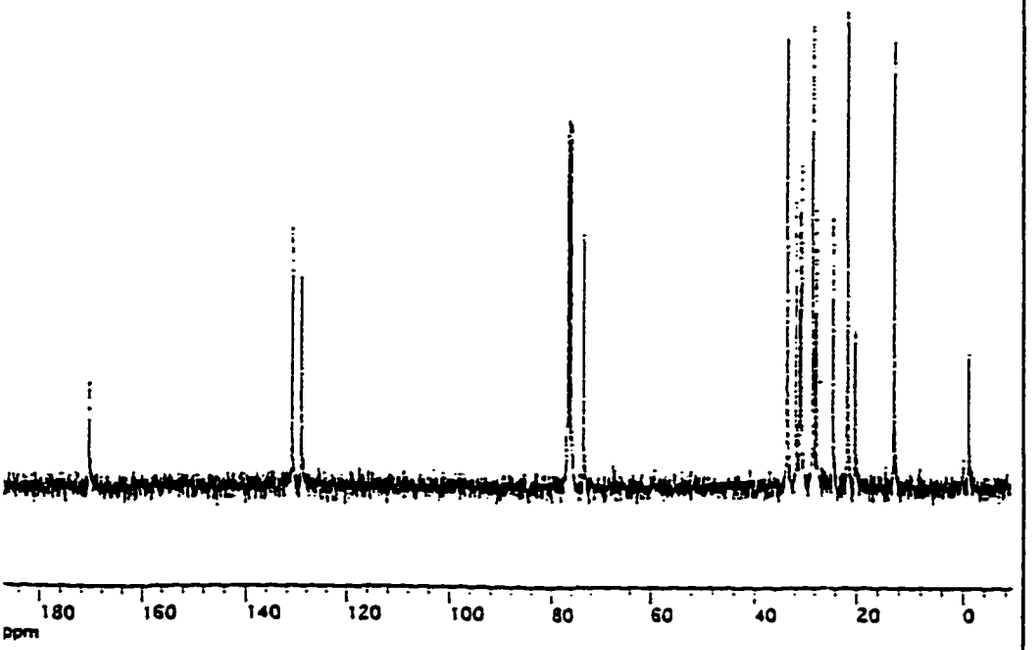

Figure 3-42. Carbon-13 NMR spectrum (75.57 MHz) and peak assignments of *trans*-10-acetoxy-6-hexadecene.

3.3.5 Bromination of Model Compound 6-Undecanol

The bromination reagents, bromine and triphenylphosphine, were reported to give no elimination or rearrangement.[23] The published procedure was modified so that the same conditions also could be used for the polymeric system. Triphenylphosphine (11.79 g, 45 mmol) and 6-undecanol (5.16 g, 30 mmol) were dissolved in 100 mL of DMF in a three-neck flask equipped with a magnetic stirrer, a nitrogen inlet tube, an addition funnel, and a reflux condenser. After a solution of bromine (0.53 g, 3.3 mmol) in 10 mL of DMF had been added dropwise at 50 °C, the temperature was maintained at 50 °C for several hours. During the reaction, several portions of the reaction mixture (*ca.* 5 mL each) were removed with a syringe, then diluted with ether, washed with water, dried with anhydrous magnesium sulfate, concentrated under vacuum, and analyzed by GC/MS (Fig. 3–43). The reaction was complete after 2 h, and there was no significant side reaction after several more hours of heating. The yield of brominated product based on bromine was estimated to be around 64%, as the area ratio of RBr/ROH in the GC/MS trace was about 7.6/100. The results were confirmed by comparison with the GC/MS and NMR data of pure 6-bromoundecane, obtained by complete conversion of the alcohol with a 1.1/1 ratio of bromine/6-undecanol under the same conditions. Mass spectrum of 6-bromoundecane, m/e (%): 155 (16), 113 (4), 99 (9), 85 (35), 71 (49), 57 (100), 43 (66), and 41 (47); ^{13}C NMR (75.57 MHz, $CDCl_3$) (Fig.

3-44) δ 58.32, 39.37, 31.44, 27.35, 22.58, and 13.93 ppm.

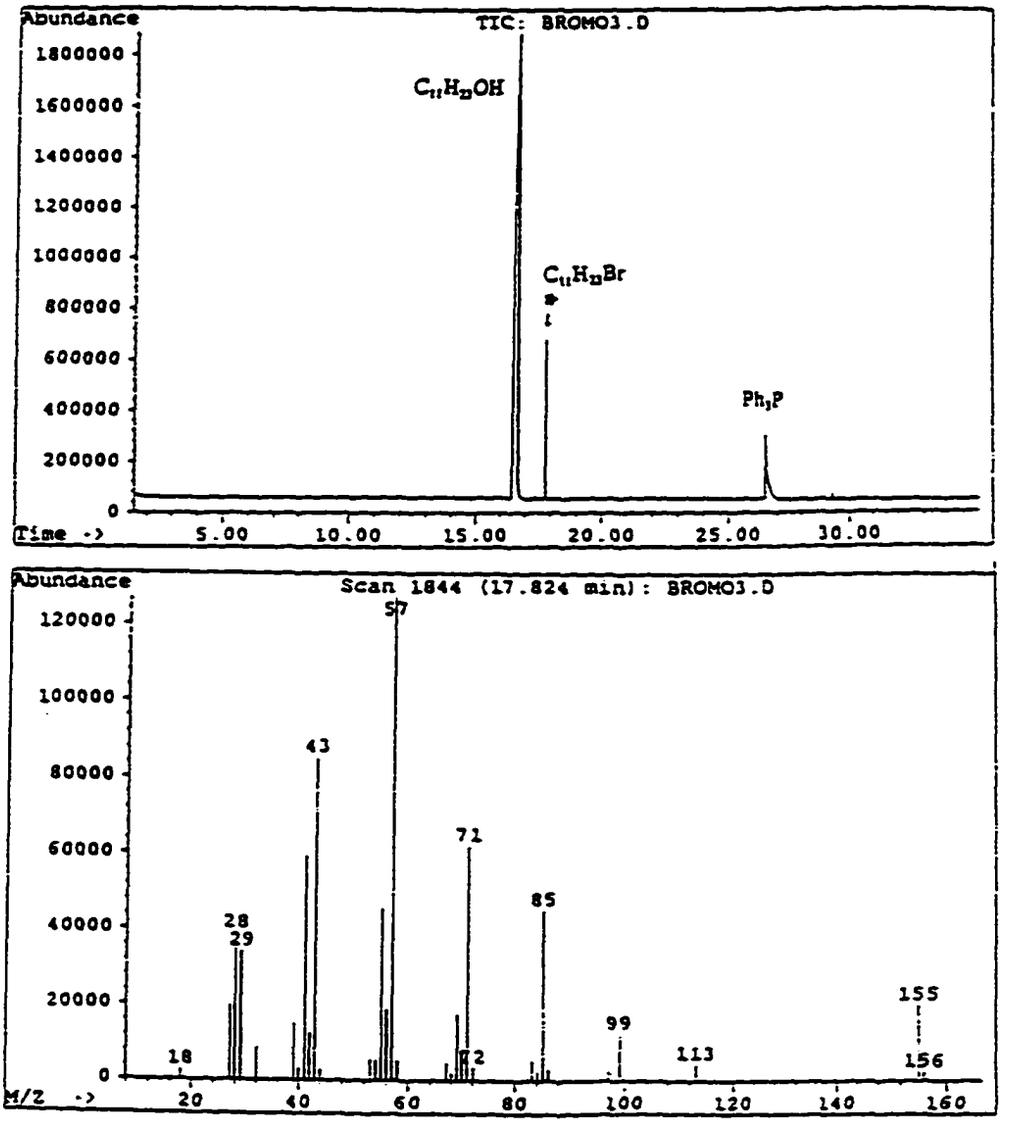

Figure 3-43. GC/MS results for the bromination product after 3 h.

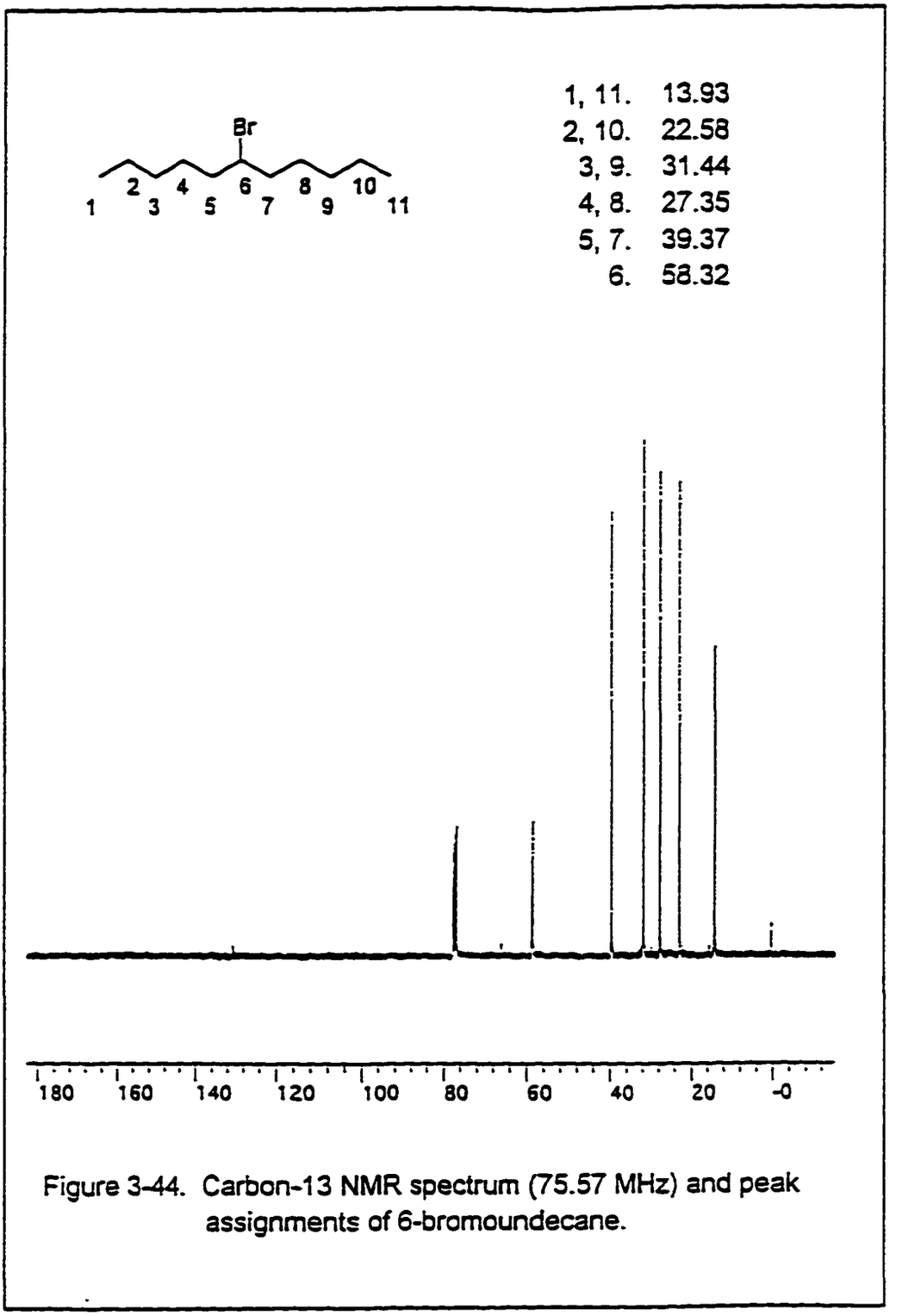

Figure 3-44. Carbon-13 NMR spectrum (75.57 MHz) and peak assignments of 6-bromoundecane.

3.3.6 Elimination Reaction of Model Compound 6-Bromoundecane

The dehydrobromination reaction was reported to proceed quite rapidly at relatively low temperature when 1,8-diazabicyclo[5.4.0]undec-7-ene (DBU) was the basic reagent.[24] A solution of 6-bromoundecane (0.30 g, 1.3 mmol), 6-undecanol (0.32 g, 1.9 mmol), and DBU (4.56 g, 30 mmol) in 50 mL of DMSO was stirred at 60 °C under a nitrogen atmosphere for several hours. During the reaction, several portions of the reaction mixture (*ca.* 5 mL each) were removed with a syringe, then diluted with ether, washed with water, dried with magnesium sulfate, concentrated under vacuum, and analyzed by GC/MS (Fig. 3−45). The elimination reaction was complete after 3 h, and there was no significant side reaction upon several more hours of heating. Mass spectrum of the elimination product 5-undecene, m/e (%): 154 (16, $M\cdot^{+}$), 111 (4), 97 (12), 83 (18), 69 (59), 55 (100), and 41 (56).

Under the same conditions, no elimination products were formed from the allylic model compounds, *trans*-9-acetoxy-7-pentadecene and 2-hepten-4-ol.

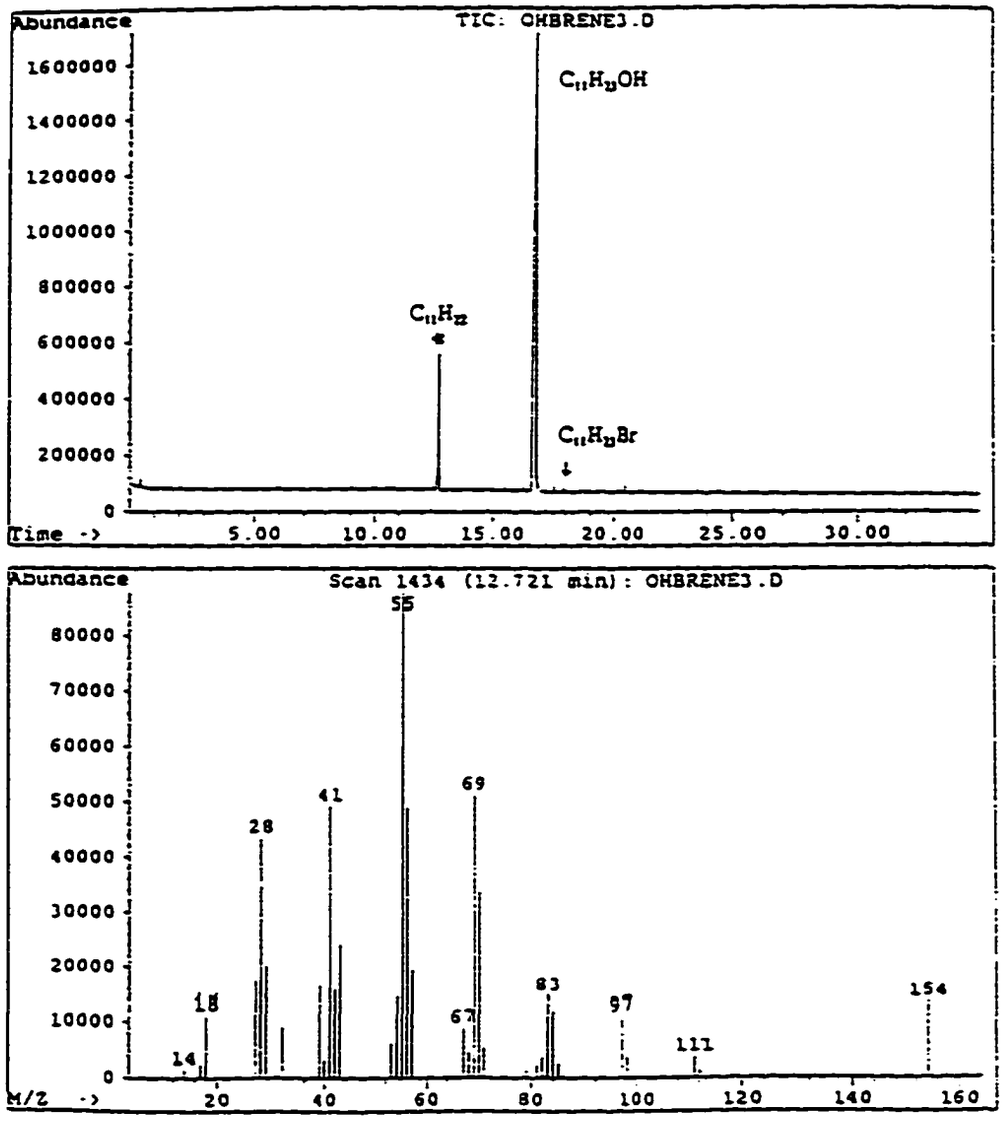

Figure 3–45. GC/MS results for the elimination product after 3 h.

3.3.7 Modification of Poly(vinyl acetate-*co*-vinyl alcohol)

General scheme 3 – 11

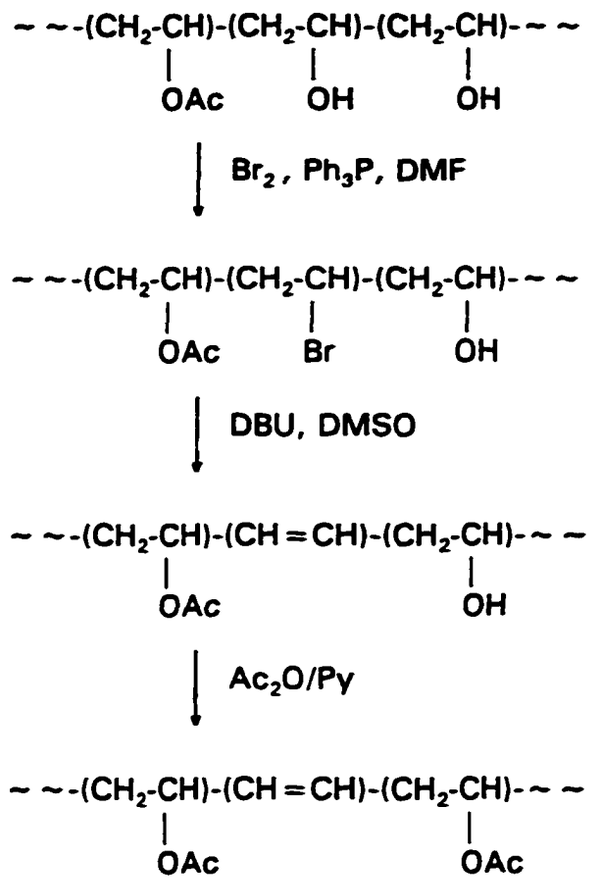

Poly(vinyl acetate) (40% hydrolyzed) (MW *ca.* 72,000) (6.92 g, 100 mmol of monomer units) was brominated with bromine (0.38 g, 2.4 mmol) and triphenylphosphine (15.74 g, 60 mmol) at 50 °C for 3 h under conditions similar to those described in Section 3.3.5. The resultant polymer was purified by successive precipitations from acetone solutions into 2% aqueous $NaHCO_3$, water, and *n*-hexane; then dried in a vacuum

oven (*ca.* 2 torr) for 1 day at room temperature.

Elimination of HBr from the brominated polymer (4.49 g, 65 mmol of monomer units) was done with DBU (4.56 g, 30 mmol) in DMSO at 80 °C for 3 h under a nitrogen atmosphere as in Section 3.3.6. The resultant polymer was purified by successive precipitations from acetone solutions into *n*-hexane, water, and *n*-hexane; then dried in a vacuum oven (*ca.* 2 torr) at 50 °C for 2 days.

The polymer was acetylated with 150 mL of acetic anhydride/pyridine (1/2, v/v) under a nitrogen atmosphere at 45 °C overnight. The resulting polymer was purified by successive precipitation from acetone solutions into *n*-hexane, water, and *n*-hexane. Then a polymer film deposited from an acetone solution was dried in a vacuum oven (*ca.* 2 torr) at room temperature for 1 day and at 60 °C for 4 days.

3.3.8 Reference Poly(vinyl acetate)

Poly(vinyl acetate) (40% hydrolyzed) (MW *ca.* 72,000) (3.46 g) was acetylated, purified, and dried in the same way as above, to get a reference poly(vinyl acetate) sample.

3.3.9 Carbon – 13 NMR Spectroscopy

The ^{13}C NMR spectra of the modified and reference polymer samples were obtained under conditions same as those given in Section 3.1.5 for the

poly(vinyl acetate) samples made by solution polymerization.

CHAPTER 4

RESULTS AND DISCUSSION

4.1 PVAc Prepared by Solution Polymerization in Benzene

4.1.1 Solution Polymerization of VAc in Benzene

The poly(vinyl acetate) samples were prepared by solution polymerization in benzene at about 80 °C under a nitrogen atmosphere, using AIBN as free-radical initiator (1.0 mM); and the conversions were kept low (*ca.* 5%) by controlling the reaction time. The conditions of high temperature and low conversion were chosen in order to increase the concentration of possible microstructures formed via chain transfer to the solvent. Several different solvent/monomer ratios were used in order to study solvent effects on the polymer microstructures.

The molecular weight (MW) of PVAc prepared with a 30/1 (mol/mol) benzene/monomer ratio was determined by the intrinsic viscosity method, using the Mark-Houwink equation: $[\eta] = K \cdot M_v^a$; where $K = 1.76 \times 10^{-4}$ (dL/g), and $a = 0.68$ in acetone at 30 °C.[1] The number-average molecular weight (M_n) was estimated from the equation: $M_n = 0.72\ M_v$.[2]

The intrinsic viscosity was obtained as $[\eta] = 0.118$ (dL/g) by extrapolation of η_{sp}/C versus C (Figure 4−1), and the M_v, M_n, and DP were then calculated to be 1.4×10^4, 1.0×10^4, and 1.2×10^2, respectively. The poor linear relationship was caused by the low polymer MW, which made the value of $\eta_{sp} = (\eta - \eta_o)/\eta_o$ too small to be measured accurately, inasmuch as the accuracy of the stopwatch was about 0.1 s. The estimated error in DP was $\pm 0.1 \times 10^2$.

4.1.2 Estimation of the Chemical Shifts of the Aromatic Carbons in the Possible Microstructures Formed via Chain Transfer to Benzene

(1) ^{13}C NMR Chemical Shift Increments of Acetoxy Group

The chemical shift increments of the acetoxy group (— OAc) on the aromatic carbons (Table 4−1) were calculated by comparing the chemical shifts of these carbons in the reference compound, *n*-octylbenzene, with those in *α*-acetoxydecylbenzene,[2] *β*-acetoxyundecylbenzene,[2] *γ*-acetoxynonylbenzene (see Fig. 3−4 in Section 3.2.3), and *δ*-acetoxydecylbenzene (see Fig. 3−9 in Section 3.2.4).

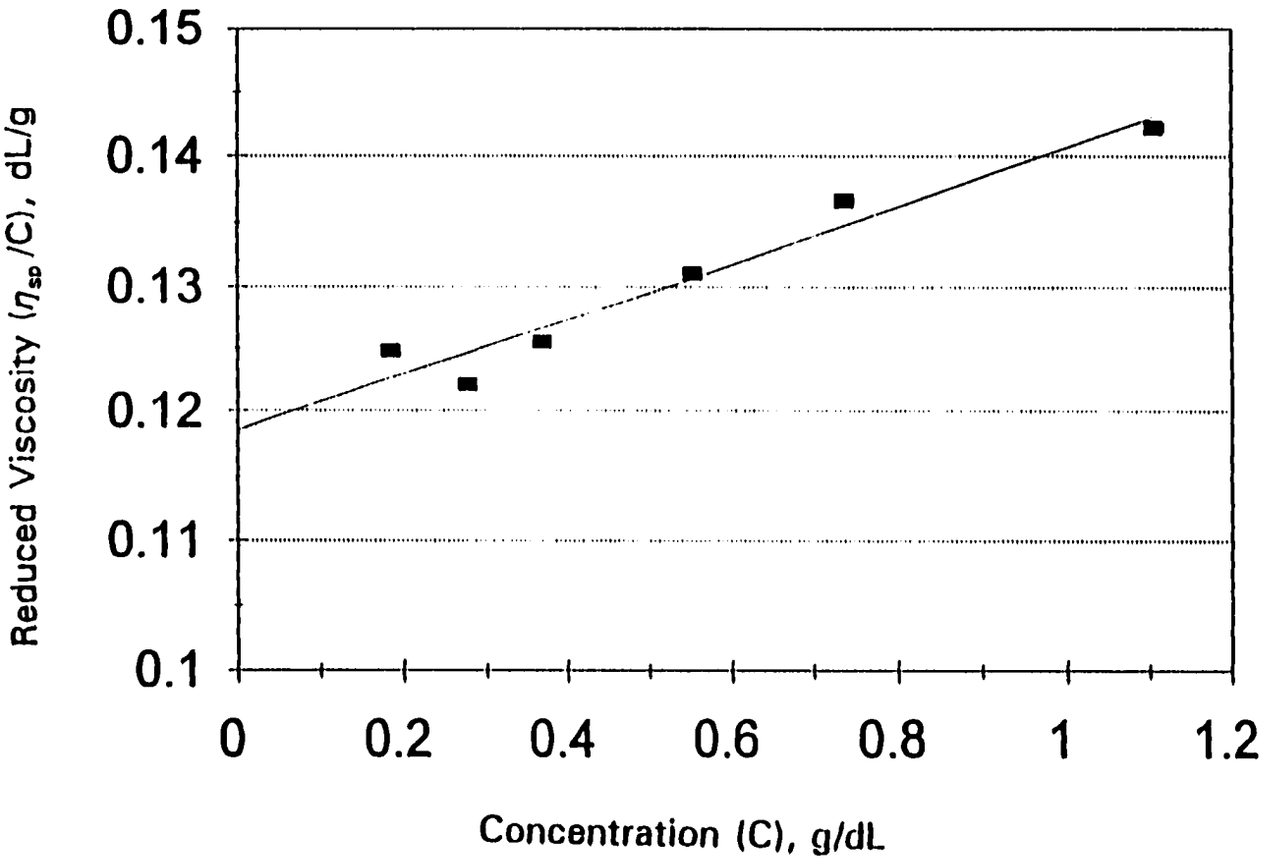

Figure 4 – 1. Plot of η_{sp}/C versus C at 30 °C for acetone solutions of PVAc prepared with a benzene/monomer ratio of 30/1.

Table 4−1. ^{13}C NMR Chemical Shift Increments $\Delta\delta_{ik}$ of the Acetoxy Group on Aromatic Carbons

	H	α	β	γ	δ
δ_1 $\Delta\delta_1$	142.96	140.97 -1.99	137.71 -5.25	141.75 -1.21	142.17 -0.79
δ_2 $\Delta\delta_2$	128.40	126.56 -1.84	129.40 1.00	128.39 -0.01	128.37 -0.03
δ_3 $\Delta\delta_3$	128.21	128.36 0.15	128.27 0.06	128.31 0.10	128.31 0.10
δ_4 $\Delta\delta_4$	125.54	127.75 2.21	126.38 0.84	125.88 0.34	125.77 0.23

i: position of acetoxy group, α, β, γ, δ;

k: position of the aromatic carbons, 1, 2, 3, 4.

(2) Estimation of ^{13}C Chemical Shifts of the Microstructures

The extended Grant-Paul additivity rule for chemical shifts can be expressed as equation 4−1:[3,4]

$$\delta_k = \delta_{k,RH} + \sum_i \Delta\delta_{ik} \qquad (4-1)$$

δ_k: chemical shift of the carbon in position k (k = 1, 2, 3, 4 in the aromatic ring, i.e., ipso-, ortho-, meta-, para-);

$\delta_{k,RH}$: chemical shift of corresponding carbon k in reference compound RH;

$\Delta\delta_{ik}$: chemical shift increment of the substituent in position i

(i = α, β, γ, δ) with respect to the aromatic ring, on the carbon in position k.

The validity of the additivity rule was confirmed by the comparisons of estimated with measured shifts that are shown in Table 4−2. Here the reference compounds used were *n*-octylbenzene and 1,4-di-*n*-butylbenzene (δ_1 = 139.99, δ_2 = 128.28 ppm).[5] The multiplicity of some peaks was caused by the diastereomeric isomerism of some of the compounds, corresponding to the n-ad microstructures of the polymer chain.

Estimated chemical shifts are given in Table 4−3 for the possible aromatic microstructures in PVAc that are formed by chain transfer to benzene (see Section 2.1 for their formation mechanisms). The expected accuracy of these shifts is around 0.2 ppm.

4.1.3 Estimation of the Concentration of the Microstructures

(1) Rate Constants at 80 °C by Arrhenius Equation

The chain transfer constant to monomer at 80 °C was calculated to be 2.23×10^{-4} from the intercept at 1/353.2 (80 °C) of a plot of $\ln(C_M)$ versus 1/T (Fig. 4−2).[6]

The chain transfer constant to initiator at 80 °C was calculated to be 0.233 from the values of 0.025 (50 °C) and 0.055 (60 °C).[6]

$$C_I = K_{tr.I}/K_p = (A_{tr.I}/A_p) \exp[-(E_{tr.I} - E_p)/RT] \qquad (4-2)$$

Table 4-2. Estimated and Measured Chemical Shifts (ppm) of the Aromatic Carbons in the Multi-acetoxy Model Compounds

Model Compounds	Estimated	Measured
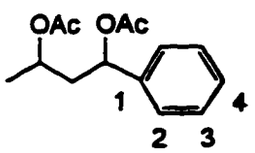	1. 139.76 2. 126.55 3. 128.46 4. 128.09	1. 140.38, 139.93 2. 126.49, 126.34 3. 128.55 4. 128.16, 128.03
	(See Fig. 3-13 in Section 3.2.5.)	
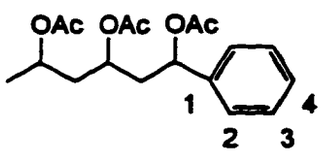	1. 139.68 2. 126.55 3. 128.46 4. 128.09	1. 140.20, 140.01, 139.71 2. 126.62, 126.53, 126.36 3. 128.57 4. 128.20, 128.09
	(See Fig. 3-18 in Section 3.2.6.)	
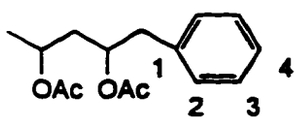	1. 136.92 2. 129.37 3. 128.37 4. 126.61	1. 137.05, 136.97 2. 129.46, 129.43 3. 128.37 4. 126.58
	(See Fig. 3-23 in Section 3.2.7.)	
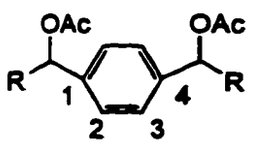	1, 4. 140.21 2, 3. 126.59	1, 4. 140.42 2, 3. 126.58
	(See Fig. 3-27 in Section 3.2.8.)	
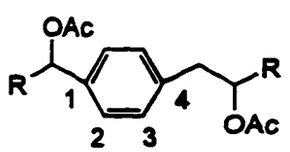 (R = -C_6H_{13} -n)	1. 138.84 2. 126.50 3. 129.43 4. 136.95	1. 138.98 2. 126.55 3. 129.44 4. 137.31
	(See Fig. 3-33 in Section 3.2.9.)	

Table 4-3. Estimated Chemical Shifts of the Aromatic Carbons in the Possible Microstructures Formed via Chain Transfer to Benzene

Polymer Microstructures	Reference Compounds	Chemical Shifts (ppm)
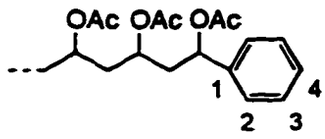 AR-II	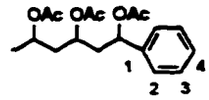	1. 139.61 – 140.30 2. 126.26 – 126.72 3. 128.47 – 128.67 4. 127.99 – 128.30
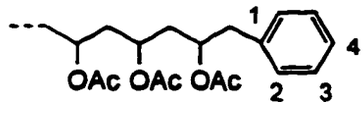 AR-I	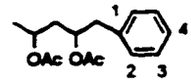	1. 136.87 – 137.15 2. 129.33 – 129.56 3. 128.27 – 128.47 4. 126.48 – 126.68
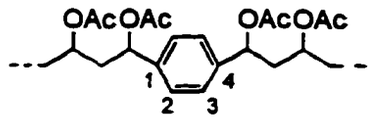 AR-IV	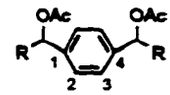	1, 4. 139.35 – 139.75 2, 3. 126.47 – 126.87
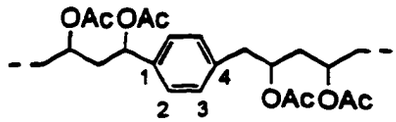 AR-III	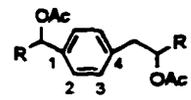 (R = -C_6H_{13}-n)	1. 137.80 – 138.20 2. 126.54 – 126.74 3. 129.31 – 129.71 4. 136.66 – 137.06

(See Schemes 2-1, 2-2, and 2-3 in Section 2.1 for the formation mechanisms.)

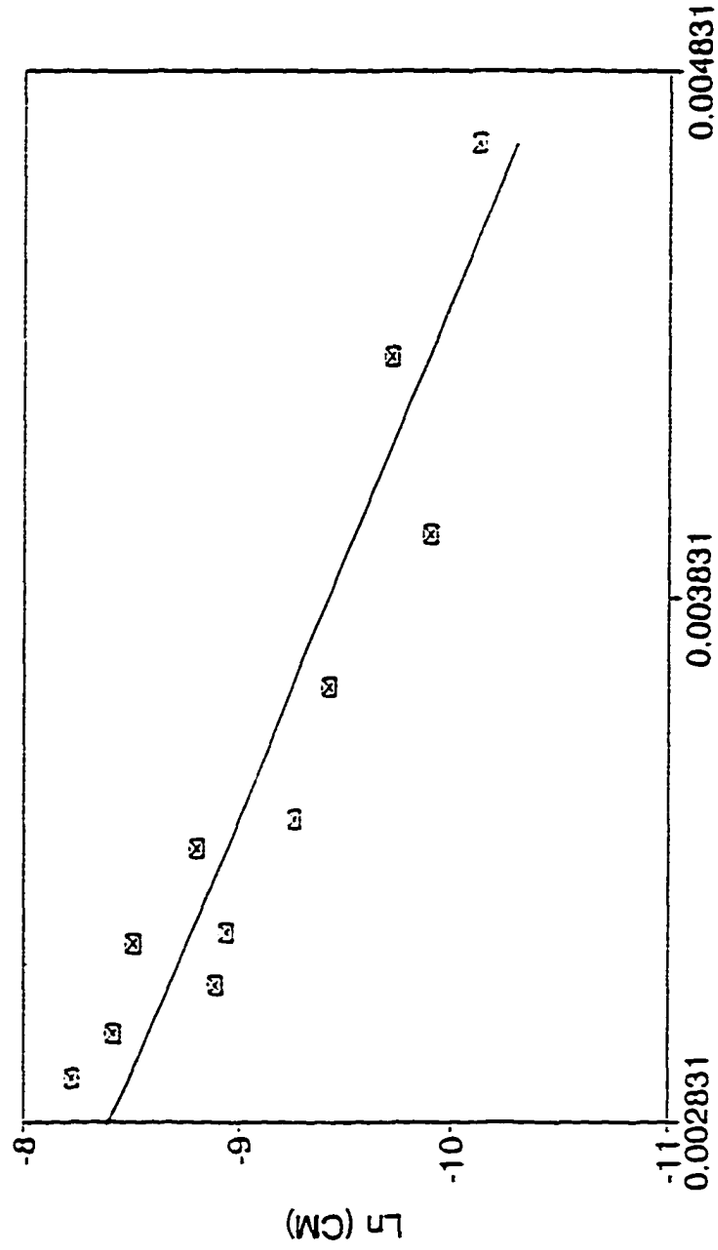

Figure 4 – 2. Plot of $Ln(C_M)$ versus 1/T for vinyl acetate.

The chain transfer constant to benzene at 80 °C was calculated to be 2.26×10^{-4} from the values of 1.77×10^{-4} (60 °C) and 2.13×10^{-4} (75 °C).[6]

$$C_B = K_{tr,B}/K_p = (A_{tr,B}/A_p) \exp[-(E_{tr,B} - E_p)/RT] \qquad (4-3)$$

The chain transfer to polymer was considered to be negligible at very low conversion (~5%) and, in any event, would not have affected the number-average molecular weight.

The rate constant of propagation (k_p) at 80 °C was calculated to be 4.3×10^3 (L/mol·s) from the following equation.[7]

$$k_p = 3.2 \times 10^7 \exp[-3150/T] \text{ (L/mol·s)} \qquad (4-4)$$

The rate constant of termination (k_t) at 80 °C was calculated to be 4.0×10^7 (L/mol·s) from the following equation.[7]

$$k_t = 3.7 \times 10^9 \exp[-1600/T] \text{ (L/mol·s)} \qquad (4-5)$$

The decomposition rate constant of AIBN (k_d) at 80 °C was calculated to be 1.33×10^{-4} (s^{-1}) from the following equation.[8]

$$k_d = 1.58 \times 10^{15} \exp[-128.9 \text{ KJ/RT}] \qquad (4-6)$$

(2) Molecular Weight Calculation

If we assume that there was no volume change during mixing, the monomer concentration is 0.375 M for the 30/1 (mol/mol) benzene/monomer mixture (Section 3.1). The concentration of AIBN is 1.0 mM, and its initiation efficiency used is 0.6. The number-average degree of

polymerization for the resultant PVAc sample was calculated from the Mayo equation[9] (Eqs. 1.3 and 1.4 in Section 1.4) to be 102 (for termination by disproportionation, a = 2) or 115 (for termination by combination, a = 1):

$$(\overline{DP})^{-1} = \frac{a(f \cdot k_t \cdot k_d \cdot [I])^{1/2}}{k_p [M]} + C_M + C_{tr,B}\frac{[B]}{[M]} + C_I\frac{[I]}{[M]} \qquad (4-7)$$

The corresponding M_n's, 8.8×10^3 and 9.9×10^3, agree with the value obtained by the viscosity method (1.0×10^4) within the experimental error.

(3) The Concentration of Microstructures

The molar ratio of benzene incorporated to VAc polymerized was calculated by considering the chain transfer and the propagation as competitive reactions.

$$\begin{aligned} [B]_p/[M]_p &= \{-d[B]/dt\}/\{-d[M]/dt\} \\ &= \{k_{tr,B}[B][R\cdot]\}/\{k_p[M][R\cdot] + \cdots\} \\ &\approx \{k_{tr,B}[B][R\cdot]\}/\{k_p[M][R\cdot]\} \\ &= C_{tr,B}[B]/[M] \\ &\approx 6.8 \times 10^{-3} \end{aligned} \qquad (4-8)$$

This corresponds to about 0.8 moieties per macromolecule derived from the chain transfer to benzene for the polymer prepared by solution

polymerization with a 30/1 benzene/monomer ratio (DP ≈ 120).

4.1.4 Microstructures Elucidated from ^{13}C NMR Spectra

(1) Qualitative Results by Peak Assignments

The ^{1}H (300 and 500 MHz) and ^{13}C (75.57 and 125.76 MHz) NMR spectra (Figs. 4−3 to 4−7) of the PVAc samples prepared by solution polymerization with a 30/1 or 2/1 benzene/monomer ratio show some resonances in the aromatic/alkene region. In the ^{13}C NMR spectra (Figs. 4−4 and 4−6), there are several groups of peaks around 140.0, 130.8, 128.5, 126.5, 125.5, 124.2, 122.8, 121.4, and 96.1 ppm.

By comparison of the chemical shifts of the polymer resonances with those estimated for the possible microstructures in Table 4−3, we can assign the peaks around 140.0, 128.5, and 126.5 ppm to the microstructure **AR-II** and exclude the presence of other aromatic microstructures. The microstructures **AR-I** and **AR-III** are ruled out because there is no major peak detected in the regions of 129.0−130.0 or 136.5−138.5 ppm. The microstructure **AR-IV** has a peak at 126.6 rather than 128.5 ppm, but its significant contribution to the peak at 126.5 ppm seems unlikely because the ratio of the peak integrals at 126.5 and 128.5 ppm (8.847/(5.574+8.131) ≈ 0.65) is the same as that of the model compound for **AR-II** (135.08/209.12 ≈ 0.65) (see Table 4−4). This conclusion is confirmed by the absence of a peak in the 139.35−139.75

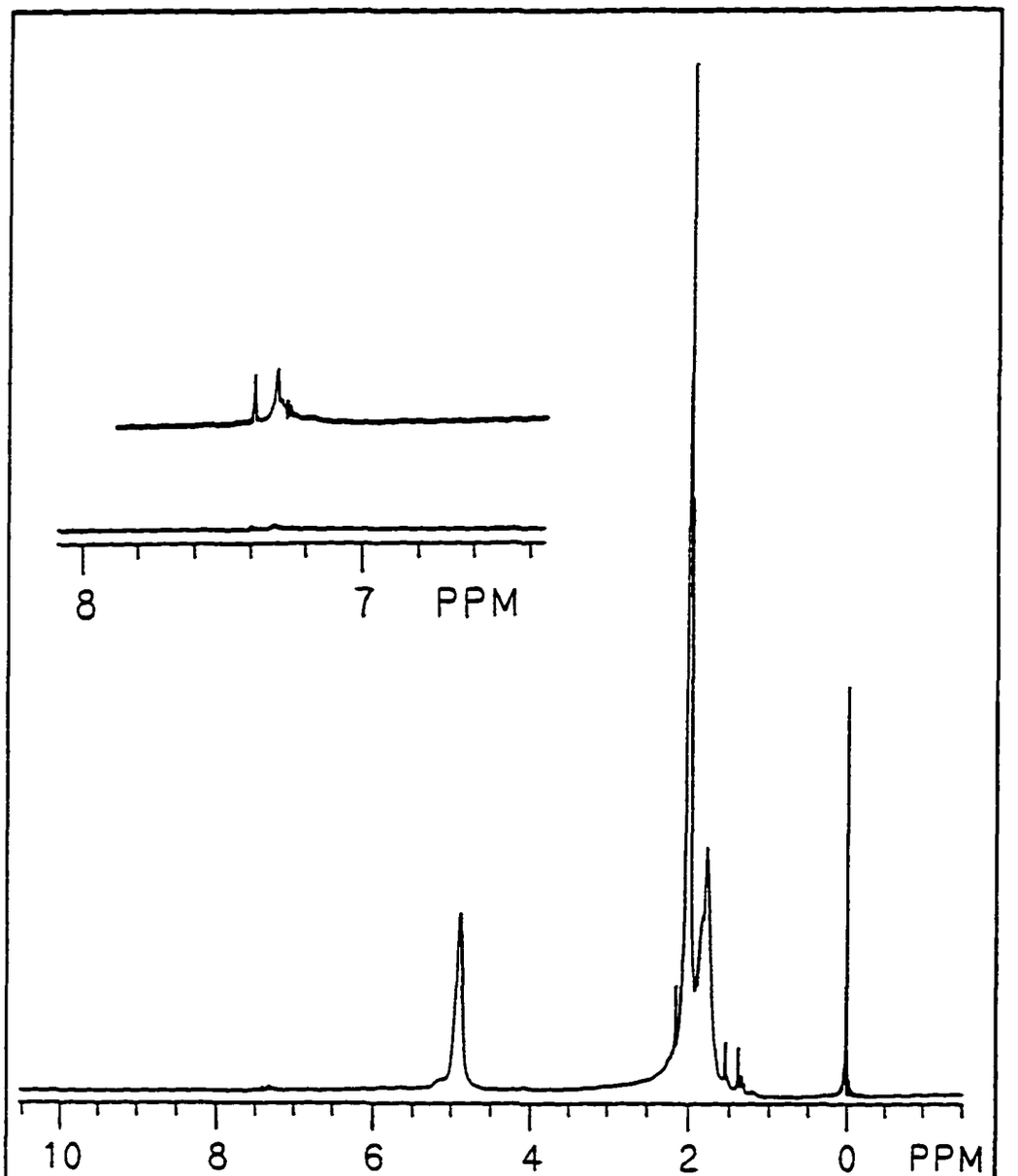

Figure 4-3. Proton NMR spectrum (300 MHz) of PVAc prepared with a benzene/monomer ratio of 30/1.

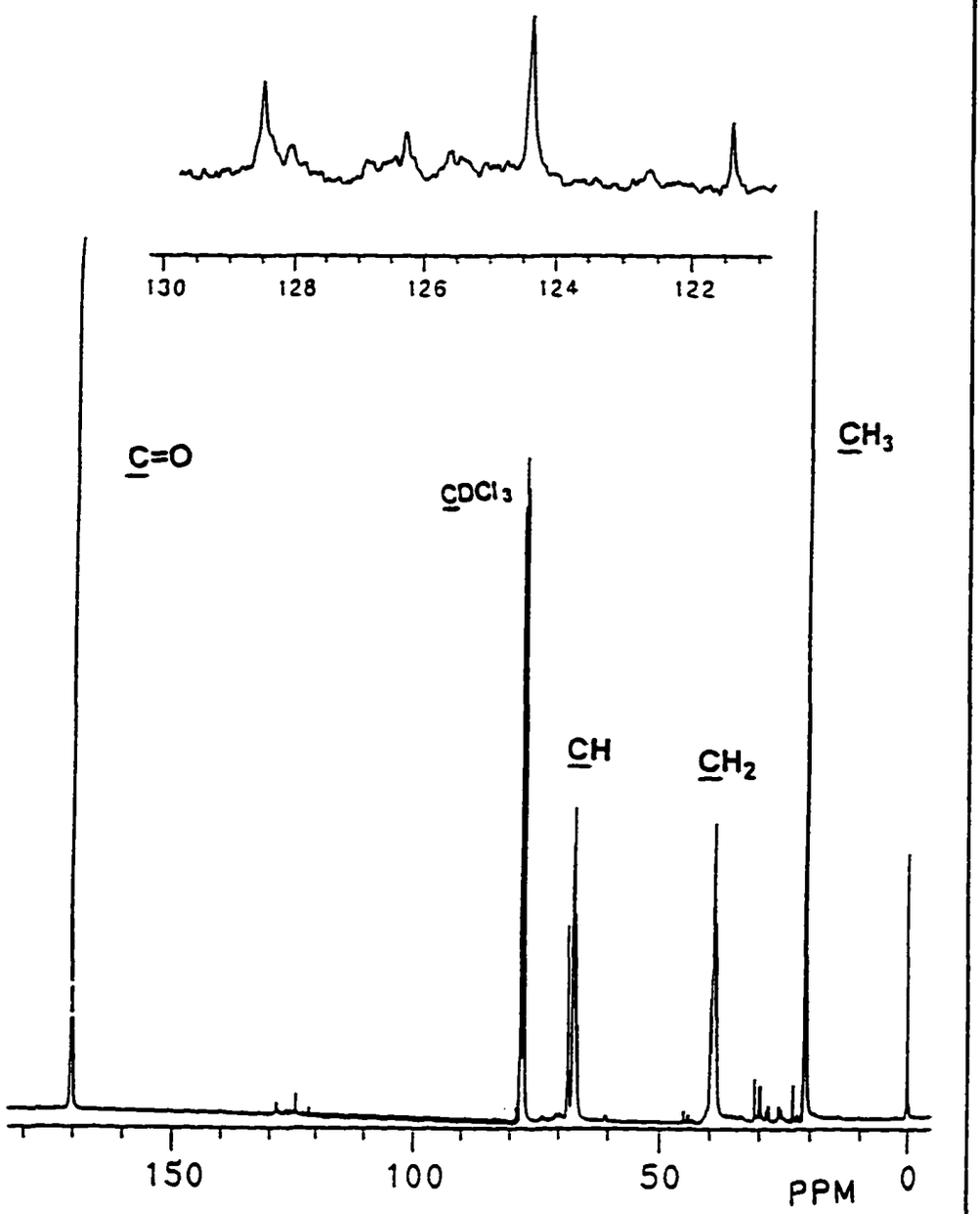

Figure 4-4. Carbon-13 NMR spectrum (75.57 MHz) of PVAc prepared with a benzene/monomer ratio of 30/1.

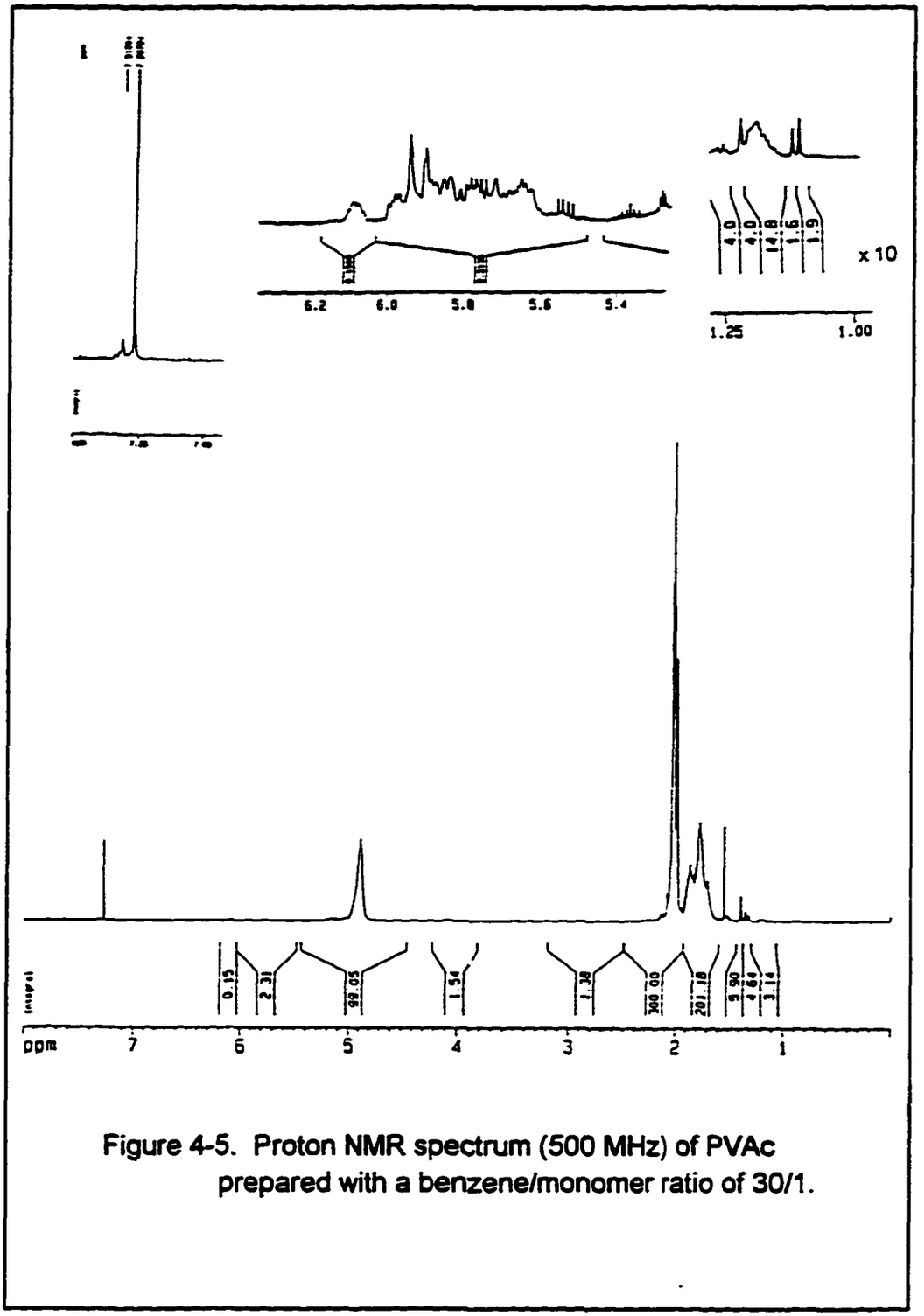

Figure 4-5. Proton NMR spectrum (500 MHz) of PVAc prepared with a benzene/monomer ratio of 30/1.

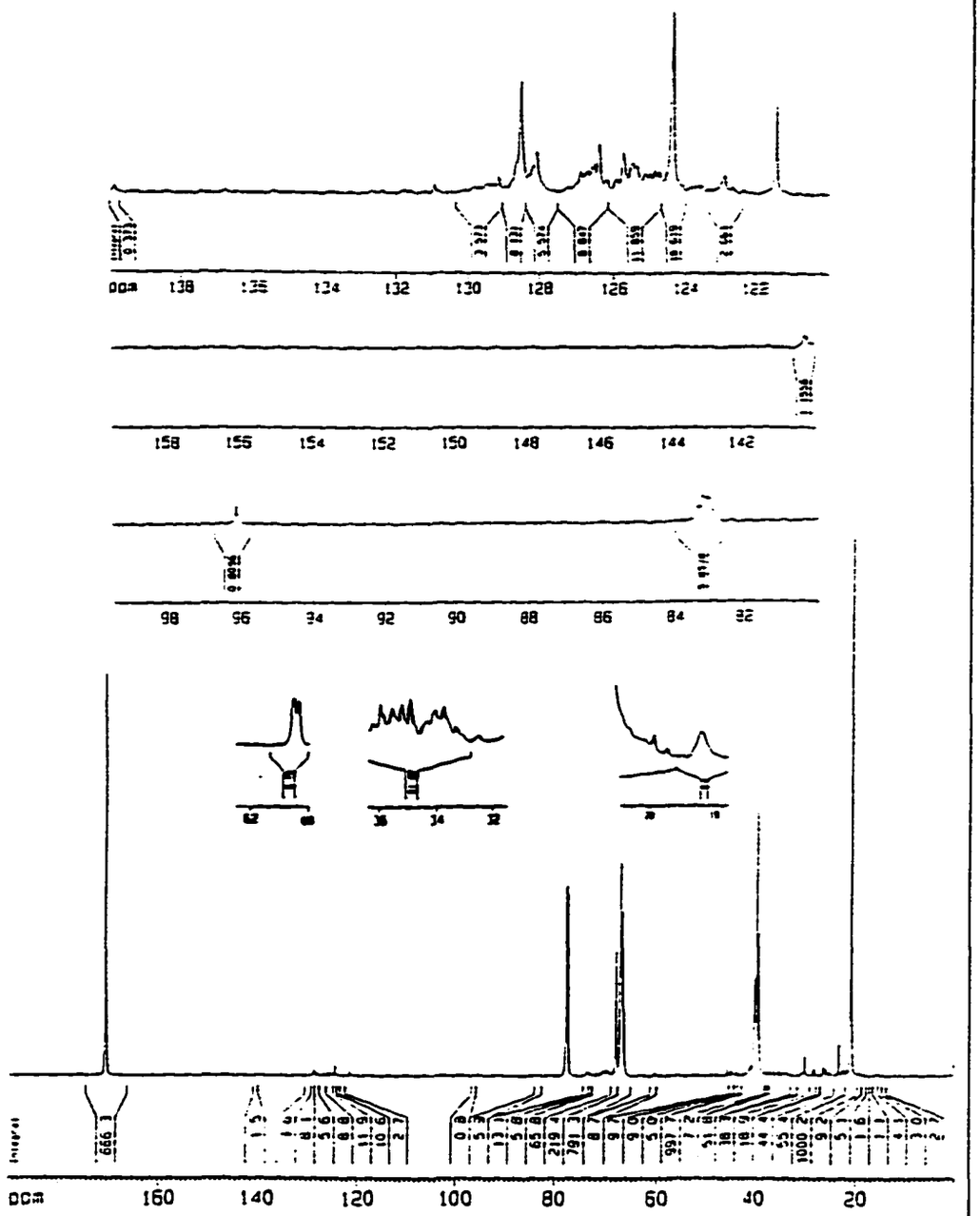

Figure 4-6. Carbon-13 NMR spectrum (125.76 MHz) of PVAc prepared with a benzene/monomer ratio of 30/1.

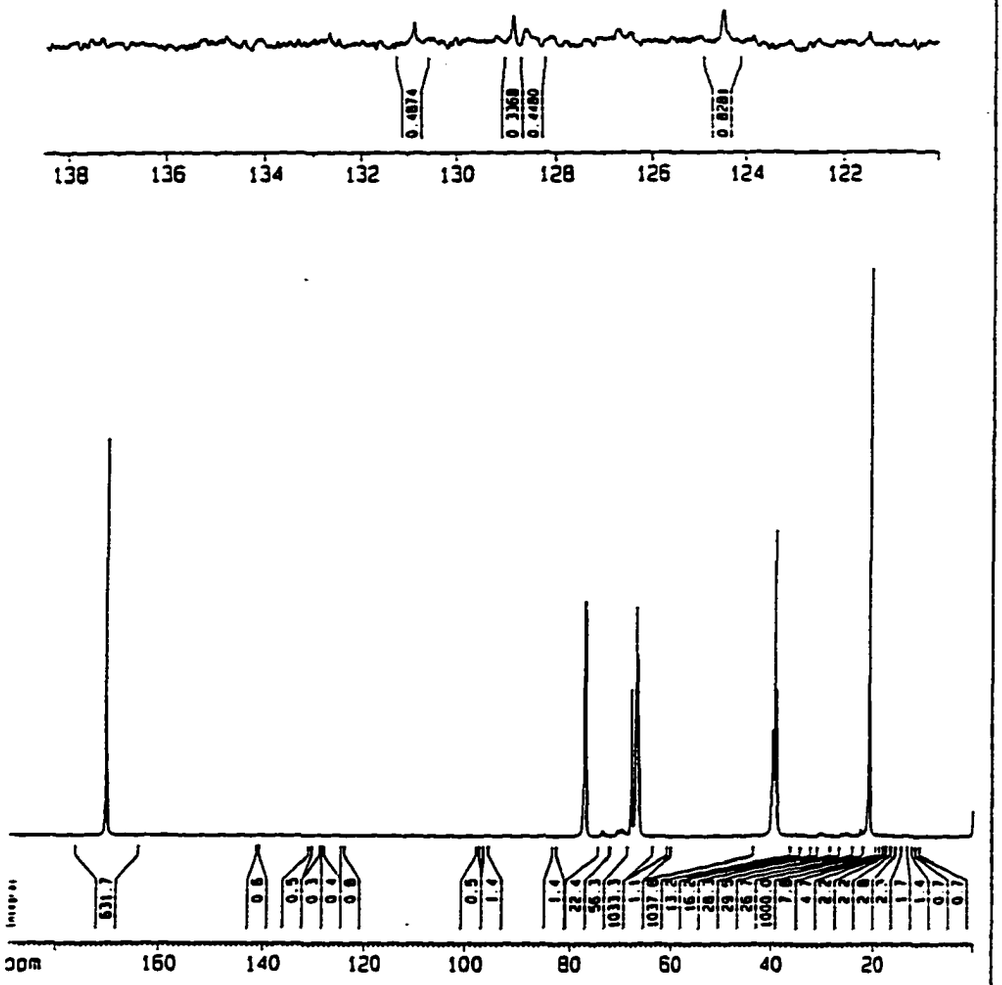

Figure 4-7. Carbon-13 NMR spectrum (125.76 MHz) of PVAc prepared with a benzene/monomer ratio of 2/1.

Table 4-4. Chemical Shifts and Integrals of the Aromatic and Methylene Carbons in the Model Compound and the Polymer Prepared with a Benzene/monomer ratio of 30/1

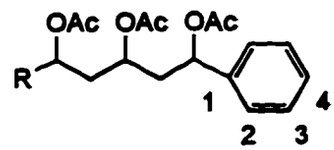

	Model Compound (R = H)		Polymer (R = -(VAc)$_n$-)	
	Chemical Shifts (ppm)	Integral	Chemical Shifts (ppm)	Integral
1.	140.20 140.01 139.71	**36.14**	140.2 139.8	**1.529**
2.	126.62 126.53 126.36	**135.08**	126.5	**8.847**
3, 4.	128.57 128.20 128.09	**209.12**	128.5 128.2	**13.705**
-CH_2 -	40.5	**126.69**	40.5	**997.7**
	(See Fig. 3-18 in Section 3.2.6.)		**(See Fig. 4-6 in Section 4.1.4.)**	

ppm region. Similarly, we can exclude any significant contribution to the peaks near 128.3 ppm from benzene trapped in the polymer. These arguments assume that the ratios of the peak integrals are the same for AR-II and its model compound.

The peaks at 124.2 and 122.8 ppm have been assigned to the nitrile carbons of initiator (AIBN) fragments at the polymer chain ends ($(CH_3)_2C(CN)$-CH_2-CH(OAc)~ ~, and $(CH_3)_2C(CN)$-CH(OAc)-CH_2~ ~), respectively.[10] The former structure is formed by normal tail addition and the latter one either by head addition or by coupling with the propagating macroradical. The peak at 124.2 also could include a contribution from copolymerized methacrylonitrile ($CH_2=C(CH_3)_2CN$) that was formed from AIBN.[11]

(2) Quantitative Results from Integrals

In addition to the molar ratios, the peak intensities in ^{13}C NMR spectra also depend on the nuclear Overhauser effect (NOE) and the rate of relaxation. Carbons in similar structural environments have similar NOE's, and at sufficiently long spectral delay times, the differences between the relaxation rates for carbons in polymer structures and models are minimized. Thus the intensity ratios for the aromatic carbons might be similar for a polymer structure and the corresponding model compound.[12] Essentially identical conditions were used to obtain the NMR spectra of our polymer

samples and models, and the very good agreement of the chemical shifts and relative intensities between the model compound, 1-phenyl-1,3,5-triacetoxybenzene, and the polymer (Table 4−4) is consistent with our assignments of the polymer resonances at 140.0, 128.5 and 126.5 ppm to the aromatic microstructure **AR-II**. However, it must be emphasized that quantitative comparisons of intensities require quantitative information about NOE's and T_1's.

The aromatic peak intensities increase with an increasing ratio of benzene/monomer. The integral ratio of the peaks at 128.5 ppm for polymer samples prepared with 30/1 and 2/1 of benzene/monomer ratios (Figs. 4−6 and 4−7) is about {(8.131 + 5.574)/997.7} / {(0.337 + 0.448)/1037.8} ≈ 18, which agrees with the expected value of 15/1 (30/2) within experimental error.

The quantitative estimation of the concentration of the aromatic microstructure from ^{13}C NMR spectra is based upon the assumption that the integral ratio of aromatic to methylene carbons is almost the same for the polymer and model under similar instrumental condition. The peak intensities of protonated carbons are much larger than those of quaternary ones and thus have higher relative accuracy. The integral ratio of the five protonated aromatic carbons (126.5 and 128.5 ppm) and the two methylene carbons (40.5 ppm) of the model compound is (135.08 + 209.12)/126.69 = 2.72. Thus the integral ratio of the protonated carbons in one aromatic

ring to one methylene carbon is 5.44. The integral ratio of protonated aromatic carbons to methylene carbons in our PVAc sample (made at a benzene/monomer ratio of 30/1) is (8.847 + 5.574 + 8.131)/997.7 = 0.0226, so the concentration of the aromatic microstructure is 0.0226/5.44 = 4.15×10^{-3}. Since there is one methylene carbon per monomer unit, there are about 4 aromatic microstructures per 1000 monomer units, or about 0.5 aromatic moiety per macromolecule with DP ≈ 120.

Within experimental error, this result agrees with the results obtained from kinetic data in Section 4.1.3 (about 0.8 aromatic microstructures per macromolecule). The measurements of chain transfer constants are known to have low accuracy, and the extrapolation to 80 °C from values at only two temperatures may lead to more error. Also, the value obtained from NMR spectra could be too low because of mechanical losses during purification by precipitation, especially losses of the low MW fractions that have the higher (chain end)/(monomer unit) ratios.

4.1.5 Formation Mechanisms of Microstructures

(1) Reactions of Propagating Macroradical with Benzene

After qualitative and quantitative confirmation of the ^{13}C NMR peak assignments for the aromatic microstructure **AR-II**, we now can discuss the possible mechanisms for chain transfer.

The microstructure **AR-II** may be formed via mechanisms that appear

in Scheme 2−1, 2−2, and 2−3 in Section 2.1.

The absence of **AR-I** excludes the conventional chain transfer mechanism of hydrogen abstraction from benzene by propagating macroradicals (Scheme 2−1), because the resultant phenyl radical is highly reactive and would reinitiate polymer chains very efficiently to form **AR-I**, rather than couple with the propagating macroradical to produce **AR-II**.[13]

According to Scheme 2−3, there is at least one **DB-V** formed for each **AR-II** produced by oxidation of **CHD-IV** (the coupling product of the cyclohexadienyl radical with a propagating macroradical). At our low conversion and low concentration, **DB-V** is not likely to be copolymerized to generate long branches. The absence of this double bond (see Section 4.2.3) excludes the mechanism of Scheme 2−3. Also, the polymerization and purification conditions (80 °C under nitrogen, air at low temperature, 60 °C under vacuum) are not likely to cause oxidation of **CHD-IV** to **AR-II**. The exclusion also is consistent with the absence of **AR-I**, the product of a process that might compete with the formation of **AR-II**.

Thus the only probable mechanism of **AR-II** formation is that in Scheme 2−2, which invovles the addition of a propagating macroradical to benzene. The **AR-II** may be formed by the reaction of the resultant cyclohexadienyl radical (**CHD**•) either with the monomer by fragmentation (hydrogen transfer) (i.e., reinitiation) or with the propagating macroradical by disproportionation. The cyclohexadienyl radical is stabilized by allylic

conjugation, and thus should have a long life which would favor the termination. Yet this route does not generate any additional polymer chain (there is either no effect on or an increase in the polymer MW), whereas the reinitiation route does (there is a decrease of polymer MW). Even though the measured MW decrease caused by chain transfer to benzene is less significant than the decrease of propagation rate, the chain transfer term still is one of the major terms in the Mayo equation. The estimation of the microstructure concentration by kinetic data agrees with that from ^{13}C NMR spectra, which favors reinitiation over disproportionation, as will now be discussed.

(2) Reactions of the Resultant Cyclohexadienyl Radical

The **CHD**· may react with monomer by hydrogen transfer to form chain end microstructure CH_3-CH(OAc)-CH_2-CH(OAc)-~ ~ (**ALK-I**) in addition to **AR-II**. The diagnostic peaks of the chain end methyl group (the 1-phenyl-1,3,5-triacetoxyhexane acts as a useful model for **ALK-I** as well) appear at 1.2 ppm in the ^1H NMR spectrum and 20.1 ppm in ^{13}C spectrum. Both peaks are present in the NMR spectra of our PVAc samples. Their intensities increase when the benzene/monomer ratio increases from 2/1 to 30/1. The concentration of **ALK-I** in the PVAc sample prepared with the 30/1 ratio is estimated from the ^1H spectrum as: (14.8/3)/999.95 ≈ 4.9 per 1000 VAc units, which is almost equal to the measured concentration of **AR-II**.

Furthermore, other possible routes to **ALK-I** via reactions of incipient hydrogen radical sources with monomer were excluded by Chung.[2]

The **CHD**· may terminate with the propagating macroradical to form chain end microstructure $CH_2(OAc)\text{-}CH_2\text{-}CH(OAc)\text{-}CH_2\text{-}\sim\sim$ (**ALK-II**) in addition to **AR-II**. The diagnostic peaks of the chain end methylene group[2] at around 4.15 ppm in the ^1H spectrum and 60.7 ppm in ^{13}C spectrum also are present in the NMR spectra of our polymer samples. This microstructure, **ALK-II**, also may be formed via other disproportionation reactions or via any chain transfer reactions involving hydrogen abstraction by the propagating macroradical (even though the labile hydrogen sources are minimized under our polymerization conditions).[2] The relative peak intensities (integral ratio over backbone methylene group intensity) increase only from 1.06 to 8.7×10^{-3} (an 8-fold increase) as the benzene/monomer ratio increases from 2/1 to 30/1 (a 15-fold increase). Thus the disproportionation mechanism is not the predominant one. However, further work is needed to elucidate fully the detailed mechanism(s) for the formation of microstructure **ALK-II**.

Our general conclusions may be summarized by the following addition/fragmentation mechanism:

$$P\cdot + C_6H_6 \longrightarrow CHD\cdot \xrightarrow{VAc} \textbf{AR-II} + CH_3\dot{C}H(OAc) \longrightarrow P\cdot$$

4.1.6 Cyclohexadienyl Structures

The chain transfer constant for benzene measured by MW decrease has been accounted for by the addition/fragmentation mechanism just described. However, this mechanism does not exclude reactions of the cyclohexadienyl radical that do not generate additional polymer chains, such as an addition/propagation sequence that forms **CHD-I** or an addition/coupling sequence that gives **CHD-II**. The microstructures **CHD-I** and **CHD-II** may be oxidized to **AR-III** and **AR-IV**, respectively (Scheme 2 – 2). However, the ^{13}C NMR spectrum of the PVAc oxidized by AIBN/O_2 (see Section 3.1.4) does not show any significant change in the unsaturated carbon region. This result may be due either to the absence of the cyclohexadienyl microstructure or to the failure of the heterogeneous oxidation of the polymer.

There are some observations that support the presence of trace amounts of cyclohexadienyl microstructure. The alkene proton chemical shifts of *cis*- and *trans*-3,6-dimethyl-1,4-cyclohexadiene were shown to be 5.50 and 5.53 ppm, respectively.[14] The corresponding chemical shifts for microstructure **CHD-I** and **CHD-II** are expected to be almost the same, since these proton shifts are not sensitive to the presence of atoms further away than the β-positions. The 500 MHz ^{1}H NMR spectrum of PVAc (Fig. 4 – 5) shows some peaks around 5.50 – 5.55 ppm. Their intensities are estimated to be lower than 2×10^{-4} of the methine proton peak, thus even if they are

peaks of **CHD-I** and/or **CHD-II**, their contributions are not significant. Due to a lack of model compounds, the ^{13}C NMR chemical shifts of the alkene carbons in **CHD-I** and **CHD-II** cannot be estimated accurately now. One obvious alternative approach to the identification of such structures is to find a mild but effective oxidation reaction for them when they occur in the polymer chain.

4.2 Alkene Groups in Poly(vinyl acetate)

4.2.1 Estimation of the ^{13}C NMR Chemical Shifts of the Carbons of the Isolated Internal Alkene Group

The chemical shift increments of the acetoxy group on the alkene carbons can be calculated by comparing the chemical shifts of the alkene carbons in the mono-acetoxyalkene model compounds, *trans*-9-acetoxy-7-pentadecene, *trans*-9-acetoxy-6-tridecene, *trans*-10-acetoxy-6-hexadecene (see Section 3.3 for their syntheses), and *trans*-1-acetoxy-5-decene,[15] with those in the reference alkenes, *trans*-7-tetradecene and *trans*-5-decene (Table 4–5).[15]

Table 4–5 ^{13}C NMR Chemical Shift Increments $\Delta\delta_{ik}$ of the Acetoxy Group on Alkene Carbons

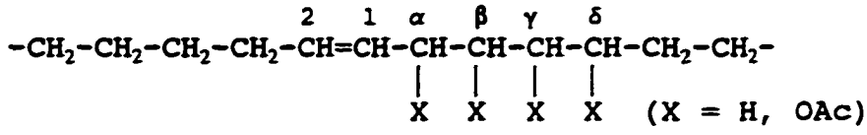

	H	α	β	γ	δ
δ_1 $\Delta\delta_1$	130.31	128.99 **-1.32**	125.13 **-5.18**	129.31 **-1.00**	129.47 **-0.84**
δ_2 $\Delta\delta_2$	130.31	134.21 **3.90**	133.89 **3.58**	131.29 **0.98**	131.03 **0.72**

i: position of acetoxy substituent, α, β, γ, δ;

k: position of the alkene carbons, 1, 2.

The chemical shifts of the alkene carbons of the microstructure, **DB-I**, can be estimated by the extended Grant-Paul additivity rule.

$$\sim\sim\text{-}CH_2CHX\text{-}CH_2CHX\text{-}CH=CH\text{-}CH_2CHX\text{-}CH_2CHX\text{-}\sim\sim \quad (X = OAc)$$

$$\delta_1 = \delta_{1,RH} + \Delta\delta_{\alpha 1} + \Delta\delta_{\beta 2} + \Delta\delta_{\gamma 1} + \Delta\delta_{\delta 2} = 132.29 \text{ ppm}$$

$$\delta_2 = \delta_{2,RH} + \Delta\delta_{\alpha 2} + \Delta\delta_{\beta 1} + \Delta\delta_{\gamma 2} + \Delta\delta_{\delta 1} = 129.17 \text{ ppm}$$

4.2.2 Modification of Poly(vinyl acetate-*co*-vinyl alcohol)

Chemically, the functional groups in polymers behave similarly to those in corresponding small analogues in a thermodynamically good solvent. By clean organic reactions (bromination, elimination, and acetylation), the poly(vinyl acetate-*co*-vinyl alcohol) (40% hydrolyzed) was converted to poly(vinyl acetate-*co*-acetylene) with only a few percent of acetylene monomer units, i.e., microstructure **DB-I**. With the estimated 60%, 95%, and 99% conversions for the bromination, dehydrobromination, and acetylation reactions for the polymeric system (see Section 3.3.7), the amount of acetylene was estimated to be $0.024 \times 0.6 \times 0.95 \times 0.99 \approx 1.35\%$.

If we assume random brominative replacement of the hydroxy group along the polymer chain, the probability of a particular alkene group to be conjugated with another one or separated from it by one monomer unit is about $2 \times 1.35\% = 2.7\%$. The chemical shift increments generally are

negligible further than the δ-position, the probability of being an isolated alkene group (separated by two or more monomer units) is about (1 − 2 x 2.7%) ≈ 95%. So the detected alkene peaks in the modified polymer are from isolated double bonds.

The 75.57 MHz ^{13}C NMR spectrum of modified poly(vinyl acetate-*co*-acetylene) (Fig. 4−8) shows peaks around 132.1 and 128.2 ppm in the region of aromatic or alkene carbons, whereas that of reference PVAc prepared by the acetylation of poly(vinyl acetate-*co*-vinyl alcohol) (40% hydrolyzed) does not. Thus these peaks are assigned to the alkene carbons in **DB-I**.

These chemical shifts differ somewhat from those estimated with model compounds (132.3 and 129.2 ppm). Possible reasons for the discrepancies are exceptionally large chemical shift increments of ϵ-, ζ-, or even η-acetoxy groups,[16] which have not been counted in the estimation, or failure of the additivity rule to work well with the alkene carbons.[17] Nevertheless, neither of these carbons has both of its peaks near those of aromatic microstructure **AR-II**, a possibility which would have complicated our discussion in Section 4.1.

The ^{13}C NMR spectrum of commercial PVAc does not show any resonance that can be assigned to alkene carbons, so there is no detectable dehydroacetation of the polymer during processing, purification, and storage.

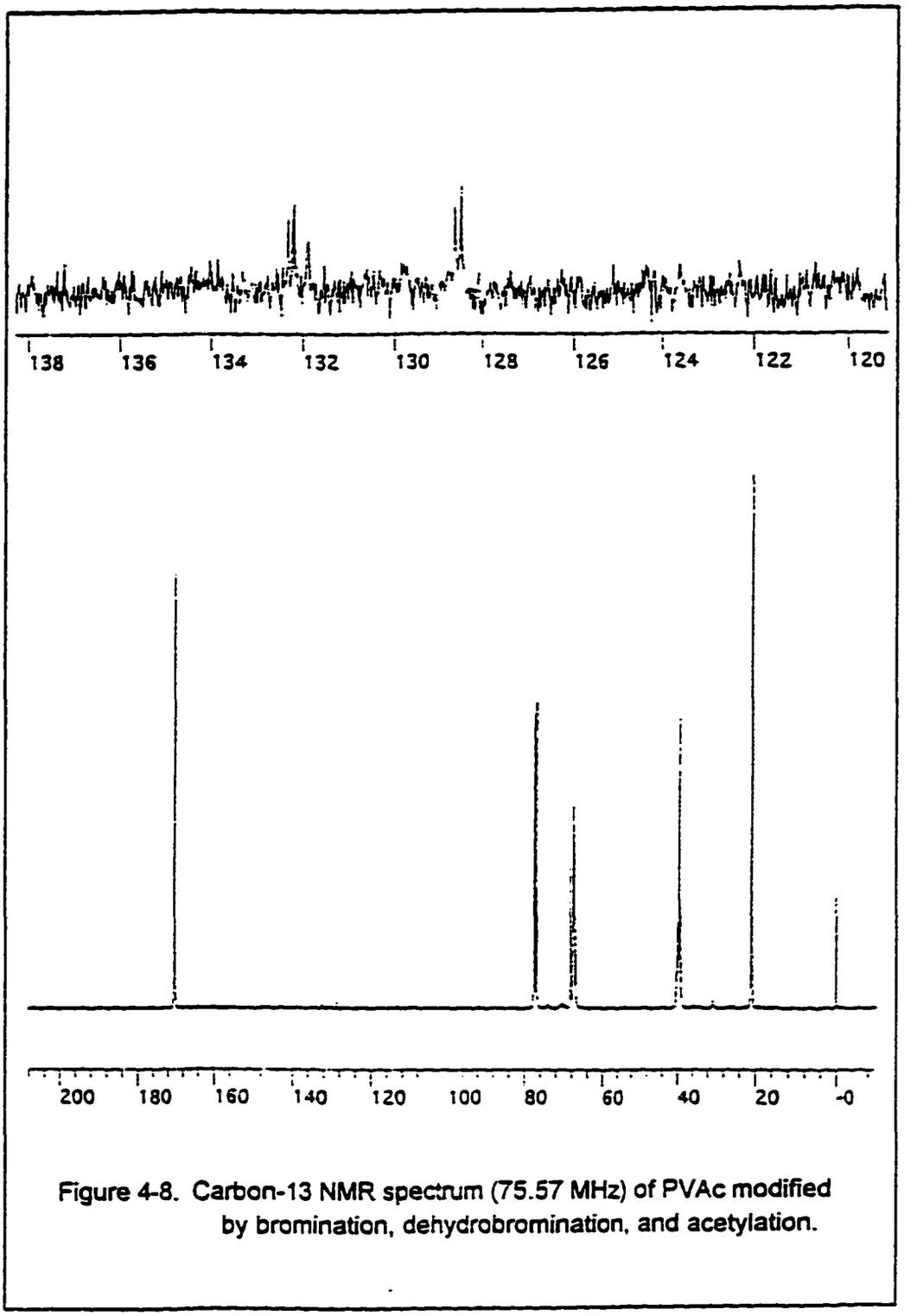

Figure 4-8. Carbon-13 NMR spectrum (75.57 MHz) of PVAc modified by bromination, dehydrobromination, and acetylation.

4.2.3 Other Alkene Microstructures

The estimated chemical shifts of the alkene carbons in some possible alkene microstructures in PVAc are listed in Table 4–6. Only the values for **DB-II** are expected to be accurate (~ 0.2 ppm), and the others are less reliable due to the lack of appropriate model compounds. However, none of those structures has both alkene peaks near those of aromatic microstructure **AR-II**.

The possibility of vinyl acetate monomer entrapment in the polymer is excluded by the absence of peaks at 97.5 and 141.2 ppm, a result which confirms our purification procedure as appropriate.

There have been different proposals for termination mechanisms, involving either disproportionation or combination with another propagating macroradical or a monomeric radical.[18–22] The NMR spectra of our polymer samples indicate the absence of **DB-V** (see Section 2.2.3.), a product of disproportionation. The presence of peaks around 73.5 and 33.6 ppm (estimated roughly for the methine and methylene carbons of the combination product,

~ ~-CH_2-CH(OAc)-$\dot{C}H_2$-$\dot{C}$H(OAc)-CH(OAc)-CH_2-CH(OAc)-CH_2-~ ~ (**HH-I**)),

supports combination during solution polymerization in benzene.[23] It is more probable that most polymer chains stop growing because of chain transfer to benzene in which no double bond is formed. More work is needed to elucidate the termination mechanisms, such as confirmation of

Table 4-6. Estimated Chemical Shifts (ppm) of the Alkene Carbons in Some Possible Alkene Microstructures

	Polymer Microstructures	Reference Compounds [2, 15]
	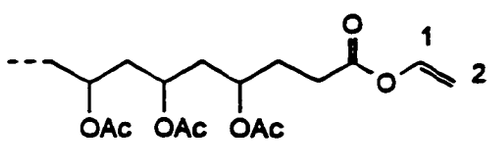	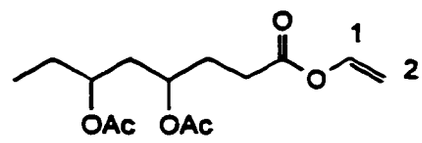
DB-II	1. 141.2 2. 97.6	1. 141.24 2. 97.58
	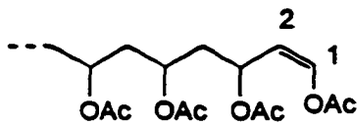	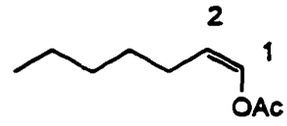
DB-V	1. 133.8 135.3 2. 117.5 117.7	1. 134.18 135.60 2. 114.63 114.82
	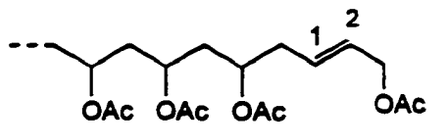	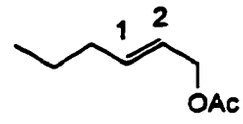
DB-VI	1. 140.6 2. 118.0	1. 136.27 2. 124.00

(See Schemes 2-5, 2-6, and 2-7 in Section 2.2.)

the absence or presence of DB-V and HH-I from the NMR spectra of better model compounds.

The other alkene peaks detected in the ^{13}C NMR spectrum of the PVAc made with a 30/1 benzene/monomer ratio are at 130.8 (*ca.* 0.5), 125.5 (11.86), 121.4 (*ca.* 6), and 96.1 (0.81) ppm (parenthesized values are integrals relative to 997.7 for methylene carbons). Their assignments need further study.

4.3 Proposed Mechanisms of Solution Polymerization of VAc in Benzene

4.3.1 Free-Radical Reactions in Aromatic Solvent

A π-complex between a chlorine atom (Cl•) and benzene was proposed in order to explain the increase of tertiary/primary selectivity during alkane chlorination in the aromatic solvent.[24-26] A time-resolved kinetic procedure (laser flash photolysis) gave new evidence for its formation.[27] The π-complex was suggested to have lower reactivity and higher selectivity than the free chlorine atom by about two orders of magnitude. The general mechanism involving this complex is shown in Scheme 4-1.[27-32]

An *ab Initio* molecular orbital calculation gave one of the stable minima as a π-complex structure with a symmetry plane passing through the midpoints of two C-C bonds and with the chlorine atom positioned slightly outside of the benzene ring (at a 101 ° angle to the ring plane).[33] The chlorine atom was 2.7 Å away from the center of the C-C bond and 3.2 Å from the center of the benzene ring. The aromatic compound acted as an electron donor to the chlorine atom to form this loosely associated charge transfer species. The calculation also gave a comparable minimum for the chlorocyclohexadienyl (CCH) radical (σ-complex) structure, a result which supported the simultaneous presence of two stable isomers.

The role of the σ-complex is not clear.[34-36] It was suggested[34] to be

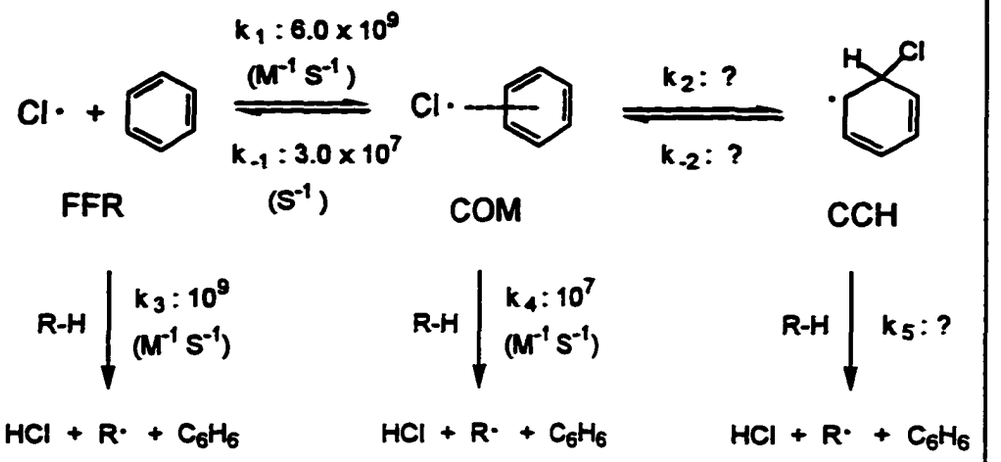

Scheme 4-1. Reactions of Chlorine Atom in Benzene.[27-32]

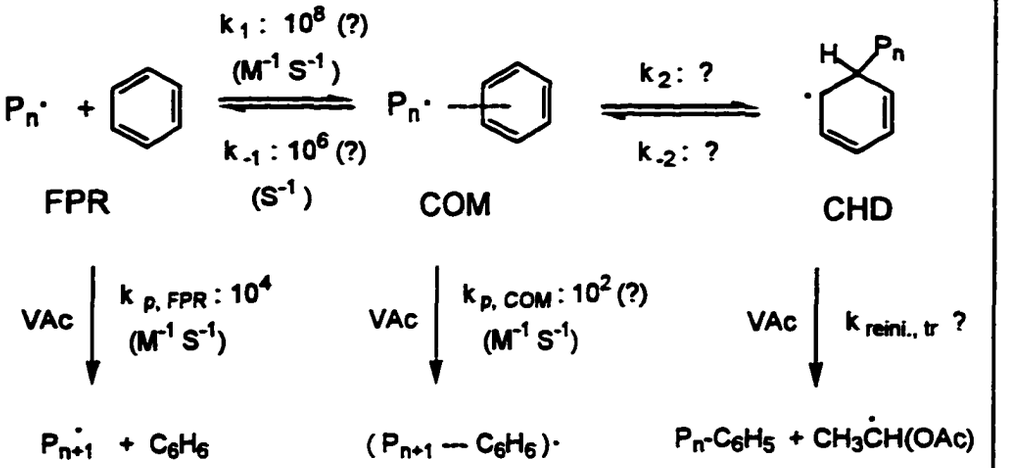

Scheme 4-2. Reactions of Propagating Macroradicals in Benzene.

low-energy stable species, yet with a high activation energy for its formation. The very low concentration CCH radical reacts with chlorine rather than with hydrogen by abstraction, forming trace amount of hexachlorobenzene.[36] Thermochemical study has suggested that the CCH radical is the major species present in the system, but that it only plays an indirect role in the chlorination process.[37] It has a half-life of ~30 ns with respect to dissociation and is in fast equilibrium with the π-complex, the real operating species for chlorination.[37] Yet a fairly strong and broad absorption band at λ_{max} ~490 nm has been assigned to the $Cl\cdot/C_6H_6$ π-complex,[27, 38, 39] because the UV spectrum of $C_6H_7\cdot$ was reported to be dominated by an absorption at 318 nm and has only weak features at 510 and 550 nm.[40, 41]

Similar schemes were also applied to free-radical reactions of chlorine or $NO_3\cdot$ in various aromatic solvents, including pyridine.[42-44]

4.3.2 Explanations of the Experimental Phenomena

The addition/fragmentation chain transfer mechanism shown above (Section 4.1) involves a cyclohexadienyl radical, that yields the aromatic microstructure **AR-II**. Even though this radical has low reactivity, its low concentration indicates that it should not significantly affect the rate of propagation. So the drastic change of propagation rate caused by benzene needs other explanations.

The mechanism of solution polymerization of vinyl acetate in benzene

was proposed in part by Kamachi[45] as in Scheme 4−2 by analogy to Scheme 4−1, and the rate constants are estimated in the present study by considering that the carbon-centered propagating macroradical has a lower reactivity than the chlorine atom. There are two mechanisms operating at the same time. One is propagation through the donor/acceptor π-complex, at a lower rate, with higher selectivity, and without changing MW. The other mechanism is chain transfer via the addition/fragmentation process, forming an aromatic microstructure in the polymer chain and decreasing the MW slightly. This scheme agrees with the recent mechanistic studies of free-radical reactions and explains almost all of the experimental data for the solution polymerization in benzene.

(1) Significant Decrease of Propagation Rate

It was assumed that there was a fast equilibrium between the free propagating macroradical and the π-complex, and the k_1 and k_{-1} were estimated to be $\sim 10^8$ and 10^6, respectively, which are much larger values than those of the propagation rate constants $k_{p,\,FPR}$ ($\sim 10^4$) and $k_{p,\,COM}$ ($\sim 10^2$). With 1 M of benzene (~1/20 benzene/monomer ratio), the concentration of the π-complex is about 100 times larger than that of the free propagating macroradical, [COM] ≈ 100 [FPR] (by $K = [COM]/\{[FPR]\cdot[M]\} = k_1/k_{-1} \approx 100$). The π-complexed macroradical still can add to monomer, though at a rate about two orders of magnitude lower.

So the total propagation rate is:

$$r_{p,TOT} = r_{p,FPR} + r_{p,COM}$$

$$= (k_{p,FPR}[FPR] + k_{p,COM}[COM]) \cdot [M]$$

where $r_{p,FPR} = k_{p,FPR}[FPR] \cdot [M] \approx r_{p,COM} = k_{p,COM}[COM] \cdot [M]$

$$\ll r_{p,O} = k_{p,FPR}[FPR]_O \cdot [M].$$

If the steady-state assumption still applies, the concentration of free propagating macroradical in aromatic solution will be much smaller than that in the bulk state: $[FPR]_O = ([FPR] + [\pi COM]) \gg [FPR]$. So the total propagation rate through the free propagating macroradical and π-complex macroradical is much smaller than that in the bulk state: $r_{p,TOT} \ll r_{p,O}$. Thus addition of a small amount of benzene (~1/20 benzene/monomer ratio) significantly decreases the propagation rate (~80-fold).

(2) Insignificant Decrease of Polymer MW

The propagation through the π-complexed macroradical does not produce additional polymer chains nor aromatic microstructures, and thus it has no effect on the polymer MW. The only route that affects the MW is the addition of propagating macroradical to benzene, followed by hydrogen transfer to monomer, forming a new polymer chain (see Section 4.1). The qualitative and quantitative results of NMR spectra explain the reported chain transfer constant of benzene. The addition/disproportionation or

addition/propagation routes in Scheme 2−2 have essentially no effect on the MW and may decrease the propagation rate slightly, but they have been shown to be negligible. The kinetic significance of this chain transfer route depends largely on the relative magnitude of the rate constants, k_2 and k_{-2}, whose estimated values are much smaller than those of k_1 and k_{-1}, based on the study of the reactions of the chlorine radical.

(3) Change of Polymer Microstructural Defects

The propagation through the *π*-complex has features which differ from those of propagation via the free macroradical. By comparison with the results for the chlorine/benzene *π*-complex, the *π*-complexed macroradical should have lower energy and higher selectivity. These factors favor the normal propagation, of lower activation energy over the side reactions with higher energies, such as head-to-head addition and chain transfer reactions. This analysis explains the experimental observations of fewer branch microstructures (formed by chain transfer to polymer) and fewer head-to-head addition units in PVAc prepared by solution polymerization in an aromatic solvent.

(4) The Unexpectedly Large Chain Transfer Constant for Benzene

The conventional chain transfer mechanism of hydrogen abstraction from benzene by propagating macroradicals involves the breakage of a very

strong sp^2 C–H bond. For this mechanism, the expected ratio of chain transfer constants for benzene/cyclohexane can be estimated by the Evans-Polanyi rule.[46-48] The activation energy of the atom abstraction reaction (R-H + R'· ⟶ R· + R'-H) is given by the equation: $E_a = \alpha E_{R-H} + \beta$, where E_{R-H} is the strength of the bond being broken, α and β are constants, and $\alpha \approx 0.5$ for most reactions.

Thus the activation energy difference between the chain transfers to benzene and cyclohexane is:

$$C_6H_5-H + P\cdot \longrightarrow PH + C_6H_5\cdot \qquad E_{a,\,tr,\,CYC}$$

$$C_6H_{11}-H + P\cdot \longrightarrow PH + C_6H_{11}\cdot \qquad E_{a,\,tr,\,BEN}$$

$$\Delta E_a = E_{a,\,BEN} - E_{a,\,CYC} = \alpha\,(E_{CYC-H} - E_{BEN-H})$$

Since the chain transfer constant is the ratio of chain transfer rate over propagation rate ($C_{tr} = k_{tr}/k_p$), the apparent activation energy of the chain transfer constant is given by: $E_{a,\,CON.\,tr} = E_{a,\,tr} - E_{a,\,p}$. Thus we have: $\Delta E_{a,\,CON.\,tr} = \Delta E_{a,\,tr} = \alpha\,(E_{CYC-H} - E_{BEN-H})$.

The values of E_{R-H} at 298K (25 °C) (E_{BEN-H} = 465.3 and E_{CYC-H} = 399.6 KJ/mol)[49] are used approximately for 60 °C, since the dependence of bond strength on temperature is very small and in the same trend for both C–H bonds. The ratio of the chain transfer constants for benzene/cyclohexane can then be estimated as:

$$C_{tr.\,BEN}/C_{tr.\,CYC} = A_{tr.\,BEN}/A_{tr.\,CYC} \cdot Exp\{-\Delta E_{a.\,CON.\,tr}/RT\}$$

$$\approx \exp\{-(32.85 \times 1000)/(8.314 \times 333)\} \sim 10^{-5}$$

The reported ratio is $\sim 10^{-1}$, much larger than the value expected.[6] The explanation derived from the addition/fragmentation mechanism is that since the reaction proceeds through addition rather than abstraction, the actual activation energy is lower than that of abstraction, and the rate constant then is higher than that estimated for the conventional mechanism.

(5) NMR Spectra

The assignments by Hatada of the aromatic peaks in the ^{1}H NMR spectrum to microstructure **AR-I** were not confirmed by our ^{13}C NMR spectra. We have shown that the microstructure present is **AR-II** (Section 4.1). The chemical shifts and spin lattice relaxation times of the aromatic protons of these two structures are expected to be the same, yet the protons have different splitting patterns (see Figs. 3–17 and 3–22 in Sections 3.2.6 and 3.2.7). Our assignments are further confirmed by the similarity of the splitting patterns of Hatada and our model compound for **AR-II**. Also, his measurements gave 0.15 phenyl groups per macromolecule prepared with a ~4.55/1 benzene/monomer ratio (DP ≈ 183), a value which agrees with the value of 0.19 which we estimated from the competitive reactions of transfer and propagation.

The ^{13}C NMR spectra reported by Chung were obtained for PVAc

samples prepared with benzene/monomer ratios of 1/1, 5/1, and 10/1 on a GE QE-300 spectrometer.[2] According to our calculation based on the competitive reactions of chain transfer and propagation, for these samples the number of aromatic moieties per macromolecule should be less than 1 (the assumption for his estimation of the concentration of solvent-participated microstructures is 1). Thus the concentration of this microstructure was just at the sensitivity limit of the instrument, so that the barely distinguishable peaks could not be assigned to the aromatic moieties in the polymer chain. With the aid of a more powerful NMR spectrometer and polymer samples prepared at higher benzene/monomer ratios, we obtained nonambiguous evidence of the benzene incorporation.

(6) Polymer Tacticity

There were no significant tacticity differences detected between polymer prepared by solution polymerization in benzene and polymer prepared in bulk.[45] The loosely associated donor-acceptor π-complex apparently has no unique preference for attack on the face of the monomer double bond, since the $P_n\cdot$ carbon center lies outside of the benzene ring.

(7) ESR Spectra

In his molecular orbital calculation, Kamachi[45] assumed that the $P_n\cdot$ lies directly above the C-C bond of the $P_n\cdot$/benzene complex, while an *ab*

Initio calculation for the Cl·/benzene complex gave a 101° angle.[33] These findings still lead to the same general conclusion about the formation and reactivity of the π-complex. The weak interactions of the unpaired electron of the propagating macroradical with the hydrogens of the aromatic solvent were used to explain the additional hyperfine splittings in the ESR spectrum resulting from the polymerization of vinyl acetate in chlorobenzene.

(8) No Isotope Effect on k_p and k_t in Deuterated Benzene

If there is R−H bond breakage during the rate-determining step, a strong kinetic isotope effect will be observed. In the mechanism established here, the rate-determining step is the addition of propagating radical to benzene rather than the fast aromatization step of hydrogen transfer, so no isotope effect is expected during polymerization in benzene-d_6. A significant isotope effect is to be expected if the chain transfer is via hydrogen abstraction from benzene by the propagating macroradical.

(9) The ^{14}C Labeling Experiments

Our result agrees with the result of about 1 rather than 20 benzenes incorporated per macromolecule,[51] on the basis of tracer experiments. This observation favors the chain transfer reaction over the copolymerization. The key "fact" for the copolymerization theory is that about 20 benzenes are incorporated per macromolecule, a result which could not be reproduced by

several researchers.[51]

4.3.3 Other Possible Theories

(1) Necessity for the π-Complex ?

The carbon-centered propagating macroradical might not form a donor-acceptor π-complex with benzene, since this radical is not as reactive as Cl•. Explanations involving only the cyclohexadienyl radical are made possible by the assumption of large values for k_2 and k_{-2} in Scheme 4−2; i.e., there is a fast equilibration of the free propagating macroradical and the cyclohexadienyl macroradical. The cyclohexadienyl radical could either be unreactive to the monomer or add to the monomer at a slower rate to form P_{n+1}•/Bz instead of the microstructure **CHD-I** (as in Scheme 2−2). Both of these possibilities would result in a lower concentration of the free propagating macroradical and a lower propagation rate. By arguments similar to those made above, it also may be possible to explain the other experimental observations.

(2) The Steady State Assumption

It is possible (but unlikely) that the steady-state assumption does not apply to the solution polymerization in an aromatic solvent. If the free-radical concentration were much lower than that in bulk polymerization, the polymerization rate would be decreased significantly without a corresponding

change of MW. This possibility needs a complex, non-steady-state kinetic treatment.

4.3.4 Some Thoughts about Future Studies

Further studies are necessary to discern the roles of the π-complex and the cyclohexadienyl radical. Those investigations could involve comparisons of the UV/Vis and ESR spectra for bulk and solution polymerizations and for alkylcyclohexadienyl radicals.

The physical properties of PVAc and its derivative, poly(vinyl alcohol), need to be to correlated with the microstructures and their formation mechanisms. Such correlations may lead to the production of some special PVAc's or PVA's with modified properties.

This solvent-modulated polymerization produces polymers with fewer microstructural defects (branches, head-to-head additions, etc) without decreasing the MW significantly. All of these parameters are crucial for polymer properties. They are difficult to vary simultaneously by using conventional chain transfer agents or other polymerization modulators. This study provides new perspectives to the challenge of the control of free-radical polymerizations. [52]

CHAPTER 5

CONCLUSIONS

Poly(vinyl acetate) samples were synthesized by solution polymerization in benzene in order to study the mechanism of chain transfer to the aromatic solvent. The high resolution NMR spectra of these samples showed the presence of microstructures formed via chain transfer of propagating macroradicals to benzene. A series of aromatic model compounds was obtained by multistep organic synthesis to aid with the chemical shift assignments. The peaks near 126.5 and 128.5 ppm in the ^{13}C NMR spectra of the polymer samples were assigned to a 1-phenyl-(2n + 1)-multiacetoxyalkane (where n = 1, 2, 3, etc.) microstructure, and its concentration obtained from NMR spectra was well-correlated with that calculated from previously reported kinetic data. The mechanism of the chain transfer reaction was shown to involve addition of the propagating macroradical to benzene instead of hydrogen abstraction from benzene. Almost all of the experimental data on the effects of aromatic solvents in this free-radical polymerization could be explained by invoking an equilibrium between the free propagating macroradical and a stabilized complex radical that is either a donor-acceptor π-complex or a cyclohexadienyl σ-complex.

References

CHAPTER 1 INTRODUCTION

1. *Chem. Eng. News*, **74** (26), 42 (1996).
2. H. F. Mark, N. G. Gaylord, and N. M. Bikales, Eds., *Encyclopedia of Polymer Science and Engineering*, 2nd ed., Vol. 17, Wiley-Interscience, New York, 1989, p. 136.
3. C. A. Finch, *Poly(vinyl alcohol) – Developments*, Wiley, New York, 1992, p. 514.
4. G. Allen and J. C. Bevington, Eds., *Comprehensive Polymer Science*, Vol. 7, Pergamon, New York, 1989, p. 136.
5. G. Odian, *Principles of Polymerization*, 3rd ed., Wiley-Interscience, New York, 1991, p. 302.
6. G. C. Eastmond, *Free Radical Polymerization*, in C. H. Bamford and C. F. H. Tipper, Eds., *Comprehensive Chemical Kinetics*, Vol. 14A, Elsevier, New York, 1976.

CHAPTER 2 BACKGROUND

1. R. Diercks and K. P. C. Vollhardt, *J. Am. Chem. Soc.*, **108**, 3150 (1986).
2. K. K. Baldrige and J. S. Siegel, *J. Am. Chem. Soc.*, **114**, 9583 (1992).
3. N. L. Frank, K. K. Baldrige, and J. S. Siegel, *J. Am. Chem. Soc.*, **117**, 2102 (1995).
4. N. L. Frank, K. K. Baldrige, P. Gantzel, and J. S. Siegel, *Tetrahedron Lett.*, **36**(25), 4389 (1995).
5. R. H. Mitchell, Y. Chen, V. S. Iyer, D. Y. K. Lau, K. K. Baldrige, and J. S. Siegel, *J. Am. Chem. Soc.*, **118**, 2907 (1996).
6. W. H. McDowell and W. O. Kenyon, *J. Am. Chem. Soc.*, **62**, 415 (1940).
7. S. I. Nozakura, Y. Morishima, and S. Murahashi, *J. Polym. Sci., Part A-1*, **10**, 2781 (1972); **10**, 2853 (1972).
8. P. J. Flory and F. S. Leutner, *J. Polym. Sci.*, **5**, 267 (1950).
9. D. W. Ovenall, *Macromolecules*, **17**, 1458 (1984).
10. F. F. Vercauteren and W. A. B. Donners, *Polymer*, **27**, 993 (1986).
11. S. Amiya and M. Uetsuki, *Macromolecules*, **15**, 166 (1982).
12. H. W. Melville and P. R. Sewell, *Makromol. Chem.*, **22**, 139 (1959).
13. W. H. Starnes, Jr., H. Chung, and G. M. Benedikt, *Polym. Prepr. (Am. Chem. Soc., Div. Polym. Chem.)*, **34** (1), 604 (1993).

14. J. C. Bevington, T. N. Huckerby, and N. W. E. Hutton, *Eur. Polym. J.*, **18**, 963 (1982).

15. G. Moad, D. H. Solomon, S. R. Johns, and R. I. Willing, *Macromolecules*, **17**, 1094 (1984).

16. G. M. Burnett and H. W. Melville, *Discuss. Faraday Soc.*, **2**, 322 (1947).

17. W. H. Stockmayer and L. H. Peebles, Jr., *J. Am. Chem. Soc.*, **75**, 2278 (1953).

18. M. Kamachi, D. J. Liaw, and S. Nozakura, *Polym. J. (Tokyo)*, **11**, 921 (1979).

19. K. Hatada, Y. Terawaki, T. Kitayama, M. Kamachi, and M. Tamaki, *Polym. Bull. (Berlin)*, **4**, 451 (1981).

20. M. Kamachi, *Adv. Polym. Sci.*, **38**, 55 (1981).

21. J. T. Clarke, R. O. Howard, and W. H. Stockmayer, *Makromol. Chem.*, **44**, 427 (1961).

22. J. Brandrup and E. H. Immergut, Eds., *Polymer Handbook*, 3rd ed., Wiley-Interscience, New York, 1989, p. V-71.

23. G. A. Mortimer and L. C. Arnold, *J. Am. Chem. Soc.*, **84**, 4986 (1962).

24. G. Henrici-Olivé and S. Olivé, *Makromol. Chem.*, **51**, 236 (1962).

25. H. C. Haas and H. Husek, *J. Polym. Sci., Part A-1*, **2**, 2297 (1964).

26. J. W. Breitenbach, G. Billek, G. Falthansl, and E. Weber, *Monatsh.*, **92**, 1100 (1961).

27. H. Chung, Ph. D. Dissertation, Polytechnic University, January, 1993.

28. M. Kamachi, Y. Kuwae, and S. Nozakura, *Polym. J. (Tokyo)*, **17**, 541 (1985).

29. T. Yamamoto, T. Yamamoto, T. Minamisawa, and M. Hirota, *Kobunshi Ronbunshu*, **36**, 557 (1979); *Chem. Abstr.*, **91**, 158200d (1979).

30. G. M. Burnett and L. D. Loan, *Trans. Faraday Soc.*, **51**, 219 (1955).

31. P. W. Allen, F. M. Merrett, and J. Scanlan, *Trans. Faraday Soc.*, **51**, 95 (1955).

32. L. H. Peebles, Jr., J. T. Clarke, and W. H. Stockmayer, *J. Am. Chem. Soc.*, **82**, 4780 (1960).

33. W. H. Atkinson, C. H. Bamford, and G. C. Eastmond, *Trans. Faraday Soc.*, **66**, 1446 (1970).

34. G. F. Santee, R. H. Marchessault, H. G. Clark, J. J. Kearny, and V. Stannett, *Makromol. Chem.*, **73**, 177 (1964).

35. T. Yamamoto, A. Mito, and M. Hirota, *Nippon Kagaku Kaishi*, 408 (1979); *Chem. Abstr.*, **91**, 193721w (1979).

36. C. H. Bamford, *Pure Appl. Chem.*, **12**, 183 (1966).

37. C. H. Bamford and S. Brumby, *Makromol. Chem.*, **105**, 222 (1967).

38. G. M. Burnett, G. G. Cameron, and M. M. Zafar, *Eur. Polym. J.*, **6**, 823 (1970).

39. N. Grassie, *Trans. Faraday Soc.*, **48**, 379 (1952); **49**, 835 (1953).

40. A. Servotte and V. Desreux, *J. Polym. Sci., Part C*, **22**, 367 (1968).

41. C. H. Bamford and A. D. Jenkins, *Nature*, **176**, 78 (1955).

42. B. L. Funt and W. Paskia, *Can. J. Chem.*, **38**, 1865 (1960).

43. A. K. Chaudhuri and S. R. Palit, *J. Polym. Sci., Part A-1*, 6, 2187 (1968).

44. W. H. Starnes, Jr., F. C. Schilling, K. B. Abbås, R. E. Cais, and F. A. Bovey, *Macromolecules*, **12**, 556 (1979).

45. D. A. Lindsay, J. Lusztyk, and K. U. Ingold, *J. Am. Chem. Soc.*, **106**, 7087 (1984).

46. W. H. Starnes, Jr., F. C. Schilling, K. B. Abbås, I. M. Plitz, R. L. Hartless, and F. A. Bovey, *Macromolecules*, **12**, 13 (1979).

47. W. H. Starnes, Jr., R. L. Hartless, F. C. Schilling, and F. A. Bovey, *Polym. Prepr. (Am. Chem. Soc., Div. Polym. Chem.)*, **18**(1), 499 (1977).

48. W. H. Starnes, Jr., F. C. Schilling, I. M. Plitz, R. E. Cais, D. J. Freed, R. L. Hartless, and F. A. Bovey, *Macromolecules*, **16**, 790 (1983).

49. J. H. Edwards and W. J. Feast, *Polymer*, **21**, 595 (1980).

50. W. J. Feast and J. N. Winter, *J. Chem. Soc., Chem. Comm.*, 202 (1985).

51. F. A. Bovey and L. W. Jelinski, *Chain Structure and Conformation of Macromolecules*, Academic Press, New York, 1982, p. 78.

CHAPTER 3 EXPERIMENTAL

1. M. Morton and I. Piirma, *J. Polym. Sci. Part A-3*, 1, 3043 (1963).
2. S. Nozakura, Y. Morishima, and S. Murahashi, *J. Polym. Sci., Polym. Chem. Ed.*, 10, 2853 (1972).
3. J. T. Clarke, R. O. Howard, and W. H. Stockmayer, *Makromol. Chem.*, 44, 427 (1961).
4. K. Hatada, Y. Terawaki, T. Kitayama, M. Kamachi, and M. Tamaki, *Polym. Bull. (Berlin)*, 4, 451 (1981).
5. R. H. Wagner, *J. Polym. Sci.*, 2, 21 (1947).
6. W. R. Moore and M. Murphy, *J. Polym. Sci.*, 56, 519 (1962).
7. J. A. Howard and K. U. Ingold, *Can. J. Chem.*, 43, 2737 (1965).
8. J. A. Howard and K. U. Ingold, *Can. J. Chem.*, 45, 785 (1967).
9. T. K. Wu and D. W. Ovenall, *Macromolecules*, 7, 776 (1974).
10. T. Moritani and Y. Fujiwara, *Macromolecules*, 10, 532 (1977).
11. M. S. Kharasch and O. Reinmuth, *Grignard Reactions of Nonmetallic Substances*, Prentice-Hall, New York, 1954, p. 138.
12. L. F. Fieser and M. Fieser, *Reagents for Organic Synthesis*, Vol. 1, Wiley, New York, 1967, p. 958.
13. A. Maercker, *Wittig Reaction*, in R. Adams, A. H. Blatt, V. Boekelheide, T. L. Cairns, D. J. Cram, and H. O. House, Eds., *Organic Reactions*, Vol. 14, Wiley, New York, 1964.
14. B. E. Maryanoff and A. B. Reitz, *Chem. Rev.*, 89, 863 (1989).

15. E. J. Corey, K. Narasaka, and M. Shibasaki, *J. Am. Chem. Soc.*, **98**, 6417 (1976).

16. J. Buckingham, Ed., *Dictionary of Organic Compounds*, 5th Ed., Chapman and Hall, New York, 1982, p. 4604.

17. S. W. Chaikin and W. G. Brown, *J. Am. Chem. Soc.*, **71**, 122 (1949).

18. M. L. Miles, T. M. Harris, and C. R. Hauser, *J. Org. Chem.*, **30**, 1007 (1965).

19. J. Cossy and P. Pale, *Tetrahedron Lett.*, **28**, 6039 (1987).

20. G. Wilke and H. Müller, *Justus Liebigs Ann. Chem.*, **629**, 222 (1960).

21. S. Warwel, G. Schmitt, and B. Ahlfaenger, *Synthesis*, **7**, 632 (1975).

22. E. Negishi, A. O. King, and S. Baba, *J. Chem. Soc., Chem. Comm.*, 17 (1976).

23. G. A. Wiley, R. L. Hershkowitz, B. W. Rein, and B. C. Chung, *J. Am. Chem. Soc.*, **86**, 964 (1964).

24. H. Oediger, H. J. Kabbe, F. Möller, and K. Eiter, *Chem. Ber.*, **99**, 2012 (1966).

CHAPTER 4 RESULTS AND DISCUSSION

1. R. H. Wagner, *J. Polym. Sci.*, **2**, 21 (1947).
2. H. Chung, Ph. D. Dissertation, Polytechnic University, January, 1993.
3. E. G. Paul and D. M. Grant, *J. Am. Chem. Soc.*, **85**, 1701 (1963).
4. D. M. Grant and E. G. Paul, *J. Am. Chem. Soc.*, **86**, 2984 (1964).
5. K-L. Noble, H. Hopf, and L. Ernst, *Chem. Ber.*, **117**, 455 (1984).
6. J. Brandrup and E. H. Immergut, Eds.; *Polymer Handbook*, 3rd ed., Wiley-Interscience, New York, 1989, p. II-86.
7. M. S. Matheson, E. E. Auer, E. B. Bevilacqua, and E. J. Hart, *J. Am. Chem. Soc.*, **71**, 2610 (1949).
8. J. P. Van Hook and A. V. Tobolsky, *J. Am. Chem. Soc.*, **80**, 779 (1958).
9. G. Odian, *Principles of Polymerization*, 3rd ed., Wiley-Interscience, New York, 1991, p. 244.
10. J. C. Bevington, S. W. Breuer, E. N. J. Heseltine, T. N. Huckery, and S. C. Varma, *J. Polym. Sci., Polym. Chem. Ed.*, **25**, 1085 (1987).
11. W. H. Starnes, Jr., I. M. Plitz, F. C. Schilling, G. M. Villacorta, G. S. Park, and A. H. Saremi, *Macromolecules*, **17**, 2507 (1984).
12. J. Schaefer and D. F. S. Natusch, *Macromolecules*, **5**, 416 (1972).
13. C. A. Barson, J. C. Bevington, and D. E. Eaves, *Trans. Faraday Soc.*, **54**, 1678 (1958).
14. F. Stoos and J. Roček, *J. Am. Chem. Soc.*, **94**, 2719 (1972).

15. C. J. Pouchert and J. Behnke, *The Aldrich Library of ^{13}C and ^{1}H FT NMR Spectra*, 1st ed., Vol. 1, Aldrich Chemical Company, Inc., 1993, pp. 28 and 965.

16. E. Wenkert, M. J. Gašić, E. W. Hagaman, and L. D. Kwart, *Org. Magn. Res.*, 7, 51 (1975).

17. W. H. Starnes, Jr., private communication.

18. C. H. Bamford and A. D. Jenkins, *Nature*, **176**, 78 (1955).

19. B. L. Funt and W. Pasika, *Can. J. Chem.*, **38**, 1865 (1960).

20. A. K. Chaudhuri and S. R. Palit, *J. Polym. Sci., Part A-1*, **6**, 2187 (1968).

21. C. H. Bamford, R. W. Dyson, and G. C. Eastmond, *Polymer*, **10**, 885 (1969).

22. M. H. Litt and K. H. S. Chung, *ACS Symp. Ser.*, **165**, 455 (1981).

23. M. Kamachi, D. J. Liaw, and S. Nozakura, *Polym. J. (Tokyo)*, **11**, 921 (1979).

24. G. A. Russell, *J. Am. Chem. Soc.*, **79**, 2977 (1957).

25. G. A. Russell, *J. Am. Chem. Soc.*, **80**, 4897 (1958).

26. G. A. Russell, *J. Am. Chem. Soc.*, **80**, 4997 (1958).

27. N. J. Bunce, K. U. Ingold, J. P. Landers, J. Lusztyk, and J. C. Scaiano, *J. Am. Chem. Soc.*, **107**, 5464 (1985).

28. C. Walling, *J. Org. Chem.*, **53**, 305 (1988).

29. K. D. Raner, J. Lusztyk, and K. U. Ingold, *J. Am. Chem. Soc.*, **110**, 3519 (1988).

30. K. U. Ingold, J. Lusztyk, and K. D. Raner, *Acc. Chem. Res.*, **23**, 219 (1990).

31. K. D. Raner, J. Lusztyk, and K. U. Ingold, *J. Am. Chem. Soc.*, **111**, 3652 (1989).

32. K. D. Raner, J. Lusztyk, and K. U. Ingold, *J. Phys. Chem.*, **93**, 564 (1989).

33. W. Jarzeba, K. Thakur, A. Hömann, and P. F. Barbara, *J. Phys. Chem.*, **99**, 2016 (1995).

34. P. S. Skell, H. N. Baxter, III, and C. K. Taylor, *J. Am. Chem. Soc.*, **105**, 120 (1983).

35. P. S. Skell and H. N. Baxter, III, *J. Am. Chem. Soc.*, **107**, 2823 (1985).

36. P. S. Skell, H. N. Baxter, III, J. M.Tanko, and V. Chebolu, *J. Am. Chem. Soc.*, **108**, 6300 (1986).

37. S. W. Benson, *J. Am. Chem. Soc.*, **115**, 6969 (1993).

38. C. Walling and M. F. Mayahi, *J. Am. Chem. Soc.*, **81**, 1485 (1959).

39. R. E. Bühler and M. Ebert, *Nature (London)*, **214**, 1220 (1967).

40. T. Shida and I. Hanazaki, *Bull. Chem. Soc. Jpn.*, **43**, 646 (1970).

41. J. E. Jordon, D. W. Pratt, and D. E. Wood, *J. Am. Chem. Soc.*, **96**, 5588 (1974).

42. R. Breslow, M. Brandl, J. Hunger, N. Turro, K. Cassidy, K. Krough-Jesperson, and J. D. Westbrook, *J. Am. Chem. Soc.*, **109**, 7204 (1987).

43. J. M. Tanko and F. E. Anderson, III, *J. Am. Chem. Soc.*, **110**, 3525 (1988).

44. T. D. Giacco, E. Baciocchi, and S. Steenken, *J. Phys. Chem.*, **97**, 5451 (1993).

45. M. Kamachi, *Adv. Polym. Sci.*, **82**, 207 (1987).

46. M. G. Evans and M. Polanyi, *Trans. Faraday Soc.*, **34**, 11 (1938).

47. J. M. Tedder, *Angew. Chem. Int. Ed. Engl.*, **21**, 401 (1982).

48. J. M. Tedder, *Tetrahedron*, **38**, 313 (1982).

49. D. R. Lide and H. P. R. Frederikse, Eds.; *CRC Handbook of Chemistry and Physics*, 77th ed., CRC Press, New York, 1996, p. 9-64.

50. J. W. Breitenbach, G. Billek, G. Falthansl, and E. Weber, *Monatsh.*, **92**, 1100 (1961).

51. G. Ayrey, *Chem. Rev.*, **63**, 645 (1963).

52. R. P.-T. Chung and D. H. Solomon, *Prog. Org. Coatings*, **21**, 227 (1992).

VITA

Hongyang Yao

Hongyang Yao was born in Zhecheng County, Henan Province, P. R. China, on March 26, 1966. He was graduated from the University of Science and Technology of China, Hefei, Anhui Province, P. R. China, in July 1989, with the degree of Bachelor of Science in Applied Chemistry. He was a candidate for Master of Science, Changchun Institute of Applied Chemistry, the Science Academy of China, from September 1989 to July 1991, with a concentration in Polymer Chemistry. The course requirements for this degree were completed, but not the thesis, which was to have been entitled "Radiation Effects on High Performance Polyimide Films".

The author entered the Department of Applied Science, College of William and Mary, in August 1991 to do doctoral research under the guidance of Dr. William H. Starnes, Jr., in the field of polymer science.